Titre: Title:	Supporting Production from a Single Surface Roughness Profile
Auteur: Author:	Paul Provencher
Date:	2017
Type:	Mémoire ou thèse / Dissertation or Thesis
Référence: Citation:	Provencher, P. (2017). Supporting Production from a Single Surface Roughness Profile [Thèse de doctorat, École Polytechnique de Montréal]. PolyPublie. https://publications.polymtl.ca/2793/

URL de PolyPublie: PolyPublie URL:	https://publications.polymtl.ca/2793/
Directeurs de recherche: Advisors:	Marek Balazinski, & Ramin Sedaghati
Programme: Program:	Génie mécanique

UNIVERSITÉ DE MONTRÉAL

SUPPORTING PRODUCTION FROM A SINGLE SURFACE ROUGHNESS PROFILE

PAUL PROVENCHER
DÉPARTEMENT DE GÉNIE MÉCANIQUE
POLYTECHNIQUE MONTRÉAL

THÈSE PRÉSENTÉE EN VUE DE L'OBTENTION
DU DIPLÔME DE PHILOSOPHIÆ DOCTOR
(GÉNIE MÉCANIQUE)
SEPTEMBRE 2017

UNIVERSITÉ DE MONTRÉAL

POLYTECHNIQUE MONTRÉAL

Cette thèse intitulée :

SUPPORTING PRODUCTION FROM A SINGLE SURFACE ROUGHNESS PROFILE

présentée par: PROVENCHER Paul

en vue de l'obtention du diplôme de : Philosophiæ Doctor

a été dûment acceptée par le jury d'examen constitué de :

M. LAKIS Aouni, Ph. D., président

M. BALAZINSKI Marek, D. Sc., membre et directeur de recherche

M. SEDAGHATI Ramin, Ph. D., membre et codirecteur de recherche

M. ACHICHE Sofiane, Ph. D., membre

M. GRZESIK Wit, D. Sc., membre externe

DEDICATION

Barbara, Daniel et Carmen

ACKNOWLEDGEMENTS

RÉSUMÉ

En production, le contrôle et la mise au point de coupes précises dépend fortement d'une approche essai et erreur et de l'expertise des spécialistes d'usinage. La manipulation des nombreuses variables du procédé en vue d'élaborer des conditions acceptables exige la fabrication de pièces d'essai. Lorsque le coût unitaire dépasse les dizaines de milliers de CAD, il est digne d'intérêt de diminuer le nombre de pièces d'essai même d'un seul exemplaire. Le contrôle du procédé est également important afin d'empêcher les pièces rebutées.

Cette thèse décrit le développement de la capacité d'acquérir un unique profil linéaire de rugosité d'une pièce soumise au tournage dur de finition, de remettre ce profil à une analyse automatisée et obtenir les contributions proportionnelles de certains mécanismes envers des paramètres arbitraires d'amplitude de rugosité.

L'évaluation en tant que contribution à n'importe paramètre facilite l'utilisation en fabrication, vu qu'en production il est normallement d'importance capitale de satisfaire aux critères spécifiques du dessin tel la rugosité moyenne R_a, plutôt qu'à des paramètres exotiques. L'analyse automatisée est importante afin d'éviter d'exiger une expertise spéciale pour appliquer les techniques chez le manufacturier. Les profils de rugosité linéaires sont attrayants pour leurs qualités d'être rapides, peu chers, non-destructifs, et dépendants uniquement d'équipements communs en atelier d'usinage.

Les défis relevés comptent la tâche non-triviale d'automatiser l'identification des traces d'outils dans les profils linéaires de rugosité, en absence de connaissance *a priori* de la morphologie des traces d'outils à cause de la déformation plastique importante lors du tournage dur de finition. La méthode créée est nommée « identification par domaine corrélé » (CDI) et exploite la variabilité aléatoire du procédé sans effectuer de régression. Des signatures de mécanismes actifs lors de la finition dure ont été identifiés en tant que modes de variabilité de la coupe, sans devoir prescrire par régression les déformations attendues. Les modes correspondent à la vibration radiale et axiale et à des réponses plastiques du matériau. Les modes ont été idéalisés mathématiquement. De plus, il a été vérifié expérimentalement que les vibrations radiales expliquent la signature de son mode associé dans sa totalité.

L'étude culmine avec une implémentation sous forme de logiciel graphique destiné à l'utilisation en production. L'analyse est conçue pour la facilité de l'utilisation et se trouve presque entièrement automatisée. Le logiciel compte aussi parmi ses fonctionnalités l'estimation par éléments finis de la concentration de contrainte microgéométrique et la génération d'hypersurfaces de réponse pour plans expérimentaux. Les codes sont structurés et documentés afin de faciliter une continuation suivant le départ de l'auteur du programme doctoral.

ABSTRACT

In production, control and optimization of precision cuts is heavily dependent upon trial and error and upon machining specialist expertise. When unit cost is in the tens of thousands of CAD, manipulation of the many process variables in order to narrow in on acceptable conditions should be done with as few trial parts as possible; reduction of the number of trial parts by even one specimen is worthwhile. Process control is equally important to maintain stable production and prevent the scrapping of parts.

This thesis describes the development of the ability to acquire a single linear roughness profile from a finish hard turned metallic part, submit the roughness profile to a computer-automated analysis, and obtain percent contributions of specific mechanisms to arbitrary roughness parameters of profile amplitude.

Expression as a contribution to any parameter facilitates applicability in manufacturing, in which production is usually concerned with meeting specific scalar surface roughness requirements such as average roughness R_a rather than exotic roughness parameters. Automated analysis is important in order to avoid requiring special expertise in the techniques developed for manufacturer implementation. Linear roughness profiles are attractive for the quick, inexpensive, and non-destructive nature of their acquisition, and for the widespread availability of linear roughness measuring machines in machine shops.

The challenges overcome include the non-trivial task of automating identification of the locations of tool traces or "feed marks" in linear roughness profiles, without any *a priori* knowledge of feed mark shape due to the significant plastic deformations in finish hard turning. The method developed is dubbed "Correlated Domain Identification" (CDI), does not depend on regression techniques, and exploits the continuous random variability of the cutting process. Signatures of specific mechanisms active during hard turning were identified as modes of cut variability without coercing the data by fitting of expected deformations. The modes identified include radial and axial cutting vibration, local ploughing, and side flow. The modes were idealized mathematically. The claim that radial vibration fully accounts for its associated mode signature was verified experimentally.

The study culminates with implementation as a graphical software program suitable for use in production. The analysis is nearly entirely automated and is designed for ease of use. Additional features of the software include finite element estimation of microgeometry-induced stress concentration and generation of response hypersurfaces of designed experiments. The codes developed are neatly organized and documented in order to facilitate development following the author's departure from the Ph.D. program.

TABLE OF CONTENTS

LIST OF TABLES

LIST OF FIGURES

LIST OF APPENDICES

LIST OF SYMBOLS AND ABBREVIATIONS

$a, b, c, d, ...$	The first few principal components of a set of feed marks, in order of decreasing importance (variance).
A	The idealized feed mark component corresponding to radial displacement of the cutting tool (see Chapter 4).
B	The idealized feed mark component corresponding to axial displacement of the cutting tool.
C	The idealized feed mark component corresponding to local, intra-mark ploughing.
D	The idealized feed mark component corresponding to side flow.
CDI	Correlated domain identification (see Chapter 3)
FEA	Finite element analysis
K_t	Stress concentration
f	The effective machining feed length, as it appears in a measured linear roughness profile
φ	Phase (measure of lateral position within a linear (*i.e.* 2D) roughness profile)
φ_m	Feed mark phase (start of the first feed mark in the roughness profile)
$q(\varphi)$	The qualifier function (see Chapter 3)
x	The axial coordinate of a cylindrical turned surface.
y	The tangential coordinate orthogonal to x and z.
z	The radial coordinate of a cylindrical turned surface.
rev	Revolution
sfm	Surface feet per minute

PREFACE

Montreal, late at night

When they offer you grad studies, they don't tell you it's aboard a submarine. Not explicitly. It's cold and I keep wishing there were windows, but even when I'm alone there's always the hum of the mini-fridge and the company of my "CDI" method and of the-part-of-my-brain-that-doesn't-care-what-I'm-working-on.

"I'm going to ad-lib a song about how to colonize Mars. It's set to the tune of 'Stressed Out' by Twenty One Pilots."

"Thanks, TPOMBTDCWIWO."

I think it's worked out all right. My work started out as a Master's degree; though the sentiment was not universal, Professor Balazinski had no hesitation in taking on a physics science major as a grad in mechanical engineering. After a year I knew I had enough material lined up to do quick Ph.D. instead, which seems to have lasted a total of three and a half years. Meanwhile, I've very nearly completed the slew of exams the *Ordre des Ingénieurs* prescribed me to qualify as a junior mechanical engineer. Still, it feels like I'm a physicist pretending to be an engineer. Eh, what's that, CDI?

"You're more of an analyst-parastatistician-manufacturing-engineer-experimental-physicist-materials-coding guy."

"Bit of a mouthful. Just go back to finding feed marks."

"I also think you should have published the finite elements part as a technical note."

"That's enough from you, CDI! I *birthed* you from my mind-vagina!" I think it sounded better when Dan Avidan said it.

Though I wish I'd gotten to build more lab setups, like I did before I came here, I might be doing that again soon; I can only suppose my work has been appreciated, seeing as the next chapter of my life looks like it might be a postdoc contract aboard a nicer submarine.

For those who will come after, if you choose to use some of my work in yours, I've made sure to organize and comment all my scripts as nicely as I can. Maybe I can get them to you, no need to reinvent everything. I'd be delighted for my work see use again. Whether or not your work is related to mine, I hope you enjoy what you're creating and don't fret working at the bottom of the sea.

CHAPTER 1

INTRODUCTION

To state the research question informally, can a single linear roughness profile from a hard finish turned part[1] be submitted to a computer, analyzed in an automated way, and yield percent contributions of specific cutting variabilities (vibrations and plastic effects) to arbitrary roughness parameters? Concluding in the affirmative, developing that ability is the goal of this thesis. Informally, the fundamental hypothesis of this thesis rests on the notion that the two-dimensional cross-sections of the tool trace on the surface of a turned part, or "feed marks", in a given profile behave as a statistical sample of the instantaneous state of the dynamic cutting interface. The feed marks behave as "snapshots" of the cut.

The context is precision finish machining, a class of techniques that is appropriate for the generation of critical surfaces having particular surface integrity requirements. The criticality of a surface is dependent upon its function: a gas turbine disk may require pronounced fatigue reliability, a gastight seal flange may require particular surface microgeometry, and an optical surface may require smoothness in the hundredths of a micron. Achieving the requirements of a surface by manufacturing successive trial parts may be demanding and costly. Similarly, it is desirable to eliminate operations entirely by producing a finished surface by cutting alone, without additional processing. Once a process is approved and a part enters production, monitoring the evolution of a production line's results is equally important to prevent the scrapping of parts.

Surface finish is highly relevant to many critical surfaces. Sadly, road pavement (Boscaino et al., 2003) and machined parts, despite very different surface generation mechanisms, are both treated using the same simple geometrical descriptors such as the ubiquitous roughness parameter R_a [2]. The typical analytical treatment of surface roughness is devoid of significance to the process having generated the surface, in no way describing the physics of the manufacturing process. Machining specialists are therefore very reliant on experience to minimize trial-and-error. Experimental tools exist, such as the insertion of a dynamometer between tool holder and turret, the measurement of the vibrational modes of the machine tool system, measurement of spindle power, high-speed video recording of the cut, and many other means of diagnosing the cutting process. However, these methods may be cumber-

---

[1] That is to say, finish turned by hard turning.

[2] R_a expresses the amplitude of a roughness profile, the mean absolute deviation from the center line (ISO 4287:1997, 1997).

some and time-consuming, requiring special equipment and experts for data acquisition and analysis, and may imply drawbacks such as the addition of new vibrational modes from the inclusion of a dynamometer.

A simple and inexpensive alternative may be the collection of linear roughness profiles[3] from machined parts. A stable cut is inevitably a dynamic stability, evidenced by the uniqueness of each feed mark in any given linear roughness profile. Each feed mark in a linear roughness profile indicates the instantaneous condition of the interface between cutting edge and workpiece. It follows that treatment of the feed marks of a profile as a statistical sample of snapshots may reveal the signatures of the dynamic processes involved in generating the surface. Linear roughness profiles are appealing for the ease, quickness, and inexpensiveness of their measurement, and for their non-destructive nature. Linear roughness profiles are commonly used in industrial practice.

There is currently an extreme dearth of research into the treatment of linear roughness profiles as snapshots of the cut. This thesis develops the ability to have a computer automatically decompose a roughness profile into quantitative information about the physics of the cut, for the sake of reducing non-trivial production expenses resulting from the trial and error methods described above. As an example, the contribution to surface roughness parameter R_a from the radial component of vibration between tool and workpiece can be quantified. Supposing that in a particular case it were ascertained that R_a could be reduced by 16% by stabilizing the cut, then the machining specialist would have that information to decide whether the surface should be improved by reducing system vibration rather than selecting another way of modifying the cut, such as a sharper edge preparation, harder tool, or any number of other approaches to process optimization.

The scope of the research in this thesis is limited to the study of linear roughness profiles resulting from hard finish turning. Nonetheless, it is expected that derivative techniques might be applicable to milling and drilling, as both those techniques produce feed marks in a manner similar to turning.

1.1   Problem Statement

In a production scenario, typical problems with microgeometry include inadmissibly large values of roughness parameter R_a, readhered material, tears, laps, poor finish due to built-up edges, white layer, scratches, waviness, traces of vibrations, and dimensional inaccuracy. To resolve this type of issue, experience is very heavily valued, and in combination with cutting tests, touch, visual inspection, and roughness measuring tools, a cutting specialist

---

[3]A "linear roughness profile" is a two-dimensional cross-section of the surface.

a)   b)
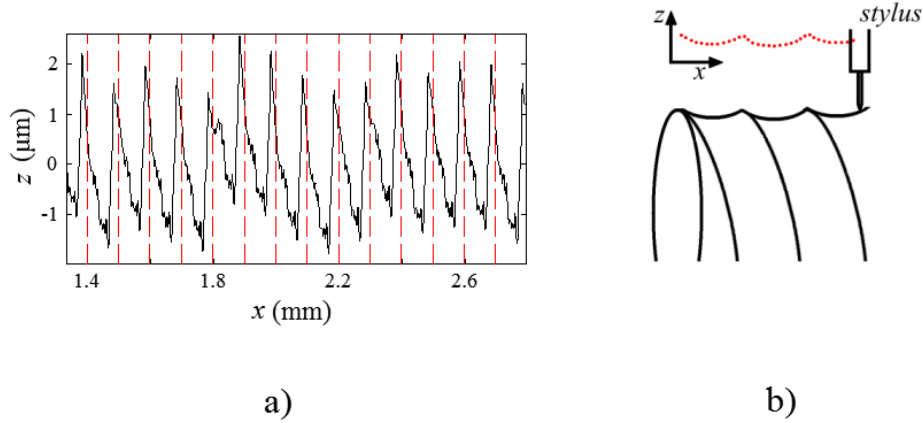
Figure 1.1: Linear roughness profiles. **a)** An example of a linear roughness profile of a cylindrical turned part. The profile was measured axially along the part, and has visually evident tool trace cross-sections, or "feed marks". The dashed lines indicate the locations of the marks, as determined using Correlated Domain Identification (CDI), the new technique described in Chapter 3. **b)** An illustration of digital encoding of linear roughness profiles using a skidless contact stylus (more details on the apparatus in Section 2.2).

may narrow in on the primary cause of the problem faced. He may then improve the cut by changing the cutting tool material, tool geometry, edge preparation, tool holder, cutting feed, cutting speed, depth of cut, coolant, method of coolant application, the order of cuts, and so forth among many ways of adjusting the machine tool-tool-workpiece system. Even a cut that satisfies the nominal requirements of a part may present a risk to its production series if the degree of control over the cut is such that an eventual part may have to be scrapped.

Furthermore, improving a cut by trial and error becomes expensive very rapidly as the number of dimensions increases; even if only feed, speed, and depth of cut considered as controlled variables, plus one response variable, exploring the resulting four-dimensional space may require many trial parts to be manufactured.

There are therefore two advantages to understanding the cutting dynamics specific to a given precision cut. "Cutting dynamics", here, should convey the notion that a cut is a *dynamically* stable process: the mercurial behavior of built-up edges, vibrations, temperature fluctuations (for example, due to coolant splashing and inconstant chip morphology), material inhomogeneity (in terms of internal stresses, work hardening, and composition), and so on, continuously agitate the interface between cutting edge and workpiece. The first advantage is to reduce the number of trial parts when optimizing the cut. The second advantage is to maintain a cutting process that is stable and consistent. Both are directly related to manufacturer expenses, particularly when unit cost is high.

Reducing the number of trial parts necessary to optimize a process may be the more important of the two advantages, simply because some processes may be costly to alter once approved for a production line, especially in aerospace, in which certification is the name of the game. In some cases, a single turned trial part may cost tens of thousands in USD for bulk workpiece material alone. By comparison, analysis of roughness costs very little, especially automated analysis. Linear roughness profiles are of particular interest because linear roughness measuring machines are common in shops and are non-destructive (see Fig.1.1).

This thesis demonstrates that a single roughness profile from a hard finish turned part can be exploited as a set of snapshots of the dynamic state of the cutting interface. That treatment may yield estimates of the percent contributions of specific cutting effects to arbitrary amplitude-based roughness parameters, in order to support production in efficiently controlling precision cuts.

1.2 Hypotheses

This work confirmed the following hypotheses:

- Random variabilities within feed marks are correlated with one another within individual feed marks, and are not correlated with each other between feed marks. This is the basis of the Correlated Domain Identification (CDI) technique developed in Article One (Chapter 3).

- Feed marks vary according to a small number of modes of variability, and those modes are associated with individual competing mechanisms active during the cut. This statement was previously made by Ancio *et al.*(Ancio et al., 2016).

- The modes of variability are largely independent, and their contributions may be treated as a sum. This is the basis for the use of principal component analysis of feed marks in Article Two (Chapter 5), revealing modes of feed mark variability that correspond with the deformations expected from specific mechanisms. Specifically, the signatures of radial and axial vibration, and of ploughing and side flow, were found. This is shown in Article Two (Chapter 4). The notion that the contributions of physical mechanisms to surface roughness may be treated as independent was previously suggested by W. Grzesik and S. Brol (Grzesik and Brol, 2011).

- The mode of variability associated with feed mark relative depths is fully accounted for by the radial component of cutting tool vibration, both in spatial frequency and in amplitude (Chapter 5).

1.3 Objectives

The general objective of the proposed research is to derive information about the cut from machined surface microgeometry. This is to be done by segmenting linear roughness profiles into individual feed marks, in order to treat the feed marks as "snapshots" of the cut, that is, as a statistical sample of the instantaneous state of the interface between cutting edge and workpiece. Snapshots in time of the interface may contain signatures of dynamic processes active during the cut, and that information may enable estimation of the percent contributions of specific mechanisms to arbitrary roughness parameters of amplitude.

This work was inspired by the following principles. In practical application as a support tool for production, the techniques developed must:

- Be inexpensive to use. (Be quick, non-destructive and not unduly laborious.)

- Make use of equipment typical of manufacturers of precise machined aerospace components. (Not require atypical equipment.)

- Have mostly automated analysis. (Not require any special expertise to employ.)

- Produce information machining specialists can immediately apply to cutting process optimization. (Be useful for production.)

Though a practical, graphical computer program implementation was developed and is shown in this thesis, these guiding stars do not imply that the thesis includes development of commercial-quality analytical tools.

As the specific objectives, an easily employed, mostly-automated analysis method was developed as a support tool for production, that can:

- Take as input a single roughness profile from a hard finish turned metallic part.

- Identify the locations of the feed marks.

- Break down feed mark variabilities by specific cutting effects such as vibration and workpiece plastic deformation

- Estimate percent contributions of those specific effects to arbitrary amplitude-based roughness parameters.

1.4 Thesis Organization

Several issues are tackled, organized by research paper:

- Automated identification of visually non-obvious feed marks. Hard finish turned surfaces often exhibit either feed marks that are severely deformed (as compared with the ideal tool nose trace) by plastic effects, or indeed no visually evident feed marks at all. How can a computer identify where the feed marks are located in a roughness profile digital signal, without *a priori* assuming a feed mark shape? This is resolved in Article One (Chapter 3).

- Decomposing feed marks into phenomenon signatures: Do feed marks from a profile, treated as a statistical sample, reveal modes of variability that are related to what is expected for feed mark deformations? Radial cutting vibration, axial cutting vibration, ploughing, and side flow as modes of variability are revealed in Article Two (Chapter 4). In the same paper, the modes are idealized and can be digitally subtracted from roughness profiles, in order to express the percent contributions of the modes to arbitrary roughness parameters.

- Validation that the mode associated with radial cutting vibration is indeed fully accounted for by radial vibration. This is achieved in Article Three (Chapter 5).

There follows a chapter on the graphical software implementation of the techniques developed, intended as a support tool for production. That software tool also includes the abilities to estimate microgeometrical stress concentration with an automated finite element model, and the ability to generate and display n-dimensional response surfaces from designed experiments.

The General Discussion chapter discusses the work of the above chapters as they relate to one another and in hindsight. It also discusses unsuccessful approaches, the main scientific results, the practical software tool developed, and the limitations of the study.

The conclusion summarises the work. Finally, the novelty of the work is stated in the Original Contributions chapter.

CHAPTER 2

LITERATURE REVIEW

This thesis concerns the development of the ability to submit a single linear roughness profile from a cylindrical, hard finish turned metal part to computer-automated decomposition of feed marks, so as to extract the quantitative contributions of the signatures of specific cutting dynamics to arbitrary amplitude-based roughness parameters.

The literature reviewed below covers the following. Beginning wide to broach the subject, surface integrity is discussed to introduce the relevance of surface roughness to manufacturing operations, and in particular the advantages of using linear roughness profiles in a production scenario. There follows a discussion of the existing microgeometry inspection methods. From inspection it is then natural to discuss microgeometry specification.

Those topics aptly frame the much narrower context of decomposition of feed marks, and the specific phenomena that influence feed mark morphology. Importantly, literature is very scarce on decomposition of feed marks, the topic most important to this thesis.

2.1 Hierarchy of Context

Surface integrity is a high-level category of manners of describing manufactured surfaces. Surface integrity includes microgeometry, and microgeometry is itself a parent notion to the sharply limited body of work on feed mark morphology. Here, we approach the importance of surface integrity to manufacturing from a top-down approach, painting surface integrity as having twofold purpose: monitoring of the stability of manufacturing processes, and gaging of part performance in service. The discussion narrows to linear roughness profiles and analysis of feed marks.

In historical perspective, it is typical (Jawahir et al., 2011; Astakhov, 2010; Griffiths, 2001) to credit M. Field and J.F. Kahles for developing "surface integrity" as a technical term (Field and Kahles, 1964; Field et al., 1972), defining surface integrity very broadly as the condition of a surface produced by any means. Field *et al.*, working from a machining standpoint, considered specific mechanisms which alter parent bulk material when machining metals. As I.S. Jawahir *et al.* remarked in a substantial 2011 CIRP keynote paper (Jawahir et al., 2011) on surface integrity, Field *et al.* identified "plastic deformation, microcracking, phase transformations, hardness variations, tears and laps related to built-up edge formation, [and] residual stress distribution", among other mechanisms affecting the integrity of newly

machined surfaces. Indeed, in the same keynote paper (which also treats surface integrity from material removal processes), the very broad definition of surface integrity offered by Field *et al.* is embraced rather than challenged, calling for collaboration between researchers and application specialists and for recognition of the multidisciplinarity of the issue of surface integrity.

In the vein of multidisciplinarity, B. Griffiths lists (Griffiths, 2001, page 2) relevant example disciplines, related by their influence on surface integrity (in the context of manufacturing): chemistry, mechanics, tribology, metrology, physics, metallurgy, manufacturing, and design. In the form of part properties, those disciplines are echoed with specific examples by V.P. Astakhov in J.P. Davim's "Surface Integrity in Machining" (Astakhov, 2010), including surface finish, resistance to fatigue, to corrosion, and to wear, and properties of adhesion, diffusion, optics, absorptivity, adsorption, bonding, friction, washability, wettability, and any other aspects relevant to any particular case.

However, for all the agreement (far beyond the texts cited above) on the vastness and multidisciplinary of surface integrity, it is common for definitions of surface integrity to differ in a particular and significant way. For illustration, Astakhov's definition expresses explicitly that for a characteristic of a surface to be considered an aspect of its surface integrity, it must affect the surface's performance in service. This definition is contradicted by G.P. Petropoulos *et al.* in the following chapter (Petropoulos et al., 2010, page 38) of the same book (!). Petropoulos explains that traditionally, surface texture (which is within the scope of surface integrity), has been used to monitor the stability of manufacturing processes such as tool wear, machine vibration, and machine damage, rather than to gauge the functional performance of manufactured parts. In effect, the Astakhov-type definition is too restrictive, because part performance does not run the show alone, industry-wide. The recognition of both process monitoring *and* part performance as distinct motivators for the analysis of surface integrity broadens the importance of surface integrity in manufacturing. Indeed, process monitoring and part performance are both motivators for the work in the current thesis.

The distinction is operationally meaningful. For academic researchers, surface integrity for part performance appears to be a hot topic (and has been for some time): it is verdant with industrially applicable research avenues for models of microstructure, of surface roughness, of the wettability of plasma-treated wood, and so on. As an example for part performance, Petropoulos notes that R_a does function as in index of various incarnations of part performance, but other parameters greatly augment it. For example, he reports that profile skewness is an indicator of tribological performance, and Zahavi *et al.* discuss profile valley curvature as an important indicator for fatigue life performance (Zahavi et al., 1996,

page 183). Compounding the limited correlability of R_a to part performance, in the 1990 NIST *Surface Finish Metrology Tutorial* (Vorburger and Raja, 1990), Vorburger *et al.* point out that R_a is not even an intrinsic property of a surface profile, and varies as a function of sampling length[1]. Surface integrity, and in particular surface microgeometry, is therefore important in many cases to part performance. Furthermore, though the temptation appears to be to reduce surface microgeometry to a single scalar value, estimation of part performance may greatly benefit from the use of a more specialized parametrization of surface roughness than R_a.

In stark contrast, and for good reason, it is discouraged for mechanical designers to require very demanding sets of surface requirements; exotic and simultaneous requirements may be prohibitively difficult to achieve on the manufacturing side of an operation, and must furthermore typically be verified by quality control (often in a non-destructive manner!). For these reasons, design requirements are typically limited to roundabout parameters that the designers deem adequate, archetypally surface roughness parameter R_a and appropriate statistical limits on surface discontinuities (Zecchino, 2003). Manufacturers will then monitor those relatively simple parameters and little else as indicators of the stability of manufacturing processes. That is to say, the convenient, limited surface descriptors do enable process monitoring, despite doing little in terms of gaging part performance directly.

The operationally-motivated distinction between the use of surface integrity for process monitoring and for part performance is widespread and manifestly useful. Nevertheless, the distinction evaporates when reframing integrity as dependent neither uniquely upon the manufacturing process nor upon the manufactured part, but upon the process, the part, and their interaction, which may be termed the machine tool-tool-workpiece system (Quintana et al., 2009, page 108). For analysis of the physics of surface generation, the machine tool-tool-workpiece system frame, being more comprehensive, may be the more appropriate frame.

To narrow the context, investigation of a part's surface microgeometry may yield information relating both to part performance (fatigue performance (Zahavi et al., 1996) e.g. tears, laps, geometrical stress concentration, and tribological performance (Petropoulos et al., 2010, page 51)(Greenwood and Wu, 2001; Brown, 2012) e.g. oil retention capability, surface roughness profile skewness R_{sk}) and to process stability (condition of the cutting tool e.g. workpiece tears and laps, and the condition of the spindle e.g. statistical ergodicity between

---

[1] Most roughness parameters from a profile sample are influenced by the sampling method. Very common and egregious, lack of understanding of profile spatial frequency filtering (ISO/TS 16610-29:2006, 2006), commonly done automatically by roughness measuring machines, skews roughness results, both in industry and academia. An unfiltered profile also suffers, as soon as the profile is corrected for inclination between the axis of stylus travel and the nominal surface of the part (hence the influence of sampling length, sampling interval, and resolution (Whitehouse, 2011, page 94))! See also footnote 14.

surfaces[2] and stationarity[3] of roughness parameter R_a). These examples and sub-examples are by no means a strict nor exhaustive categorization.

Narrower still, measurement of linear roughness profiles is often quick (compared, for example, to metallographic cuts), inexpensive (in terms of materials, personnel-time, and required training), and non-destructive[4].

Focusing upon the subject of this thesis, linear roughness profiles of turned parts are composed of feed marks. As stated above, the aim is to treat roughness profile structure at the feed mark level in order to estimate the quantitative contributions of mechanisms active during the cut to arbitrary surface roughness parameters. What literature exists on the topic is discussed further below.

2.2 Microgeometry Inspection

This thesis develops a method of describing the surface microgeometries of parts to aid the machining specialist in controlling cuts. A brief discussion of roughness profile acquisition is therefore warranted.

Inspection of microgeometry begins with visual and tactile inspection. A machining specialist may tell without tools if a surface is wavy, rougher than expected, subject to readhered material, scratched, microstructurally altered or damaged by chatter. A magnifying lens and a portable roughness gauge or roughness measuring machine may often be enough for preliminary inspection. Detailed and quantitative inspection of roughness requires instruments. Two classes of instruments exist: contact and non-contact. Significantly, the work of this thesis is applicable to linear roughness profiles obtained by any method.

Contact methods are simpler and more common and rely on contact between the measured surface and a stylus (with or without a skid[5]). To orient the reader, a common detector scheme is shown in Fig. 2.1. D.J. Whitehouse explains in his *Handbook of Surface and Nanometrology* (Whitehouse, 2011) the involved details of analysis of contact stylus methods, especially for surfaces that deform elastically or plastically when touched. For this research

---

[2] "Ergodicity between surfaces" means that the results of repeated operations under the same nominal conditions are consistent.

[3] A process is said to be statistically stationary if statistical parameters describing it (e.g. surface roughness parameter R_a) are stable i.e. do not follow any trends. Mathematically, a process is stationary if the probability distribution governing its stochastic component is invariant.

[4] Although usually considered non-destructive, the use of a contact stylus to measure surface roughness may in some cases be considered a destructive measurement by mechanically damaging a very finely finished surface. Non-contact alternatives exist, such as laser confocal microscopy and other optical means.

[5] A skidless contact stylus has only the stylus in contact with the measured surface. A skid eliminates some long spatial wavelengths by resting on the surface around the stylus, so that the roughness measurement at any lateral position is always made relative to the immediate surroundings. A skid also reduces vibrations, for example from the cantilever arm of the stylus.

proposal, surface deformation during measurement is neglected, as the metals used are hard (>45 HRC) and stylus contact is gentle. Considerations such as stylus tip radius and angle are treated according to ISO standards (ISO 4287:1997, 1997) (save for some liberties in frequency filtering). Whitehouse comments on the damage a stylus or skid may cause to a surface, which in practice, for machining of hard metals, even for fatigue-sensitive applications, is neglected. Whitehouse also details signal artifacts caused by the measurement apparatus, which again, are so so subtle as to be neglected for the purposes of this thesis[6]. The experiments in this thesis make use of contact topographical measurements in order to scan over several millimeters; methods such as atomic force microscopy are too slow or impractical for characterization of feed marks, and such methods are also quite rare in machine shops, which would limit the applicability of the results. Contact methods may also be used to generate areal maps (3D topography) of a surface by rastering.
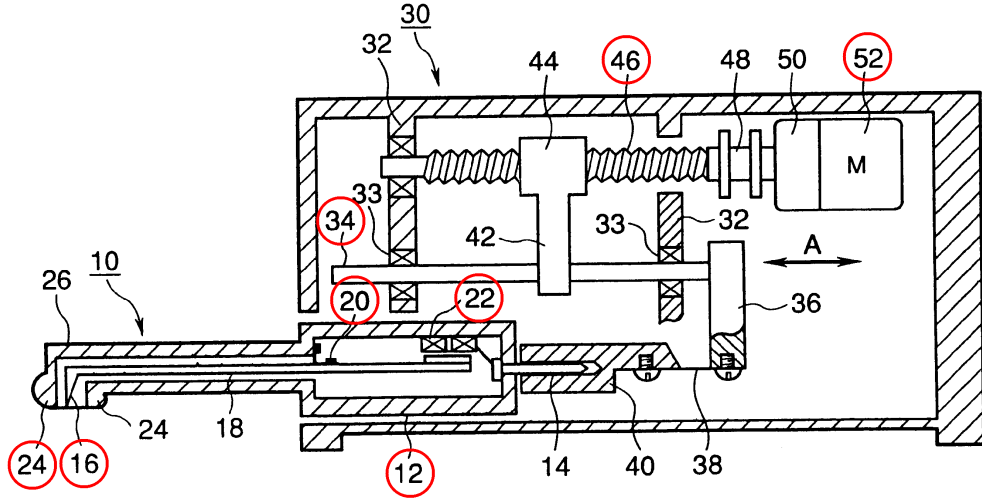
Figure 2.1: Figure 22 of a patent (Fujii and Shirai, 2000) owned by Mitutoyo Corporation illustrating common elements of a skidded contact stylus roughness measuring machine detector. The stylus 16, housed behind skid 24, pivots on fulcrum 20, and its motion is picked up by magnetic inductance-type detectors 22. Motor 52 feeds detector case 12 along feed screw 46 and sliding shaft 34. Signal processing accounts for gain calibration, stylus radius compensation, and other errors. (*Copyright information:* As a US patent figure, this image may be freely copied (USPTO, 2017), and this image does not appear to be subject to any other copyright.)

---

[6]Signal artifacts due to the apparatus are subtle, but more to the point, barely affect the decomposition of feed marks in this thesis. Signal artifacts generally produce aberrations in the frequency domain (Whitehouse, 2011), which average out over a statistical sample of feed marks, because the wavelengths of these aberrant frequencies are much shorter than the feed marks. In effect, the frequency domain measurement artifacts appear at "random" phases in individual space-domain feed marks, vanishing statistically for samples of many feed marks.

Non-contact methods are dominated by optical techniques, but other, more exotic methods exist, listed by Whitehouse: capacitive, eddy current, pneumatic, and other methods. Optical methods have the advantage of causing no damage to the surface and of producing areal scans quickly. Interferometry and confocal microscopy in particular offer rapid, non-contact measurement of surface roughness, but, for the moment, optical measurement of surface roughness in machine shops is uncommon.

Electron microscopy deserves mention because microstructure and surface discontinuities of machined parts (such as tears, laps, scratches, and readhered material) are often evaluated using scanning electron microscopy (SEM), and the technique is utilized in production by some manufacturers. SEM provides a topographical[7] assessment of a surface, but on a scale too small to obtain linear roughness profiles with multiple feed marks at the scale studied.

2.3 Microgeometry Specification

Description of surface roughness is at the heart of this thesis concerned with quantifying cutting mechanism contributions to arbitrary roughness parameters. It is paramount to discuss how microgeometry is specified in the literature.

At the top level, machined surfaces often exhibit lay (Petropoulos et al., 2010, page 39), which is the primary direction of any anisotropic pattern. Surface texture may then be divided into "orders" of deviation from the nominal part geometry (adapted from Deutches Institut Fuer Normung (national German standardization institute) (DIN 4760, 1982) and Petropoulos):

- Macrogeometric deviations: they are due to machine tool errors, deformation of the workpiece, erroneous setups and clamping, vibration and workpiece material inhomogeneities (Benardos and Vosniakos, 2003)(Klocke and Kuchle, 2011, page 11).

  - 1st order: Form errors (flatness, roundness, straightness, cylindricity, etc.).
  - 2nd order: Waviness. To obtain the waviness profile, a long-pass filter and a short-pass filter are applied to a raw surface profile waveform (ISO/TS 16610-29:2006, 2006).

- Microgeometric deviations: 3rd- and 4th-order deviations are often caused by the cutting process; 5th- and 6th-order deviations are due to physico-chemical processes on the crystal grain and lattice scales (Benardos and Vosniakos, 2003). Penetration of the tool into the workpiece may cause grooves; the higher orders are primarily random and are linked to the chip formation process (Klocke and Kuchle, 2011, page 11).

---

[7]SEM is not purely topographical, due to the different electronic affinities of microstructural phases.

- 3$^{\text{rd}}$ order: Grooves. This would include traces of chip formation and the helical feed mark on a turned part and other sorts of tool marks.
- 4$^{\text{th}}$ order: Cracks, for example as a result of thermal contraction after cutting.
- 5$^{\text{th}}$ order: Polycrystalline structure, including crystallization mode, corrosion, and other chemical alterations of the order of crystal grains.
- 6$^{\text{th}}$ order: Lattice-level crystalline structure.

Surface finish is the superposition of the orders of deviations. This thesis is primarily concerned with feed marks, which are 3$^{\text{rd}}$-order deviations (grooves), and the higher-order deviations within (up to 5$^{\text{th}}$ order).

For profile analysis, it is often desirable to separate 1$^{\text{st}}$- and 2$^{\text{nd}}$-order deviations from the other orders (see Fig. 2.2). The ISO standards for surface roughness treat those low orders as "waviness", and treat the high orders, together, as "roughness"[8] (ISO 4287:1997, 1997). The following is written with respect to the ISO standards.

Separation of waviness and roughness is done very simply by filtering of spatial frequencies. The raw, as-measured profile is treated to remove form (by simple subtraction), and a low-pass frequency filter is applied to remove whatever high frequencies do not represent the surface due to the measurement process. ISO filters are Gaussian[9], and this initial filtering is done from wavelength λ_s. Correction may also be performed for stylus radius[10] and other experimentally-induced aberrations. The result is the "primary profile", which is appropriate for analyses where additional filtering would destroy relevant information (such as evaluation of cracks, for example using the deepest valley in the profile as a parameter, or estimation of microgeometrical stress concentration for fatigue). The primary profile may then be filtered again at cutoff wavelength λ_c to separate the long wavelengths from the short ones: the longer ones are the "waviness", and the shorter ones the "roughness".[11]

Frequency filtering is typically followed by evaluation of roughness parameters. Roughness profiles are treated in a variety of ways, including many arithmetic and statistical (ISO 4287:1997, 1997), motif (ISO 12085:1996, 1996), areal (ISO 25178-2:2012, 2012), and fractal (Petropoulos et al., 2010) parameters, wavelet analysis (ISO/TS 16610-29:2006, 2006),

---

[8]The ASME standards make the waviness-roughness distinction, too (ASME B46.1 - 2009, 2009). ISO and ASME standards are commonly used in North America for evaluation of surface finish.

[9]Gaussian frequency filters are symmetrical filters chosen to limit windowing artifacts. In particular, they are "non-oscillatory" and prevent Fourier ringing. (Allen and Mills, 2004, page 652)

[10]Because the surface of the part is not flat and the stylus probe tip has a nonzero size, the angle of incidence between the stylus tip and the surface causes an error.

[11]Other methods of separating roughness and non-roughness exist. Wavelet transforms and the motif method (discussed below) are alternative means of creating a reference line to be subtracted from the measured profile. Other authors have proposed methods for specific circumstances: X. Rimpault *et al.* in our own research group have proposed a method for the difficulties the plies in laminated composites cause to roughness profiles (Rimpault et al., 2016).
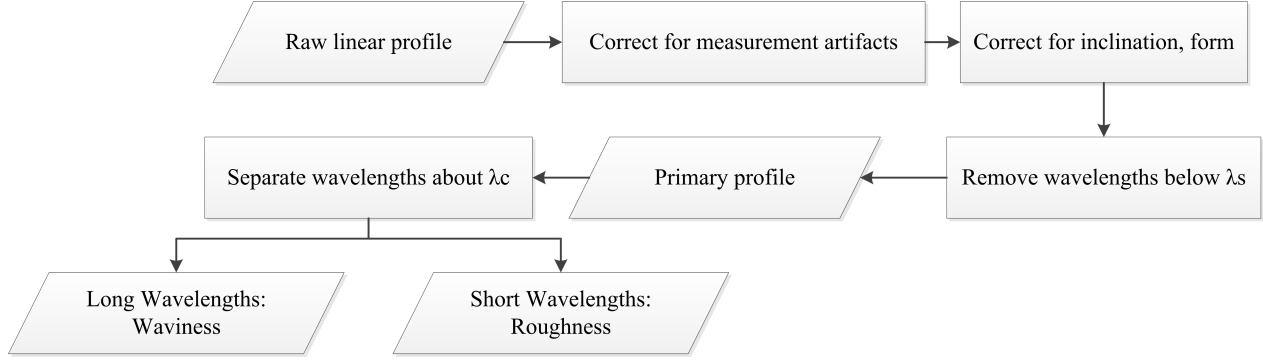
Figure 2.2: Simplified process for generating the primary, waviness, and roughness profiles

Fourier transformation, and autocorrelation (Petropoulos et al., 2010), among others. They are not related to the means by which the surfaces were manufactured. Table 2.1 lists some common arithmetic and statistical parameters.[12]

Table 2.1: Some arithmetic and statistical parameters of roughness profiles

R_a	The arithmetical mean absolute deviation from the profile mean line. The most common roughness parameter for machined parts.
R_q	Serving the same function as R_a, R_q sums quadratic deviations and is more sensitive to extremes.
R_{sk}	Skewness. Represents how positive (or negative) the profile deviations are about the mean line. Sometimes significant to oil retention.
R_{ku}	Kurtosis. Represents how concentrated the profile deviations are around the mean line. Relevant to friction.
R_v	The absolute value of the maximum profile valley depth. Relevant to fatigue.
R_z	Maximum profile height as of ISO 4287:1997. This is a source of confusion, as the older definition (10-point mean) is well-established and widely used.
R_{zJIS}	The ten-point mean, commonly referred to as R_z (JIS B 0601-2001, 2001). Relevant to fatigue and tribology.
R_{Sm}	Mean width of the profile elements. Used for feed mark spacing, for example.
R_{dq}	Root mean square slope. Relevant in some optical applications.

Linear profiles can also express material distribution. The cumulative distribution (integral) in the z-direction (perpendicular to the nominal surface) of the linear profile is called the bearing area curve and has its own, if less commonly used, scalar descriptive parameters. The bearing area curve is of particular importance for cases where oil retention for surfaces in contact is of interest.

Motif parameters are an alternative to frequency filtering[13] (ISO 12085:1996, 1996). D.J.

---

[12]These roughness parameters have areal equivalents for 3D topographies, for which an S is substituted for the R (ISO 25178-2:2012, 2012). Primary and waviness profiles may be treated similarly, in which case a P or W is substituted for the R, respectively.

[13]Motif parameters can also be used in combination with frequency filtering.

Whitehouse (Whitehouse, 2011, page 41) describes the appeal of motifs as being adaptive ("intrinsic") to surfaces rather than prescriptive as frequency cutoffs are. Used mainly by the French automotive industry, the motif method deconstructs profiles into "motifs", which are patterns identified using a set of rules; it is a form of pattern recognition. It may also (Dietzsch et al., 1998) be described as a good method for surfaces with unknown nominal microgeometry, for inquiries into the envelopes of surfaces, and for surfaces with waviness and roughness that are difficult to separate by frequency filtering due to similar wavelengths. For applications where envelope is more meaningful than mean line, motifs may be a better choice than frequency filtering.[14]

Like motifs, fractal or "chaotic" parameters are "intrinsic" to surfaces. According to Whitehouse (Whitehouse, 2011, page 94), the interest in treating roughness with fractal analysis is to produce scalar roughness parametrizations with reduced dependence on metrological measurement method. Fractal dimension (a measure of structure complexity) and topothesy (a measure of structure scale) are usually cited (Petropoulos et al., 2010; Whitehouse, 2011) as fractal parameters for roughness, each with multiple methods of mathematical evaluation from a profile. The reason for the existence of multiple methods is the nature of experimental roughness profile measurements as discrete, digital signals, which enable only approximations of fractal parameters. Though interesting, fractal roughness parameters are as far as we know unrelated to the mechanisms of surface generation, and are also, by themselves, incomplete descriptions of surfaces, lacking absolute indications of amplitude and lateral spacing. Furthermore, Whitehouse believes, on the basis of fracture mechanics, that chaotic treatment of roughness is unjustified for processes involving plastic flow.

Complementary to the above methods, Fourier transformation and autocorrelation show the degree of periodicity of a roughness profile (Petropoulos et al., 2010). The power spectrum plots the profile in the frequency domain, with periodic components differentiating themselves as peaks from nonperiodic components. The autocorrelation function is an alternative representation of the degree of periodicity in a profile.

Assessments of periodicity also lack information on profile non-stationarity. Grzesik and Brol described the continuous wavelet transform (CWT) as an alternative to Fourier transformation by transforming the profile not to a basis of sinusoids, but to a basis of wavelets, and can detect disturbances and non-stationary behavior in profiles of turned parts (Grzesik and Brol, 2009). Wavelet analysis of roughness profiles is also an alternative method of de-

---

[14] A comment complementing footnote 1: the motif and fractal analysis methods are examples of profile parametrizations that are more "intrinsic" to surfaces than others, avoiding some of the difficulties with sampling. The problem reduces to subtracting nominal part geometry or microgeometry from the measured profile; stated as such, motif and fractal methods are subject to the problem too (though resistant), not immune to it as some authors (Whitehouse, 2011, page 41)(Petropoulos et al., 2010, page 48)(Sahoo et al., 2011, page 4) suggest.

termining the profile reference line (non-roughness additive component of the profile) (Chen et al., 1999).

In addition, it is worth mentioning that scalar roughness parameters reduce roughness profiles to a finite set of scalars, simplifying description but necessarily destroying information; although not considered a roughness parameter, a plot of the surface roughness profile *itself* may be a useful addition to any roughness report, and may reveal problems with machine tool axis motion, workpiece bending, failure to engage the tool, tool failure, or any other unexpected eventuality.

It may be concluded that literature on parameters quantifying cutting dynamics from linear roughness profiles is very limited. It has of course been mentioned that introducing "custom" parameters should be done cautiously to avoid superfluous or erroneous methods (Tabenkin, 2001). Naturally, many alternative roughness parameters have been proposed for various purposes. Grzesik and Brol suggested roughness parameters relating to the vertical and lateral displacement and elongation of feed marks of imposed nominal shape, especially in relation to plastic flow (see Section 2.4). The work of this thesis is designed in part to avoid creating spurious new roughness parameters that will be difficult to apply in practice in the communication between manufacturer design and production teams.

2.4   Decomposition of Feed Marks

In this work, we consider surface roughness of hard finish turned parts. Specifically, we exploit the fact that a single linear roughness profile that crosses the helical tool trace multiple times contains "snapshots" in time of the state of the cut. That statistical sample can be leveraged to quantify process dynamics. "Dynamics" here is intended in a broad sense, including not only vibration but also plastic side flow, ploughing, and all other mechanisms that exhibit a dynamic stability, rather than static contribution to post-machining part microgeometry. Dynamometers and accelerometers measuring during the cut are widely used by researchers, but analysis of feed mark morphology is very sharply limited, and is the concern of this thesis.

A matter of scope, it is important to note that the topic here is decomposition of feed marks, which should be distinguished from the modeling of machining. Decomposition estimates the influence of machining effects from a roughness profile, whereas modeling of turning, much more common, starts from machining effects to simulate surface generation. Benardos and Vosniakos authored an important review paper on predicting roughness (Benardos and Vosniakos, 2003).

Work closely related to this thesis includes that of F. Ancio *et al.*, who have been able to reconstruct part microgeometry from online readings of cutting tool acceleration, beginning

with a paper in 2012 (Ancio et al., 2012) and developed further in 2014 (Ancio et al., 2015). In 2013, Ancio *et al.* introduced the use of principal component analysis on roughness profiles of machined parts (Ancio et al., 2013), demonstrating that a superposition of a few patterns suffices to describe most of the roughness of the surfaces studied. In 2016, Ancio *et al.* suggesting a methodology for principal component analysis on turned parts (Ancio et al., 2016). Significantly, they suggested that cutting traces contain information about the physical processes generating machined surfaces, which includes vibrations and material responses. They did not publish in detail on feed mark morphology.

W. Grzesik has also published on the relationship of cutting effects and intra-feed mark surface roughness morphology. In 2011, W. Grzesik and S. Brol published a simple method for describing feed marks (Grzesik and Brol, 2011), consisting of fitting parabolas to linear profiles. That method is sometimes justified for round-nosed cutting tools, but is somewhat limited in finish hard turning where plastic effects may dominate even the scallop-shaped ideal tool nose trace. Grzesik and Brol used that method to measure the vertical and lateral displacements of feed marks and feed mark elongations, expressing belief that those deformations relate to plastic side flow, spring-back, cutting edge preparation, cutting edge wear, and other considerations. Importantly, Grzesik and Brol acknowledge that roughness profiles contain information about the surface-generating physical mechanisms. Crucially, Grzesik and Brol also expressed the belief that the relative depths of feed marks are due to material response. While true, in the current thesis it is demonstrated that the radial component of tool vibration is a direct, clear, and sufficient explanation for variation in feed mark depth across a roughness profile.

In J.P. Davim's *Metal Cutting: Research Advances*, W. Grzesik and S. Brol published a chapter (Grzesik and Brol, 2010) about generation and modeling of surface roughness. The paper describes surface roughness generation as a dynamic process of material removal and elastic-plastic deformation, with the analytical nominal shape of feed marks based on tool geometry and minimal undeformed chip thickness. The chapter also discusses plastic flow and numerical treatment of other effects such as cutting edge preparation. The chapter also introduces plastic flow, shown in Fig. 2.3 and other elements[15].

Importantly, no literature at all was found detailing how a computer can find the feed marks in a linear roughness profile without assuming some manually input feed mark shape. More subtle and just as important, expecting a particular feed mark shape does not indicate where, laterally, feed marks begin and end, due to deformations (particularly plastic) not accounted for by nominal feed mark shape.

---

[15]The other elements discussed are a numerical treatment of the influence of cutting edge preparation and a treatment of feed mark decomposition as in the previously discussed paper by Grzesik and Brol (Grzesik and Brol, 2011). Also shown is a visualization of feed mark disturbances by continuous wavelet transform.
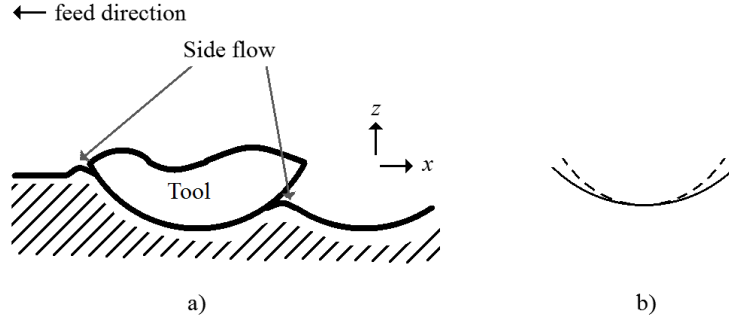
Figure 2.3: Plastic flow in turning and a model of its effect on roughness profiles. The images are redrawn from Grzesik and Brol (Grzesik and Brol, 2010). **a)** Side flow. **b)** Distortion of the surface profile (dashed line).

2.5 Cutting Dynamics

Typically, authors will dub only the effects of vibrations and forces "cutting dynamics". In this thesis, the term should suggest all processes that are inconstant in time that affect the interface between tool and workpiece. This thesis considers vibrations (radial and axial), and plastic flow (side flow and ploughing).

Vibrations affect tool wear and tool failure, surface finish, residual stresses, microstructure, chip formation, and machine spindle wear. It is therefore of interest to quantify the influence of vibrations during cutting; doing so directly from a linear roughness profile rather than an accelerometer or dynamometer would be convenient. Fig. 2.4 illustrates the machine tool-tool-workpiece system as a pair of oscillators. When considering the cross-sectional traces of the tool, as in a roughness profile, the number of degrees of freedom of the system may be reduced to two; the relative vibrational motion of the tool with respect to the workpiece is then two-dimensional, as suggested in Grzesik and Brol's 2011 paper on feed mark decomposition (Grzesik and Brol, 2011), where they considered both the lateral and vertical displacements of feed marks.

Machining vibrations may be either free, forced, or self-excited (Cheng, 2008, page 10). The cause of self-excited vibrations is internal to the process (for example, interrupted chips, or stick-slip), and self-excited vibrations usually result in chatter. A cut with chatter is not considered a stable process, and so for the current thesis, self-excited vibrations are neglected. Free vibrations in turning may be caused by material inhomogeneity, by external agitation of the machine tool base, or other one-time excitations, and dissipate. Forced vibrations are different in that their energy source persists in time. As examples, an unstable spindle, uneven workpiece surface geometry, interrupted cutting (in the case of milling), or other time-dependent forces. For this thesis, the important remark is that in two-dimensional
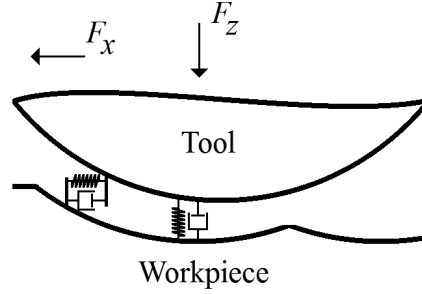
Figure 2.4: A model of the vibrational dynamics of the machine tool-tool-workpiece system. Note that vibration into the page is not depicted but of course exists. The components have effective masses and are subject to the elastic and damping responses. The damped-elastic model corresponds to the elastic-plastic behavior of the workpiece, and the gap shown between tool and workpiece is imaginary. The diagram is inspired by a figure in *Machine Tool Vibrations and Cutting Dynamics* by B.C. Gegg *et al.* (Gegg et al., 2011, page 103).

roughness profiles, vibrations should influence feed mark depth and lateral displacement. The quantitative import of vibration on surface microgeometry could therefore be estimated from the morphologies of the feed marks in a linear roughness profile.

As noted in Section 2.4, decomposition of feed marks should be distinguished from modeling the influence of dynamics on surface roughness. Although it is not directly involved in the work in this thesis, modeling of roughness from dynamics is common and should be mentioned. Benardos and Vosniakos (Benardos and Vosniakos, 2003), in their review paper on prediction of surface roughness, note some classes of approach: analytical machining theory, experimental investigations, designed experiments, and artificial intelligence. They note Ehmann and Hong's (Ehmann and Hong, 1994) 1994 paper modeling tool runout, machine deformation, and higher-order kinematics to the estimation of surface finish. In 1998, Lin and Chang's (Lin and Chang, 1998) kinematic simulation demonstrated the radial component of vibration as much more significant to the resulting roughness profile than the other components. Other works have built on simulation of microgeometrical surface generation for vibration, developing models involving simulation of the milling cutter, workpiece, machine spindle, and so on. In particular, and important to this thesis, superposition of microgeometry from multiple simultaneous mechanisms appears to be valid (at least sometimes) (Kim and Chu, 1999). Note also that extensive modeling of workpiece, tool, machine, and so on may be warranted in some industrial cases, but that realistic modeling is time-consuming and expensive.

For the influence of vibrations on feed marks, F. Ancio *et al.*'s 2014 paper (Ancio et al., 2015) deserves special mention, and is discussed in Section 2.4.

Plastic flow[16] is also recognized as influencing surface roughness, and includes ploughing (Fig. 2.5) and side flow (Fig. 2.3). Ploughing may or may not involve a built-up edge. The effects of ploughing on surface roughness are poorly understood (and has been commented on as such (Zhang and Liang, 2005)), with no literature expliciting an analytical model or simulation for surface roughness from ploughing, though the importance of ploughing (particularly with a built-up edge) to roughness is recognized. The effects of side flow on surface roughness are better understood. W. Grzesik, in J.P. Davim's *Machining of Hard Materials* (Grzesik, 2011, page 108), explains side flow as a phenomenon characteristic of hard turning. It consists of hard, ductile material undergoing plastic flow, possibly due to it squeezing between the workpiece and flank face or worn trailing edge of the tool. Grzesik has published on decomposition of feed marks to estimate side flow (see Section 2.4). Fig. 2.6 illustrates sidewall formation in milling, which is closely related to side flow as shown in Fig. 2.3. The equivalent phenomenon in turning is illustrated in Article Two, in Fig. 4.7.
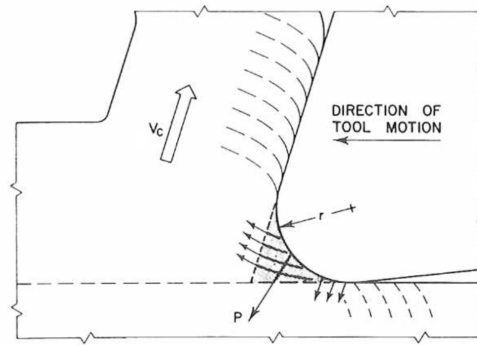
Figure 2.5: Illustration of ploughing, with material flow indicated by the arrows. The diagram is from P. Albrecht (Albrecht, 1960) (*Copyright information:* Image is Copyright © 1960 by the American Society of Mechanical Engineers (ASME). Image used with permission).

Plastic flow is permanent deformation; elastic recovery of the workpiece after machining is the spring back effect. Grzesik has recognized spring back as significant to surface roughness (Grzesik and Brol, 2011), as have Schaal *et al.* (Schulze et al., 2015), but neither have published on obtaining spring back estimates from linear roughness profiles. Not much has been published on the contribution of elastic recovery to surface roughness. In 2006, M.C. Kong *et al.* described elastic-plastic recovery as being heavily dependent on crystal structure (in the case of single-point diamond turning) (Kong et al., 2006). In 2013, S.J. Wang *et al.* (Wang et al., 2013) proposed a roughness parameter simply comparing measured profile to

---

[16]"Plastic flow" also sometimes refers to swelling (Kong et al., 2006), which implies either elastic-plastic response or elastic response of the workpiece.
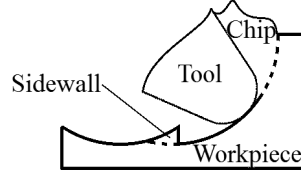
Figure 2.6: The phenomenon of sidewall surface generation in milling. The illustration is redrawn from Zhanqiang *et al.* (Zhanqiang et al., 2013). Part of each feed mark is subject to an improper cut due to failure of the tool to engage, because the cut is locally below the minimal chip thickness. The same principle applies to turning, which may result in "local ploughing" (see Fig. 4.7) and side flow when hard turning.
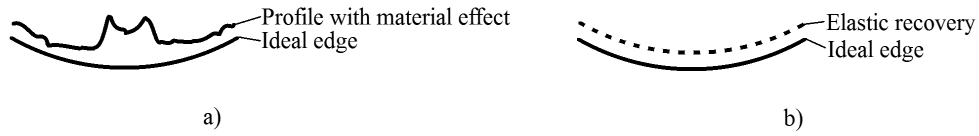
Figure 2.7: Description and modeling of elastic-plastic material influence on surface roughness. **a)** Redrawn version of Wang *et al.*'s comparison of real profiles and ideal profiles for roughness description (Wang et al., 2013). **b)** Redrawn version of Zong *et al.*'s simple model of spring back for roughness prediction (Zong et al., 2014).

ideal profile in the case of milling (see Fig. 2.7). In 2014, W.J. Zong *et al.* (Zong et al., 2014) published their analytical model, shown in Fig. 2.7. They model elastic recovery as a swell of constant amplitude across the entire feed mark, proportional to the tool nose radius, workpiece material hardness, and inversely proportional to the workpiece's elastic modulus. Perhaps real elastic recovery should be uneven across the feed mark due to uneven work hardening from the previous feed mark's pass and uneven pressures from the situation's geometry, even more so with thermal effects considered. In 2015, C.L. He *et al.*, in collaboration with Zong, published a model predicting surface roughness involving side flow and spring back in addition to the system's kinematics, but published roughness predictions from kinematics only (He et al., 2016).

CHAPTER 3

ARTICLE 1: AUTOMATIC IDENTIFICATION OF FEED MARKS IN MACHINED SURFACE ROUGHNESS PROFILES BY CORRELATING RANDOM VARIATIONS

ABSTRACT

A new method is detailed to identify the positions of the ends of the tool marks in linear surface roughness profiles. No feed mark shape must be assumed and the process is entirely automated. The approach may find applications in automated quality control, surface texture classification, and modeling of metal cutting processes. Validation was done with forty finish hard turning specimens. The method relies on the justified hypotheses that a feed mark profile is a superposition of a fixed and a random component, and that the random component has a spatial period equal to one feed mark length. A brief typology of tool mark particularities revealed by the method is presented as well as observations on the correlation of the random events within marks and between marks, both at short and at long range. Feed marks difficult to identify by visual inspection were easily identified with the method and evidence of overlapping tool marks and unstable regions was discovered. The limits of the method are also explored.

3.1 Introduction

The surface integrity of a machined part is significantly influenced by its surface roughness. It is common in industrial application for the roughness of a machined part to serve as an indication of the condition of the machining operation (Petropoulos et al., 2010), and, less commonly, as an index of part performance, for example tribologically (Brown, 2012) or for fatigue life (Zahavi et al., 1996). The microgeometry of a part's surface is commonly described and manipulated in many ways, including a host of arithmetic and statistical

(ISO 4287:1997, 1997), motif (ISO 12085:1996, 1996), areal (ISO 25178-2:2012, 2012), and chaotic (Petropoulos et al., 2010) parametrizations, wavelet analysis (ISO/TS 16610-29:2006, 2006), and Fourier transformation and autocorrelation (Petropoulos et al., 2010), to name but some. A linear roughness profile from this microgeometry will in many cases include a regular pattern left by the cutting tool. Identification of tool mark *patterns* has been done before, for example by filtering the texture's Fourier transform (Carroll et al., 1989).

There are three categories of application for the identification of *individual* tool marks. First, theorists interested in modeling surface generation from machining may benefit from statistically validated identification of tool marks, and visual identification may be difficult in some cases. Grzesik and Brol decomposed feed marks to study the mechanisms of their generation (Grzesik and Brol, 2011). Secondly, the identification of tool marks may be useful in quality control; Carroll *et al.* explain that there is value in automatically distinguishing defects from the rest of a machined surface (Carroll et al., 1989). The third category is surface texture classification. It may be worthwhile to devise surface finish parameters specific to the morphologies of tool marks rather than to holistic, undivided tool mark patterns, so as better to describe the underlying physical mechanisms of their generation. In the same vein, it may be desirable to devise parameters related to the relationships between tool marks, for instance in the study of vibrations during machining. Ultimately, Petropoulos *et al.* suggest that surface typology may be a worthwhile although ambitious goal (Petropoulos et al., 2010); the development of such a taxonomy may be aided by the ability to divide a roughness profile into segments of physically asynchronous origins. The ability to identify individual feed marks automatically may therefore provide added value to manufacturing operations as a technique for the characterisation of surface texture.

Somewhat surprisingly, to the best of the authors' knowledge, there is very little literature on the identification of individual marks. Grzesik and Brol identified marks by fitting parabolas to profiles (Grzesik and Brol, 2011). However, fitting in such a manner requires the selection of an assumed tool mark shape, which limits the ability to automate the analysis. Doing so also relies on the analyst's intuition to impose where marks begin and end (by virtue of assuming some shape). Indeed, this paper's results show that visual identification of marks and statistical evidence do not quite match, and furthermore that some tool marks have ends that are difficult to identify visually.

In contrast, the present authors have devised a new method of analyzing 2D surface roughness profiles to reveal individual machining feed marks without assuming a particular feed mark shape, and the ends of the marks are discovered, not imposed. The method is based on compelling experimental statistical evidence of the separate physical origin of each mark. This evidence can be extracted from a profile in a completely automated fashion, with

no user input whatsoever other than the profile itself. The method is to divide a roughness profile into statistically distinct portions, which the authors refer to as "correlated domain identification" (CDI) as a convenient handle. The method and underlying hypotheses were successfully validated with all 200 roughness profiles evaluated from 40 finish hard turning specimens from 11 cutting conditions. A drilled laminated composite was also analysed to demonstrate the limits of CDI in the case of an extremely irregular profile.

This paper describes the CDI method in detail and discusses tool mark particularities revealed using CDI concerning correlation of random events with feed marks. Random events bridging multiple feed marks were also indirectly observed. Other results include identification of visually non-obvious marks, measurement variability, regions influenced by multiple tool passes, unstable regions, and the effects of profile length.

3.2   Theory

It is important first to specify the meaning intended here by the interchangeably employed terms "feed mark" and "tool mark". The authors's meaning is "a trace left by the passage of a cutting edge". For a cutting operation with a continuous cut and a single cutting edge, with a profile taken parallel to the machining feed, the feed is equal to the period of the tool marks. However, when machining with multiple cutting edges, such as when drilling, or when machining with repeated disengagement, such as when milling, multiple tool marks may occur per feed length, and the apparent spatial period of the cutting edge passes in the measured profile is called the "effective feed" f, hereafter referred to simply as the "feed".

The CDI method is summarised in Fig. 3.1 and the first step is the division of the roughness profile into a set of segments, each with a length equal to $2f$, shown as step a) in Fig. 3.1. This step requires knowing the feed f. If the feed is not known, it may be estimated from the autocorrelation function of the profile, or from its frequency power spectrum. The CDI method should also work with a non-constant feed, provided the instantaneous feed is known at all locations in the profile..

The CDI method relies on two principal hypotheses:

H1. Because the cutting tool has a defined shape, the feed marks share a common shape. The common shape is summed with random deviations from that shape.

H2. Because the totality of an individual tool mark is generated with one passage of the cutting tool, the deviations within one tool mark are correlated with each other. Conversely, because the generation of each tool mark is a physically distinct event, the deviations in one tool mark are not correlated with the deviations of any other tool mark.

a) Divide the profile into lengths of (2 × effective machining feed f)

Roughness profile

Set of profile segments

b) Take point-by-point arithmetic mean of the profile segments

Mean segment

c) Subtract mean segment from each profile segment

Set of segment deviations from the mean segment (exaggerated)

d) Perform point-by-point correlation across the deviation segments

Segment deviation correlation map

p-values of the segment deviation correlation map

e) Use these matrices to evaluate each phase with which the segments may be divided into feed marks

Qualifier function

f) Fit theoretical curve to qualifier function

Identified feed mark phase

Feed marks

Figure 3.1: A summary of the CDI method. The x-direction is defined at the top, in the depiction of a roughness profile.

The model of hypothesis H1, that there is a common shape summed with random deviations, is called a linear mixed model[1]. To implement it, the profile is discretized into points, with deviations measured normally to the machined surface (z-direction), because that is how roughness profiles are encoded using the stylus method. With this implementation, the set of segments is arithmetically averaged, creating a mean segment of length $2f$, which is step b) in Fig. 3.1. The mean segment therefore includes an estimate of the common shape (which has a length equal to f), somewhere within its length. The position of the common shape within the mean segment may be called its phase φ_m ("m" for "mark"), as in Fig. 3.2.
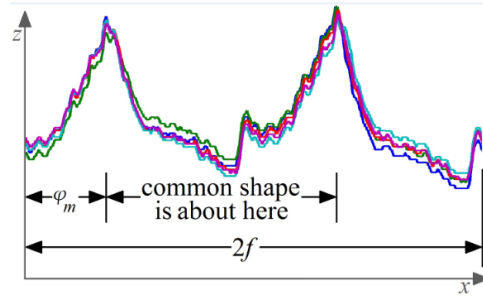
Figure 3.2: Explanatory illustration of a profile dissected into segments of length $2f$ and superimposed. For clarity, only a few segments are shown. At this stage in the analysis (step a) in Fig. 3.1), the shape and location of the common shape are unknown, but for the sake of explanation, the "common shape" of hypothesis H1 is located approximately as shown. That location, expressed as φ_m, is determined in step f).

As in Fig. 3.1, the following step, step c), is arithmetically to subtract the mean segment from each segment, yielding the set of deviations from the mean segment. The amplitude of the deviations is exaggerated in the result of step c) in Fig. 3.1. Thereafter, Step d) is to estimate the correlation coefficient of the z-values of the deviations at x-coordinate x_i with respect to the z-values of the deviations at all other x-coordinates x_j, and to repeat for all i:

$$\operatorname{corr}(i,j) \equiv \frac{\operatorname{cov}(i,j)}{\sqrt{\operatorname{cov}(i,i)\operatorname{cov}(j,j)}} \tag{3.1}$$

where cov is the covariance:

$$\operatorname{cov}(i,j) \equiv E\left((z_i - \mu_i)(z_j - \mu_j)\right) \tag{3.2}$$

and μ_i represents the mean of the z-values at x_i. E is the expectation value of its argument. Note that the covariance of a variable with itself is identically its variance.

---

[1]A model is said to be "mixed" when it includes both a fixed and a random component.

The pairwise correlations compose the segment deviation correlation map as shown in Fig. 3.3 a) and Fig. 3.1. The reason that the correlation map is used rather than the covariance map is that in the rest of the analysis, the variances of different x-positions must be compared; the variance varies across tool marks[2], so the covariance coefficient is normalised to become the correlation coefficient, with the result that neither variance dominates the other in any combination of i and j. Fig. 3.3 b) and Fig. 3.1 also show a matrix of the p-values associated with the correlation matrix. A small p-value indicates that the corresponding correlation coefficient is statistically significant.
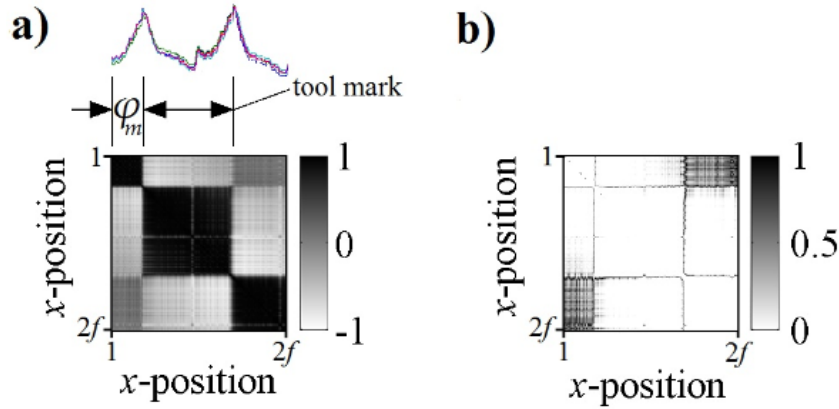
Figure 3.3: Graphs aiding the explanation of step d) of Fig. 3.1. Note that these two maps have different color scales, and that each map is necessarily symmetrical. **a)** Correlation map of the segments of Fig. 3.2. Most significantly, notice that the "common shape" (indicated as the "tool mark") from Fig. 3.2 is aligned with a correlated domain in the correlation map (centermost dark square). **b)** The p-values of a).

Step e) of Fig. 3.1 evaluates the correlation matrix and its p-value matrix to generate what the authors dub the "qualifier function" $q(\varphi)$ that is used to determine the tool mark's phase φ_m. (φ is a variable from 1 to $2f$. The correct mark phase φ_m is $\in \varphi$.)

Hypothesis H2 supposes that the generation of each tool mark is a distinct event. Nonetheless, the deviations of a tool mark may be correlated with the deviations of an adjacent tool mark if some random physical phenomenon persists between the two. For example, a built-up edge might last long enough to travel around a turned part, influencing multiple feed marks in a correlated fashion. Naturally, that sort of random phenomenon ought not to "persist" through multiple feed marks if the turned part is diametrally "large". Periodic vibrations, however, might produce periodic long-range correlation.

If "persistent" phenomena are ignored, hypothesis H2 implies that the correlation matrix

---

[2]The fact that the variance is not constant across tool marks is expected because the physics of the cutting process are inhomogeneous across the engaged portion of the cutting tool.

should be block-diagonal, meaning that it contains correlated blocks along the diagonal, as in Fig. 3.3 a). H2 also implies that the width of the blocks should be f. The manner of evaluating $q(\varphi_m)$ is illustrated in Fig. 3.4 and is defined as the mean, weighted by $(1 - $ the p-values$)$, of the diagonal blocks for each possible phase $q(\varphi)$. The result is a $q(\varphi)$ function as in Fig. 3.5.
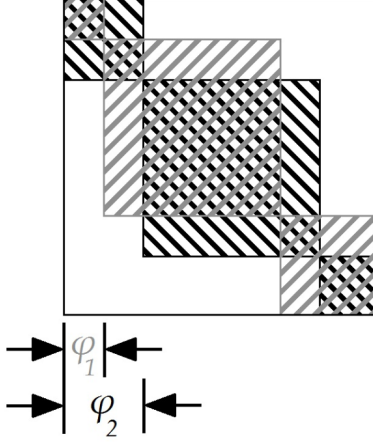
Figure 3.4: Illustration of the method of evaluating $q(\varphi_m)$. For each value of φ, q is the mean of the correlation matrix values (shown in Fig. 3.2) within the block diagonal region of that phase. Each element of each mean is weighted by $(1 - $ its p-value$)$. Here, two phases are shown, φ_1 and φ_2, but $q(\varphi)$ is evaluated for all possible phases φ, as in Fig. 3.5. Note that the computational weight of the whole analysis is made very light (less than a second on a typical desktop PC) by recycling each calculation for the following iteration, because only the edges of the region of interest change as it shifts from one iteration to the next across φ.

Fig. 3.5 also includes the theoretical curve of step f) of Fig. 3.1. It has the following form:

$$q(\varphi) = a_0 + \left[1 - 2\frac{\varphi - \varphi_m}{f} + 2\left(\frac{\varphi - \varphi_m}{f}\right)^2\right] a_1 \tag{3.3}$$

This equation is derived geometrically from the block-diagonal pattern of Fig. 3.4. If it is assumed that at $\varphi_m = \varphi$ the mean correlation in the hatched region is 1, then the equation is

$$q(\varphi) = \frac{[f - (\varphi - \varphi_m)]^2 + (\varphi - \varphi_m)^2}{f^2} \tag{3.4}$$

That assumption is equivalent to the assumption that the deviations of any given tool mark are perfectly correlated (corr $= 1$) with each other, and that they are perfectly uncorrelated (corr $= 0$) with the deviations of the other tool marks. This assumption can be softened by admitting the effects of noise in the correlations by including fitting parameters a_0 and a_1,
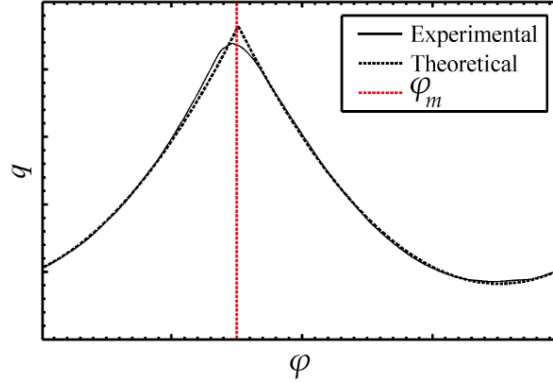
Figure 3.5: Visual aid for the explanation of steps e) and f) of Fig. 3.1. The experimental curve (determined as in Fig. 3.4) is overlaid with the theoretical curve of Eq. 3.3. Note that this curve, although it is coincidentally scallop-shaped, is completely unrelated to the common scallop shape of tool marks, and remains valid for any tool mark shape.

resulting in Eq. 3.3[3]. By regressing to minimise residuals, φ_m can be estimated. With this estimate of φ_m, which is manifestly the beginning of a tool mark[4], it is trivial to dissect the roughness profile into tool marks.

It is preferable to fit to the q function rather than simply find its maximum. By considering the entire q function, information from across the entire correlation map is preserved; i.e., the *degrees* of "correlatedness" of the various phases are more informative than merely the phase of maximum correlation, because lack of correlation is as significant as correlation in the search for the tool mark. It is also for this reason that segments of length $2f$ are employed rather than of length f, so that lack of correlation may be exploited.

Naturally, the accuracy of the estimate of φ_m depends on the length of the roughness profile analyzed. The more feed marks it contains, the better the estimate will tend to be.

3.3   Experiment

The CDI method was tested on cylindrical samples of AISI 4340 tempered to 48 HRC with $\varnothing 2$", turned on a Mazak QT-Nexus-200 lathe equipped with a DCLNL-12-4B tool holder from SECO. A new, unworn edge of a CNMG120408-FF1, grade TP1500 (multilayer Al2O3, Ti(C,N)) cutting insert manufactured by SECO was used for each cut. The cutting fluid was Cimstar 60 undyed metalworking fluid, which is largely water-based.

---

[3]If the "ideal" correlation matrix includes only ones and zeroes, then random noise will diminish the ones and augment the zeroes (the matrix will go from monochrome black and white to grey). The fitting parameters allow for this effect.

[4]Strictly, φ_m may be interpreted as the beginning of a tool mark if the definition of the tool marks in the manner of hypotheses H1 and H2 is admitted.

The roughness was evaluated by the skidless contact stylus method using a Mitutoyo Formtracer SVC4000 surface roughness measuring machine, using 1997 ISO procedures and a 2 µm radius stylus with a 60° tip angle. The sampling length was 0.8 mm. Five roughness measurements of 20 sampling lengths each (a non-standard number of sampling lengths) were made on each of the 40 specimens. All the profiles considered are R-profiles (ISO 4287:1997, 1997).

The cutting conditions are summarised in Table 3.1. They were chosen to provide a range of roughnesses and for a designed experiment not discussed in this paper.

Table 3.1: The cutting conditions and numbers of replicates of each experimental treatment

Ident.	Replicates	Feed		Cutting speed	
		(mm/rev)	[in./rev]	(m/min)	[sfm]
1	3	0.30	0.0118	250	820
2	3	0.30	0.0118	164	538
3	3	0.30	0.0118	78	256
4	3	0.25	0.0098	121	397
5	3	0.20	0.0079	250	820
6	10	0.20	0.0079	164	538
7	3	0.20	0.0079	78	256
8	3	0.15	0.0059	207	679
9	3	0.10	0.0039	250	820
10	3	0.10	0.0039	164	538
11	3	0.10	0.0039	78	256

3.4   Results

3.4.1   Identified marks

Fig. 3.6 illustrates the mean feed marks identified from 33 machining tests. In that figure and all others, the direction of machining is leftwise. The R_a of the roughness of the profiles varies from 3.1 to 0.4 µm. All the p-values considered in this paper are at 95% confidence.

3.4.2   Crisp results

Fig. 3.7 illustrates a profile with a particularly "crisp" correlation matrix, meaning the latter is strongly block-diagonal. The off-diagonal dark patches are not statistically significant, as evidenced by the p-values.

Compare Fig. 3.8, appearing noticeably less crisp, yet possessing a very crisp qualifier function.
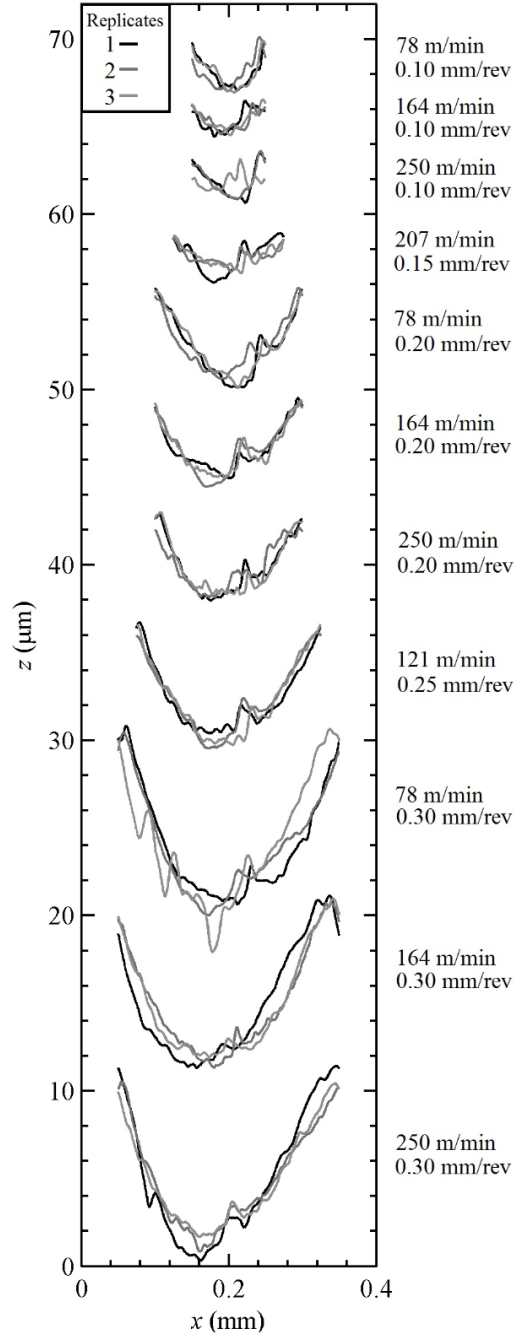
Figure 3.6: The mean feed marks identified from 33 of the 40 machining tests, each one taken from one profile. The 7 undisplayed tests are additional replicates of the 164 m/min, 0.2 mm/rev tests, and are similar to the three shown. For each condition, from the top, the numbers of segments of length $2f$ used to obtain each mark are 159, 159, 159, 106, 79, 79, 79, 63, 52, 52, and 52 (the numbers of feed marks are therefore double these numbers). There is no significance to the z-direction stacking of the marks on this graph.
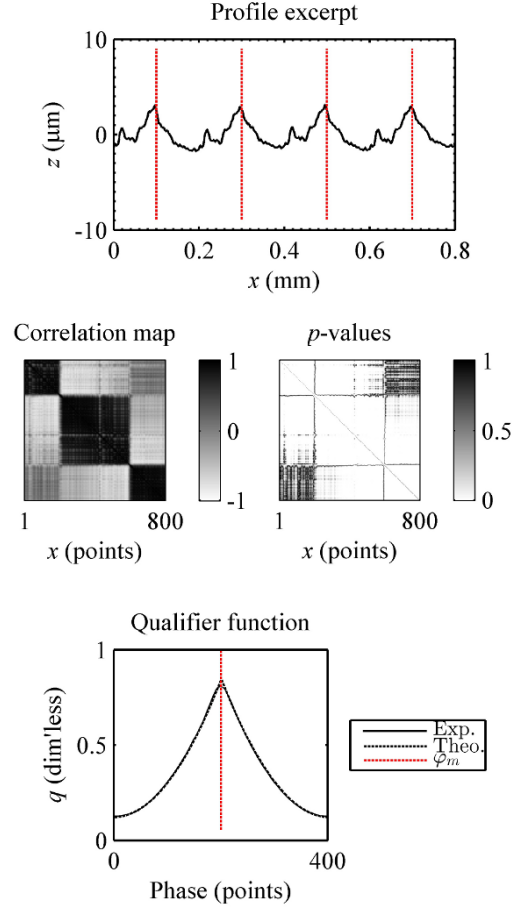
Figure 3.7: A profile with a particularly crisp correlation matrix, belonging to the 164 m/min, 0.2 mm/rev treatment.

3.4.3 Detection of visually non-obvious or misleading marks

Without CDI, some marks may be difficult to identify visually or by fitting curves such as a parabolas. Fig. 3.9 exemplifies this fact.

3.4.4 Correlation between adjacent marks

Sometimes, profiles exhibit considerable correlation between adjacent marks, as in Fig. 3.10. Nearly the entire correlation matrix is statistically significant, as demonstrated by its p-values. This example nonetheless retains a crisp qualifier function.
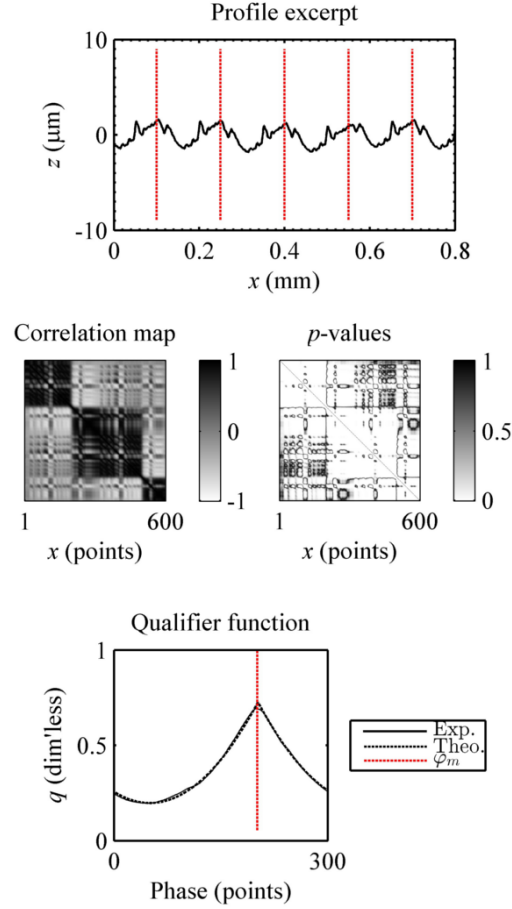
Figure 3.8: An uncrisp correlation matrix with a crisp qualifier function, from the 207 m/min, 0.15 mm/rev treatment

3.4.5 Long-range correlation

Some profiles exhibit periodic, long-range, inter-mark correlation, as shown in Fig. 3.11. The correlations are reasonably statistically significant, as evidenced by the p-values.

3.4.6 Correlation matrix blurriness

Some correlation maps may be "blurry", meaning the diagonal blocks have indistinct edges. Fig. 3.12 demonstrates this common phenomenon.

3.4.7 Variability of repeated profile measurements

Multiple profile measurements were performed on each experimental specimen. Fig. 3.13 and Fig. 3.14 demonstrate the common phenomenon of repeated measurements that produce
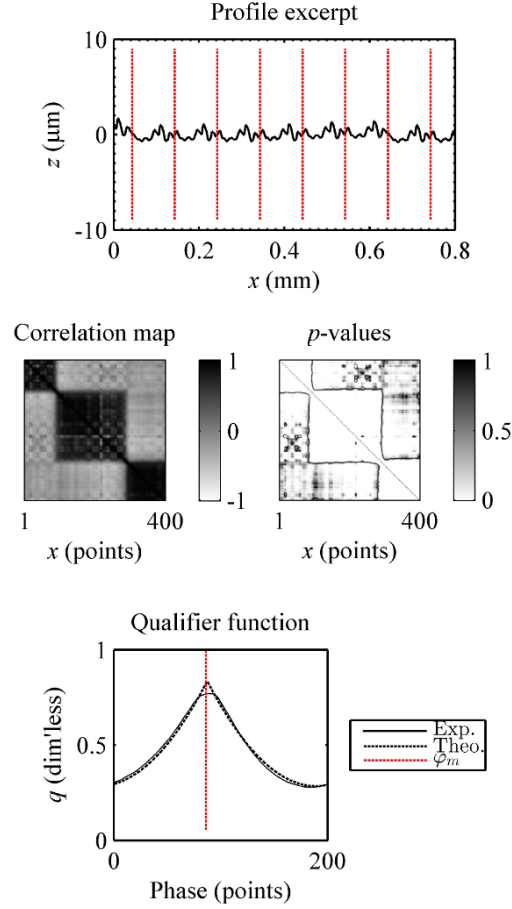
Figure 3.9: An example of a visually non-obvious feed mark, from the 250 m/min, 0.1 mm/rev treatment

dissimilar, statistically significant inter-mark degrees of correlation (varying amounts of off-diagonal darkness in the correlation matrix with corresponding white p-values).

3.4.8 Qualifier function error

Identification of φ_m inevitably includes error. The correlation matrix of Fig. 3.14 demonstrates a case where fitting Eq. 3.3 to the qualifier function produced an identified phase that is not quite in agreement with the intuitively visible diagonal blocks.

3.4.9 Limitations of the model

The model of Eq. 3.3 may in some cases produce a poor fit. Fig. 3.15 illustrates this phenomenon.
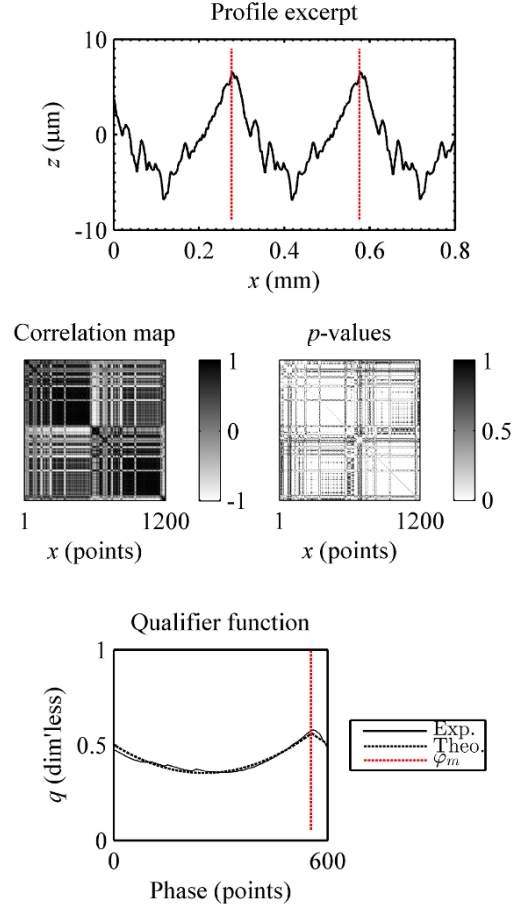
Figure 3.10:   An example of considerable correlation between adjacent feed marks, for 78 m/min and 0.3 mm/rev
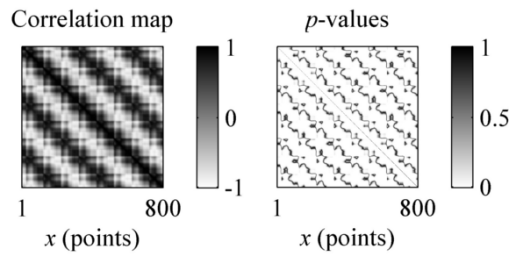
Figure 3.11:   An example of periodic, long-range, inter-mark correlation, from the 164 m/min, 0.2 mm/rev treatment. Here, the width of the correlation matrix is more than $2f$.

3.4.10   Negative correlation of adjacent marks

Often, adjacent marks demonstrate negative correlation, as in Fig. 3.13.
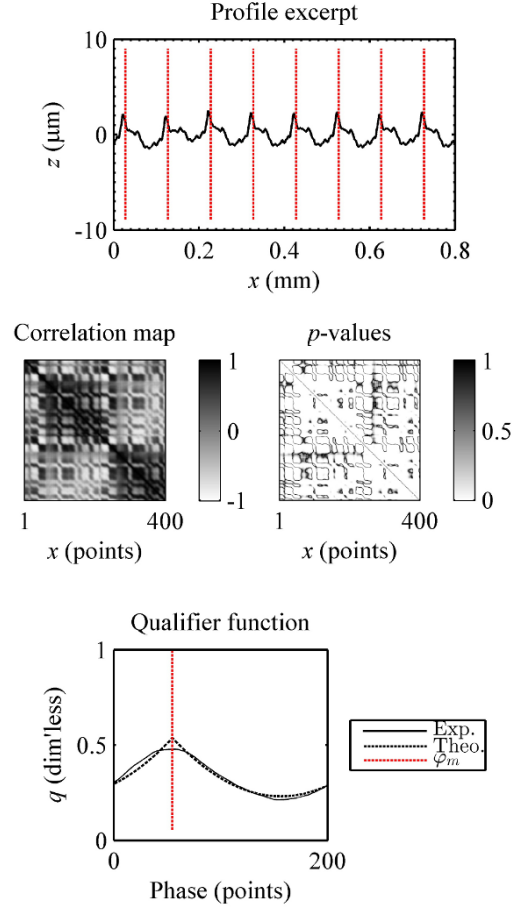
Figure 3.12: An example of a profile with a blurry correlation matrix from the 78 m/min, 0.1 mm/rev treatment

3.4.11 Some limits of CDI

Fig. 3.16 shows the effect that the length of a roughness profile has on the qualifier function. Also, CDI failed to extract meaningful information from exceptionally irregular roughness profiles taken from holes drilled in a laminated composite.

3.5 Discussion

The validation of the CDI method may begin with appeal to intuition. The identified marks shown in Fig. 3.6 agree well with the feed marks intuitively suggested by the scallop-shapes (for the profiles that have scallop-shapes). As such, CDI immediately appears reasonable.[5]

---

[5]The marks of Fig. 3.6 are of course not intended to be compared with each other. Rather, the quality of the division into segments of each individual profile is of interest.
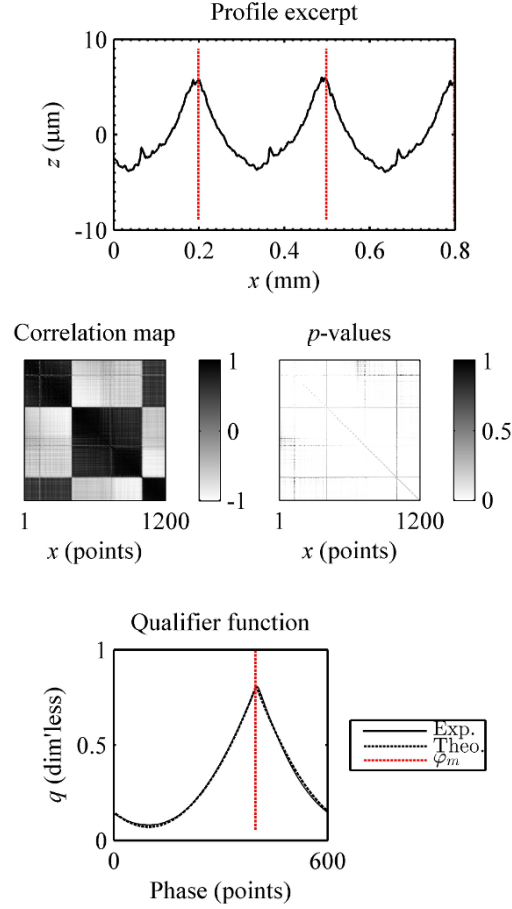
Figure 3.13: This figure and Fig. 3.14 are repeated measurements on one experimental specimen, from the 78 m/min, 0.3 mm/rev treatment. The correlation map here also demonstrates negative correlation between adjacent marks.

Crisp correlation matrices (as the example in Fig. 3.7) provide a stronger basis for validation. Hypothesis H1 is made compelling by the discovery of the block diagonal correlation pattern, because the block-diagonal pattern is revealed by subtracting the mean mark from the feed mark deviations. In the same figure, the apparent off-diagonal dark regions in the correlation matrix are statistically insignificant because of the large p-values of those regions. The excellent agreement of the theoretical q-curve with the experimental data in Fig. 3.8, even with such an uncrisp correlation matrix, strongly supports the model of Eq. 3.3. In addition, Fig. 3.13 in comparison with Fig. 3.14, both taken from the same experimental specimen, show that the model is reasonably robust versus the variability discovered from repeated measurement.

Hypothesis H2 is similarly confirmed by the block-diagonal structure of the correlation maps. The fact that the off-diagonal correlation is weaker than the block-diagonal correlation
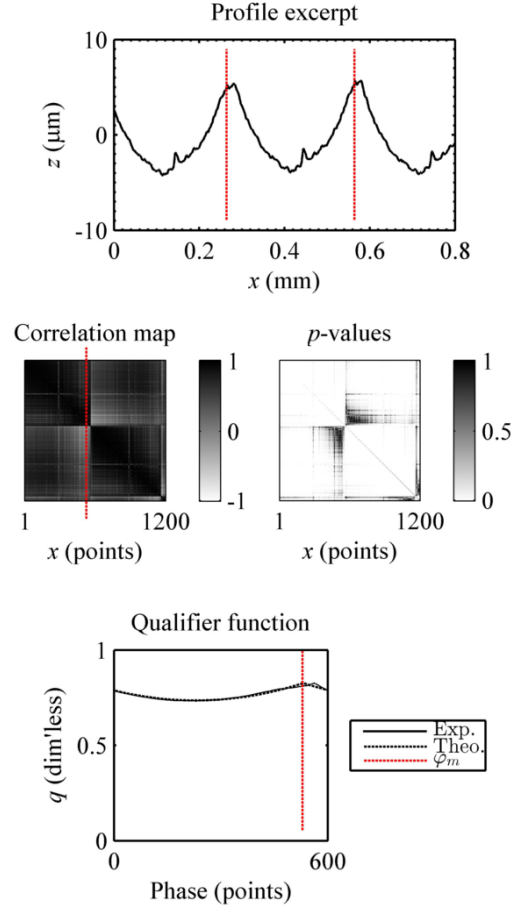
Figure 3.14: This figure and Fig. 3.13 are repeated measurements on one experimental specimen, from the 78 m/min, 0.3 mm/rev treatment. The dotted line indicates the identified phase φ_m.

also supports hypothesis H2, but situations like Fig. 3.10 make H2 less compelling. H2 could be amended to include exceptions for the "persistent" phenomena suggested previously, such as periodic vibrations.

The usefulness of CDI is made apparent by the successful identification of tool marks that are not scallop-shaped, as Fig. 3.9 (which is manifestly not scallop-shaped) and similarly oddly-shaped marks in Fig. 3.6. The odd shape of the tool marks evidently did not damage the excellent quality of the q-function fit. The results demonstrate strong statistical evidence of the physically distinct origins of the tool marks. The emergence of such evidence from a profile lends a physically meaningful basis for the identification of individual tool marks. It is furthermore suggested that mechanisms investigated by Grzesik and Brol such as plastic flow, friction, and elastic recovery (Grzesik and Brol, 2011) may obfuscate the ends of tool marks in visual inspection, but not affect CDI.
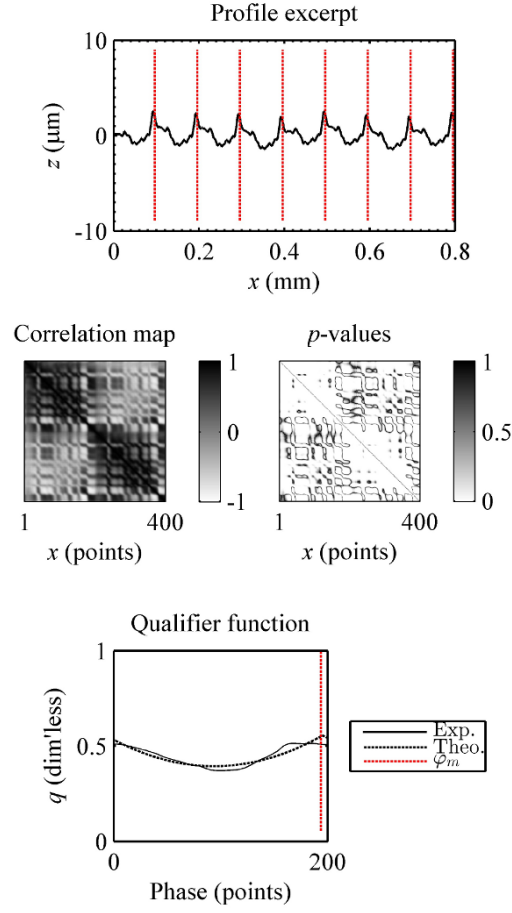
Figure 3.15: An example of a profile where the model of Eq. 3.3 fits the q-function poorly, from the 78 m/min, 0.1 mm/rev treatment.
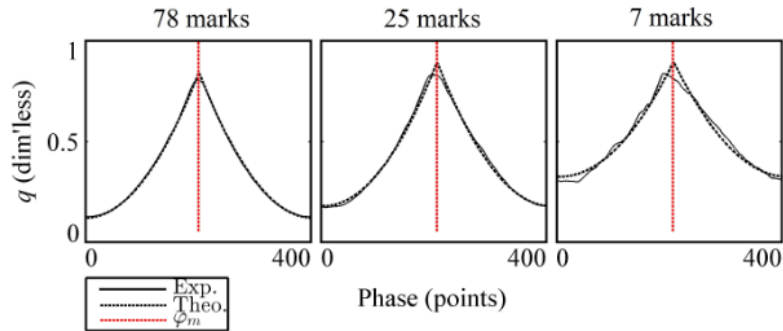
Figure 3.16: The effect of the length of the profile on the qualifier function. To generate these graphs, the profile of Fig. 3.7 was cropped to 1, 1/3, and 1/9 of its total length, approximately.

The obfuscation of the ends of the tool marks is demonstrated by blurry correlation blocks, as in Fig. 3.12. The authors suggest that correlation blocks with indistinct edges physically signify that between two feed marks, there is a region that was created by mechanisms from both passes of the cutting tool. That intuitively expected result is therefore experimentally demonstrated.

Despite crisp q-functions, there nonetheless exists at least one flaw in the model of Eq. 3.3 that is present in all the qualifier function fits: the roundess of the experimental peak in comparison with the sharp cusp of the model. This roundness means that the covariance block of any given tool mark is not purely a matrix of ones. Noise might account for some of the roundness of the peak, but perhaps more interesting are the white and grey vertical and horizontal stripes in many of the dark diagonal blocks shown in this paper. Lighter stripes in a dark block signify small regions of irregular variance, in the deviations of the feed mark from the mean mark. Such regions might be called "unstable".

While Fig. 3.10 demonstrates correlation between adjacent marks, Fig. 3.11 shows long-range correlation of the random deviations, made apparent by statistically significant off-diagonal "darkness" in the correlation map. The only explanation the authors are able to suggest at this time for long-range correlation of deviations is periodic vibration with a half-period equal to one revolution of the lathe. This is the explanation proposed in this paper for the fact that Fig. 3.13 shows marks that are positively correlated with their *second* neighbours, as well as pronounced negative correlation with their first neighbours.

On the subject of error, the CDI method as implemented for this paper is limited by the qualifier function model in at least one way: the simplicity of the model of Eq. 3.3 may cause the fact that Fig. 3.14 shows that the identified phase is not quite in agreement with the intuitively visible diagonal blocks. Fig. 3.15 shows a case where the model fits poorly to the qualifier function. It is conceivable that more sophisitcated methods of identifying the block diagonal structure of a correlation matrix could be employed, such as machine vision techniques which could include edge detection. Beyond using the p-values for weighting, the patterns in the p-value matrices might also contain useful information for identifying $u(\varphi_m)$.

When CDI is employed, the profiles used ought to be as long as possible. The number of feed marks in a profile will determine the statistical sampling of the feed marks' deviation distributions from the mean feed mark, meaning longer profiles tend to produce better results, as shown in Fig. 3.16. Indeed, CDI failed to identify feed marks in exceptionally irregular profiles taken from holes drilled in a laminated composite. It is mathematically expected that CDI could in principle extract meaningful information from any profile with regular feed marks, but practically speaking, in extreme cases the profiles required to do so may be entirely too long.

3.6 Conclusion

The CDI method identified feed marks from 200 profiles from 40 specimens and 11 experimental treatments in an intuitively reasonable manner. The model agrees very well with experimental results. The discovery of the block diagonal patten in the correlation maps justifies the hypotheses concerning feed mark shape and correlation within tool marks, but the discovery of correlation and negative correlation between adjacent marks and at long range suggests an amendment for random phenomena that "persist" between multiple feed marks. Significant variability was observed in the correlation maps from repeated measurement of an individual specimen, but in the experiments performed, CDI was able to contend very well with repetition variability. The CDI method handily identified visually non-obvious feed marks. CDI revealed overlapping feed marks, meaning regions experimentally shown to have been contributed to by two tool passes. Unstable regions throughout the feed marks were discovered. The quality of the results of CDI depends on the length of the profile considered, and CDI may fail for extremely irregular profiles. The ability to identify tool marks from profiles fully automatically may provide added value to manufacturing operations by aiding identification of surface finish defects in quality control, by benefitting surface texture classification, or by augmenting theory and modeling of metal cutting processes.

3.7 Conflict of Interest

The authors declare that they have no conflict of interest.

3.8 Acknowledgements

CHAPTER 4

ARTICLE 2: PRINCIPAL COMPONENT IDEALIZATIONS OF THE DOMINANT MODES OF VARIABILITY IN THE MECHANICS OF THE CUTTING PROCESS IN METAL TURNING

ABSTRACT

Quantitative information about the contributions of individual cutting phenomena to linear roughness profiles may aid in optimizing processes with fewer expensive successive trial parts. Linear roughness profiles of metallic hard turned parts contain feed marks, each mark representing a snapshot in time of the state of the cut. This suggests that roughness measuring machines may be an attractive avenue for offline, inexpensive, non-destructive, quantitative evaluation of the time-dependent mechanisms active during the cut. Principal component analysis of feed marks reveals theoretically expected feed mark deformations without coercing the data by fitting. Novel in this paper, we show that those components of feed mark variability appear to correspond to radial and axial displacement of the cutting tool, ploughing, and side flow. Those components are sufficient to explain nearly all the variability between feed marks. The components are easily idealized in a general manner, and their influences on experimental profiles are quantified as percentage contributions to ordinary roughness parameters.

Keywords: Cutting process; Surface roughness; Feed marks; Metal cutting; Profile decomposition

4.1 Introduction

How does a machining specialist alter a cutting process to improve the microgeometry resulting from a precision cut? Typical problems with microgeometry include inadmissibly large values of roughness parameter R_a, readhered material, tears, laps, poor finish due to built-up edges, white layer, scratches, waviness, traces of vibrations, and dimensional inaccuracy. To

resolve this type of issue, experience is very heavily valued, and in combination with cutting tests, touch, visual inspection, and roughness measuring tools, a cutting specialist may narrow in on the primary cause of the problem faced. He may then improve the cut by changing the cutting tool material, tool geometry, edge preparation, tool holder, cutting feed, cutting speed, depth of cut[1], coolant, method of coolant application, the order of cuts, and so forth among many ways of altering the setup of the machine tool tool-workpiece system. Even a cut that satisfies the nominal requirements of a part may present a risk to the production series if the degree of control over the operation is such that an eventual part might have to be scrapped.

There are therefore two advantages to understanding the cutting dynamics specific to a given precision cut. "Cutting dynamics", here, should convey the notion that a cut is a dynamically stable process: temperature fluctuations (for example, due to coolant splashing and inconstant chip morphology), material inhomogeneity (in terms of internal stresses, work hardening, and composition), the mercurial behaviour of a built-up edge, vibrations, and so on, continuously agitate the interface between cutting edge and workpiece. The first advantage is to reduce the number of trial parts when optimising the cut. The second advantage is to maintain a cutting process that is stable and consistent. Both are directly related to manufacturer expenses, particularly when unit cost is high.

Reducing the number of trial parts necessary to optimise a process may sometimes be the more important of the two advantages, simply because some processes may be costly to alter once approved for a production line. In some cases, a single turned trial part may cost tens of thousands in USD. By comparison, analysis of roughness costs very little, especially automated analysis. Linear roughness profiles are of particular interest because linear roughness measuring machines are common in shops and are non-destructive.

A matter of scope, decomposition of feed marks (the subject of the present paper) should be distinguished from prediction of the influence of machining effects on surface roughness. The prior estimates the influence of machining effects starting from a roughness profile, and the latter, much more common, starts from machining effects and simulates surface generation. Benardos and Vosniakos authored an important review paper on predicting roughness (Benardos and Vosniakos, 2003).

The most relevant by far of the literature studied is the recent work of F. Ancio *et al.* of the University of Sevilla. In 2013, Ancio *et al.* published a paper introducing the use of principal component analysis on roughness profiles of machined parts (Ancio et al., 2013), demonstrating that a few principal components (that is to say, a linear superposition

---

[1]It is well known that cutting force, and consequently vibrational amplitude, depend upon depth of cut. As we consider time-variation in surface roughness in this paper, depth of cut can be relevant, despite being usually less important to roughness than feed and cutting speed.

of a few patterns) sufficed to describe most of the roughness of the surfaces studied. In 2016, Ancio *et al.* again published on principal component analysis of surface roughness of machined parts, suggesting a methodology (Ancio et al., 2016). Significantly, they suggested that cutting traces contain information about the physical processes generating machined surfaces, including cutting vibrations and material responses.

W. Grzesik and S. Brol have perhaps published the most on the explicit relationship of feed mark morphology and cutting dynamics. In 2011, Grzesik and Brol published a simple method of decribing feed marks (Grzesik and Brol, 2011): fit parabolas to the linear profile, of the form $z \propto x^2$ (with vertical and lateral displacement, as well as scaling in x), which is justified for roundnosed cutting tools.[2] By doing so, they could measure the vertical and lateral displacements of each feed mark and their elongations, which they believed relate to plastic side flow, spring-back, cutting edge preparation, cutting edge wear, and other mechanisms. They treated these effects as independent, that is, treating the effects on surface roughness as a sum. Grzesik and Brol's paper describes how to relate feed mark displacement and elongation to cutting dynamics in a simple way. Importantly, their paper's conclusions acknowledge that roughness profiles contain information about the mechanisms having generated the surface, connecting feed mark distortions to physical mechanisms. It is also our contention that feed mark vertical displacement, though not explicitly mentioned by Grzesik, are caused not only by plastic flow, but in large part by vibrations. That concention will be investigated in a later paper. Furthermore, an important drawback of Grzesik's method is that it assumes a nominal feed mark shape; even if other nominal tool shapes are used for other tools, real feed marks often do not resemble the nominal tool shape due to plastic effects.

In J.P. Davim's Metal Cutting: Research Advances, W. Grzesik and S. Brol published a chapter (Grzesik and Brol, 2010) about generation and modelling of surface roughness using defined cutting tools. Again, those authors explain their belief that understanding surface roughness involves the dynamic process of material removal and elastic-plastic deformation. The paper describes the analytical nominal shape of feed marks based on tool geometry and minimal undeformed chip thickness. The chapter also introduces plastic flow and other elements.

It is critical that no literature at all was found detailing how a computer can *find* the feed marks in a linear roughness profiles without assuming some manually input feed mark shape (such as, in the case of Grzesik and Brol, a parabola). More subtle and just as important, given that true feed mark shape is unknown *a priori*, expecting a particular feed mark shape

---

[2] "Ideal" feed marks mimic the shape of the cutting tool perfectly, as smooth scallops. As shown in the figures below, real feed marks don't behave so nicely, and for finishing conditions, the profiles often don't resemble the nominal scallops at all. These plastic effects are especially important in hard turning.

does not indicate where, laterally, feed marks of arbitrary geometry begin and end, due to deformations not accounted for by nominal feed mark shape. These issues were resolved by P.R. Provencher and M. Balazinski (Provencher and Balaziski, 2016).

Closely related to Ancio *et al.*'s work, the present paper discusses the use of principal component analysis to allow the components of variability of the cut to arise naturally from the data, without imposing expected shapes. The manner in which the modes of variability are found in the data is secondary to the realization that we can connect those modes with theoretically expected feed mark deformations, and idealize those signatures in convenient ways. Crucially, the feed marks in a given profile are effectively a statistical sample of the instantaneous state of the dynamic cutting interface, or "snapshots" of the cut. Experiments for this paper have shown that principal component analysis on the feed marks of a profile reveals components of feed mark variability that are theoretically expected in terms of the physics of metal cutting. Specifically, the radial component of vibration, the axial component of vibration, and plastic flow (ploughing and side flow) appear to show up as principal components. Those components, by themselves, explain around 95% of feed mark variability within a roughness profile of a metallic hard turned part. The principal components can furthermore be idealized to a simple form, and be used to quantify the relative contribution of each mode of variability to the roughness parameters of the profile. This is accomplished *without* resorting to introducing new, exotic parameters, simply by assessing the percentage contribution of each mode of variability to ordinary roughness parameters such as R_a (or indeed any other parameter).

Coming full circle, as introduced above, we believe that because measuring linear roughness profiles in a shop environment is quick, convenient, and non-destructive, automating the analysis of roughness profiles with the intention of quantifying the percentage contributions of physical phenomena to existing roughness parameters may assist machining specialists in resolving process optimization with fewer trial parts. If that goal can be achieved in practice, it will impress directly upon material manufacturer expenses.

As our statement of novelty, to the best of our knowledge, idealization of the feed marks in terms of analytically expected machining effects is novel, with the quantification of side flow and local ploughing of particular note. We believe that quantifying the percentage contributions of specific physical effects to arbitrary roughness parameters is novel, too. Furthermore, the present work makes use of automated feed mark identification as developed by Provencher and Balazinski (Provencher and Balaziski, 2016). Importantly, the methods developed in this paper are designed to be employed utilizing a single linear roughness profile from a turned part, and analysed in a fully automated way, with the intention of suitability to production environments.

4.2 Theory

The concept of feed marks in a linear roughness profile as samples in time of the state of the cut is introduced below. "Correlated Domain Identification" is then described, the technique used to automate locating the feed marks in the profiles. Principal component analysis of roughness profiles follows, as does a discussion of the modes of feed mark variability. Finally, a method is proposed to quantify the influence of each mode of variability in a practical way, without introducing new, exotic parameters.

4.2.1 Feed marks in linear roughness profiles as snapshots of the cut

The measurement of a linear roughness profile is illustrated in Figure 4.1, where the red dots above represent the digital signal recorded. When the surface was generated, the cutting tool followed a helical path around the part, to the effect that the feed marks in the measured roughness profile represent the state of the cut at moments in time (denoted in the figure as t_1, t_2, t_3). The dashed lines on the part represent other profiles that could have been measured instead, in each case containing feed marks.
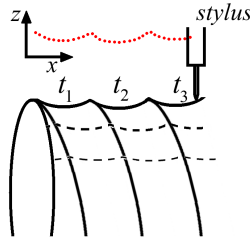
Figure 4.1: Illustration of a digitally encoded linear roughness profile. The feed marks in a profile are as snapshots in time of the state of the cut.

Crucially, each feed mark in a given linear profile is unique, as a result of the variabilities of the cutting process, keeping a stable cutting zone constantly in a state of change. As this paper reveals, the variability between feed marks is far from random, and is almost entirely accounted for by a handful of modes of variability.

4.2.2 Use of Correlated Domain Identification (CDI) to verify feed mark phase

To automate analysis of roughness profiles, it is critical to identify the feed marks in a profile in a reliable, automated way. For this paper, the identification of the feed marks by the computer is done by the method described in a previous paper (Provencher and Balaziski, 2016) by P.R. Provencher and M. Balazinski, in which they developed a method to identify the locations of feed marks in roughness profiles, completely independently of feed mark shape,

calling that method Correlated Domain Identification (CDI). The method is illustrated in Figure 4.2. With the CDI method, it is the fact that the feed marks behave as snapshots in time that allows the marks to be distinguished using correlation maps. Within a feed mark, the variabilities are correlated with one another; between marks, they are not, generating the clear block-diagonal structure.

In other words, in order to analyze the feed marks in a profile, knowing the period of the roughness signal (which is equal to the machining feed length) is *not sufficient*; the phase of the periodic signal must also be known, that is to say, where the feed marks begin and end relative to lateral zero within the measured roughness profile. Sometimes, particularly for hard turning finishing conditions, the plastic behavior of the workpiece material is such that the feed marks are not obvious scallops like the ideal ellipses in the schematic of Figure 4.1. Rather, they may resemble Figure 4.3, where the feed marks have been identified using CDI, and are not obvious from visual inspection of the profile.
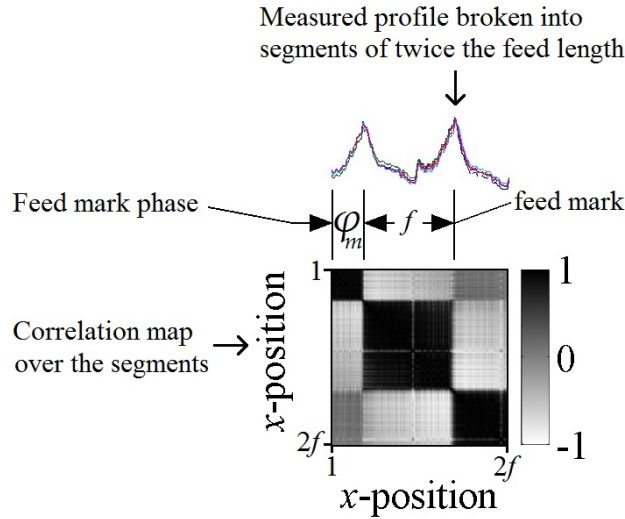
Figure 4.2: Illustration of the CDI method for identifying feed mark phase by exploiting cutting process variabilities and the snapshots in time that feed marks represent. This method has the advantages of requiring no assumptions as to nominal feed mark shape, and may reveal the feed mark locations even when the feed marks are not identifiable by visual inspection, as in Fig. 4.3.

4.2.3   Principal component breakdown of feed marks

Principal Component Analysis (PCA) is a standard statistical method. Given a set of signals (in our case, a set of individual feed marks from a given roughness profile), PCA expresses each signal as a linear combination of principal components. This is done such that the first principal component is defined so as to account for as much of the variability between the
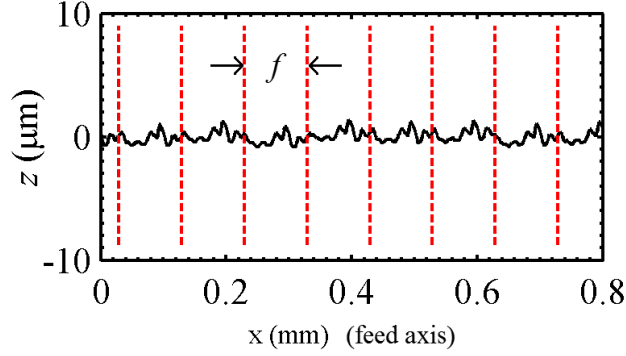
Figure 4.3: A measured profile from finish hard turning. The feed marks are not obvious from visual inspection, but have been identified (as delimited by the dashed lines) using CDI.

signals as possible, the second pricipal component accounting for as much of the remaining variability as possible, and so on. Applied to feed marks from a profile, PCA would express each feed mark as a linear combination of components common to the feed marks of that profile.

The PCA method is common in statistics, and it is not in the scope of the current paper to explain general PCA in rigorous detail. The application here is transformation from the basis of the digital encoding of the feed mark profile ($z(x_i)$) to an efficient new basis consisting of a set of functions, called principal components, which when summed account for the variations between the feed marks of a roughness profile.

Most importantly, the new basis of principal components arises naturally out of the data, without imposing expected component shapes (as would be the case with regression techniques).

4.2.4 Effects of common modes of cutting variability on feed marks

This paper is concerned with the effects of cutting mechanics on intra-feed mark roughness profile morphology. Several effects have been identified by other authors, briefly discussed here. The modes of continuous, tumultuous variability during the cut that are considered here are shown in Figure 4.4, simplified. We also refer to the "modes" of variability as "components". The modes are explained below, and expanded to greater detail. Each of these modes is further justified in the Results and Discussion, arising naturally out of the measured data.
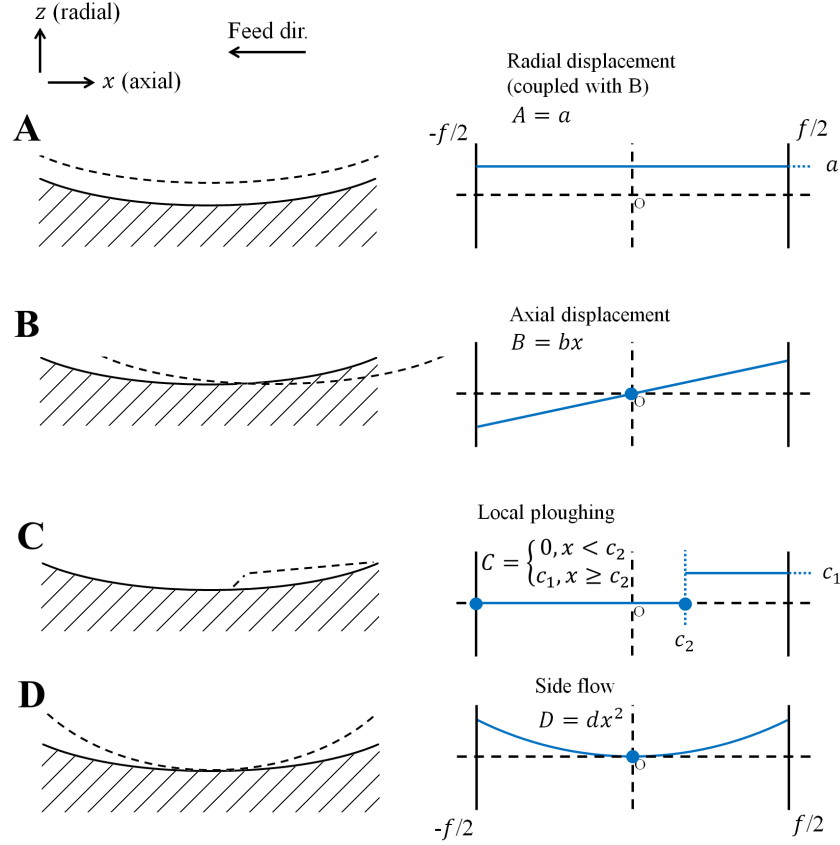
Figure 4.4: The modes of variability due to cutting mechanics considered, and their simple-form idealizations. The cutting mechanics would generate the dashed profiles. The expanded, more detailed idealizations are explained in Fig. 4.6, accounting for mathematical coupling between the modes.

Radial and axial displacement

Radial displacement of the feed mark is shown in Figure 4.4 A in simplified form. Feed marks may vary in depth relative to one another, as discussed (Grzesik and Brol, 2011) in 2011 by W. Grzesik and S. Brol. Though Grzesik and Brol expressed the belief that plastic flow is responsible, we contend that variations in feed mark depth are the result of the radial (as in the depiction of Figure 4.1) component of vibration, as examined in F. Ancio *et al.*'s 2014 paper (Ancio et al., 2015) on vibrations and feed marks. It should also be noted that elastic recovery of the workpiece may also vary feed mark depth, but supposing that the elastic recovery is similar between feed marks, the global swelling of elastic recovery should not appear in linear roughness profiles, because the z-axis zero in a measured profile is arbitrary. Radial displacement, idealized as a horizontal line component added to feed marks, may be positive or negative in z, and is coupled with axial displacement, as follows.

Similarly to radial displacement, axial displacement of the feed mark is shown in Figure 4.4 B, in simplified form as well. Radial displacement of feed marks on a turned surface may be due to the axial component of vibration between the cutting tool and the workpiece. That explanation has not been proven, but as elaborated in the Results and Discussion section, this sort of inclined line component appears to emerge naturally from the data. Axial displacement may be to either side (up-feed or down-feed, i.e., b in Figure 4.4 may be positive or negative.). Note that as defined, the inclined line component is fixed at its center on the origin.

Figure 4.5 explains the coupling of the horizontal line and inclined line components. As shown, the lateral displacement of the tool edge h and the vertical displacement v are related to the component parameters a (horz. line height) and b (inclined line slope) as in Fig. 4.6. (The figure also summarises local ploughing and side flow, discussed below.)
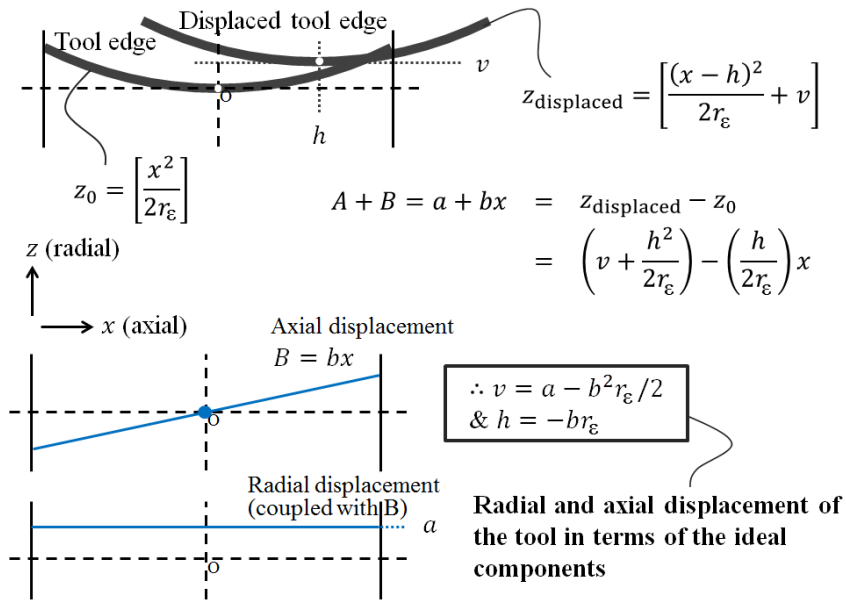
Figure 4.5: The coupling of the horizontal line and inclined line components. r_ϵ is the tool nose radius. v and h are the vertical and horizontal displacements, respectively.

Local ploughing

In addition to radial and axial displacement, turning feed marks are expected to show a local ploughing phenomenon on part of the feed mark, related to minimum chip thickness, i.e., sub-feed-mark local failure of the tool to engage the workpiece material, causing a kind of local ploughing/burnishing instead of shear removal of workpiece material. H.A Kishawy
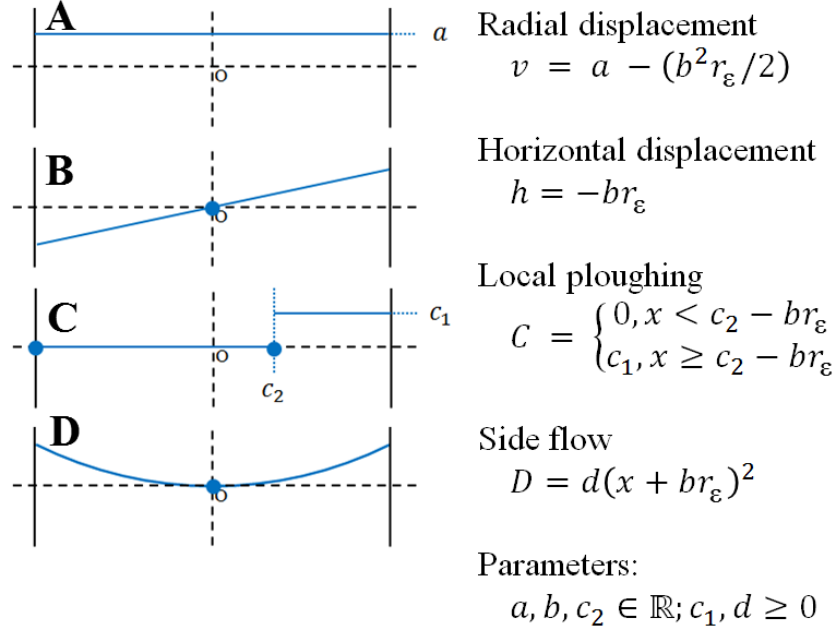
Figure 4.6: Summary of the mathemetical definition of the feed mark components v, h, c_1, c_2, d

and M.A Elbestawi succinctly explained the notion, in the context of side flow (Kishawy and Elbestawi, 1999) (see Fig. 8 of Kishawy and Elbestawi). Side flow is closely related in that, beneath the minimum chip thickness, failure of the cutting tool to engage the workpiece material leads to elastic-plastic displacement of the material, which includes material swelling (elastic-plastic recovery), ploughing, and side flow. Fig. 4.7 also illustrates the local ploughing/burnishing phenomenon. Local ploughing is accounted for using the function in 4.4 C, shown in greater detail in Fig. 4.6. Like the radial displacement, local ploughing is coupled with axial displacement.

Side flow

Grzesik and Brol suggested (Grzesik and Brol, 2010) the deformation of the feed mark shown in Fig. 4.4 D, to account for side flow, shown in more detail in Fig. 4.6. This component, too, is coupled with the inclined-line axial displacement component. Again, side flow is the plastic response of the workpiece as a result of failure of the cutting tool to engage the workpiece material locally, within a feed mark, due to the minimum chip thickness phenomenon.
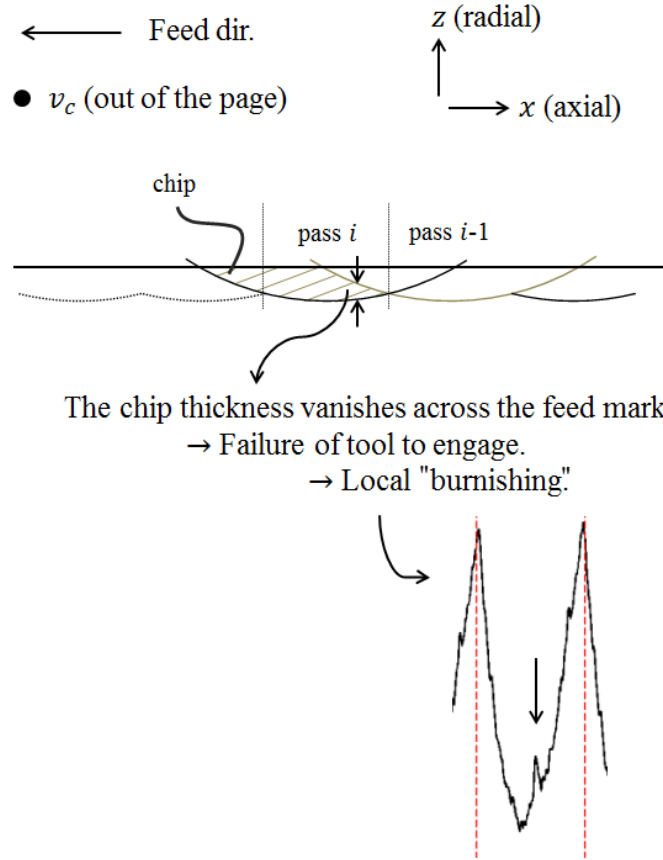
Figure 4.7: Illustration of local, sub-feed-mark failure of the cutting tool to engage the workpiece material, as a result of the minimum chip thickness phenomenon and the geometrical situation of turning with fully round engaged tool nose profile.

4.2.5 Method of quantifying the influences of modes of cutting variability on roughness parameters

Once the modes of variability have been quantified in a profile, the quantity of any mode in each mark can be mathematically subtracted. The result of doing so is a hypothetical profile in the absence of the removed mode of variability. Ordinary roughness parameters may be evaulated on that hypothetical profile, and compared to the same roughness parameters of the original, measured profile. Quantifying the effects of the modes of variability in this way prevents the creation of new, exotic, abstract parameters, enabling the modes' influences to be expressed as percentage effects on any ordinary roughness parameter, such as R_a.

4.3 Materials and Methods

Forty specimens were turned from ⌀2" AISI 4340 tempered to 48 HRC. The machining was done on a Mazak QT-Nexus-200 lathe using a DCLNL-12-4B tool holder from SECO. Each specimen was cut using a new edge of CNMG120408-FF1, grade TP1500 (multilayer Al2O3, Ti(C,N)) cutting inserts manufactured by SECO. Metalworking fluid was used.

A Mitutoyo Formtracer SVC-4000 roughness measuring machine was used to measure the roughness profiles by the skidless contact stylus method, with a 2 μm radius, 60 μm tip angle. The measured length on each specimen was 160 mm. Table 4.1 lists the cutting conditions. The conditions were chosen to provide a range of roughnesses.

Table 4.1: The cutting conditions and numbers of replicates of each experimental treatment

Ident.	Repli-cates	Cutting speed (m/min)	[sfm]	Feed (mm/rev)	[in./rev]
1	3	250	820	0.30	0.0118
2	3	164	538	0.30	0.0118
3	3	78	256	0.30	0.0118
4	3	121	397	0.25	0.0098
5	3	250	820	0.20	0.0079
6	10	164	538	0.20	0.0079
7	3	78	256	0.20	0.0079
8	3	207	679	0.15	0.0059
9	3	250	820	0.10	0.0039
10	3	164	538	0.10	0.0039
11	3	78	256	0.10	0.0039

4.4 Results and Discussion

First, a brief account of an unexpected result, the necessity of fine-tuning the effective feed length in the measured roughness profile as opposed to using the slightly longer (due to parallax) nominal machining feed length. Then, experimental principal components are shown. Arguably the most important result, it is shown that about five components account for nearly all the variability between feed marks, strongly suggesting that a handful of competing physical phenomena account for almost all the variability. Furthermore, those components match the theoretically expected components quite nicely. The idealized versions of the components are fit to profiles for illustration. Finally, examples are given of quantitative, percent contributions of components of variability to ordinary roughness parameters.

4.4.1 Fine-tuning of effective feed for Correlated Domain Identification (CDI)

CDI as presented previously (Provencher and Balaziski, 2016) did not account for the fact that the effective feed length in a roughness profile is usually slightly shorter than the machining feed length, due to parallax error between the axis of the turned part and the axis of motion of the rougness measuring machine. The effect is small, but has a significant effect on results. Figure 4.8 shows the effect of using the nominal feed versus using the effective feed. In a), the correlation map exhibits structures that do not appear when using the effective feed length of the measured profile as in b). The effective feed was chosen from the maximal peak in the Fourier spectrum of the profile.[3] Selecting the effective feed length correctly was vital to yielding principal components that were consistent from profile to profile.
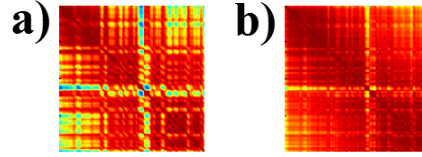
Figure 4.8: In a), the correlation map of the feed marks of a roughness profile, using the nominal machining feed length. In b), the same, but using the effective feed of the measured profile. The salient property is structure, as discussed in-text.

4.4.2 Experimental principal components of feed marks

Figure 4.9 shows the principal components of cutting condition 1 in Table 4.1. Principal component analysis, again, allows these components to arise naturally from the data, without imposing expected components as with fitting. The components shown are chosen for their relative clarity; not all the profiles measured showed the upper two components as clearly. Nonetheless, in all cases, five principal components were sufficient to account for around 95% of the variance between the feed marks of a profile, from 600 principal components for a profile. In other words, the variability of the cut was reduced from 600 dimensions to around 5 dimensions. This suggests that about five independent phenomena account for nearly all the variation between the feed marks of a profile (not counting microstructure-level roughness, not considered in this paper). This is supported by Fig. 4.10, which shows the variance explained for all 200 of the profiles taken from the 40 specimens.

---

[3]A detail on selecting effective feed based on the frequency of maximal power of the roughness profile. In fact, it was not the maximal peak due to the limitations of the *discrete* Fourier transform, as the peak was narrow compared with the frequency resolution. The true maximal power frequency can be implied to be somewhere between the maximal discrete frequency and the next highest neighbour.
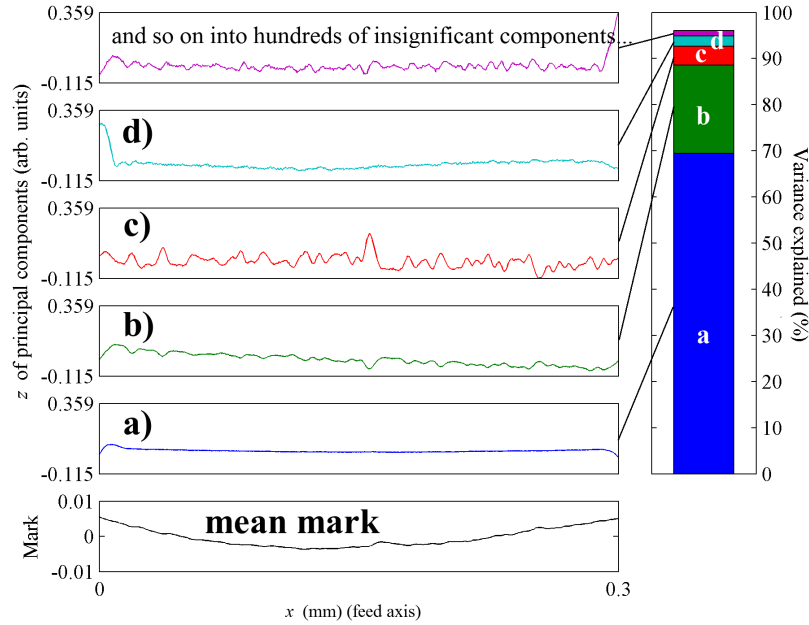
Figure 4.9: The principal components from condition 1 in Table 4.1. On the left at the bottom, the average feed mark. Upwards from there, the first principal component (explaining the most variance), second (explaining the most of the remaining variance), and so on to the fifth component. On the right, the proportions of variance explained by those five components, the sum of which exceeds 95%.

4.4.3 Idealizations of feed mark principal components and relationships with cutting mechanics

The principal components shown in Fig. 4.9 bear a striking resemblance to the corresponding theoretically-motivated A, B, C, and D idealized components of Fig. 4.4. This is a great result, considering that principal component analysis in no way coerces the data into yielding these components rather than any arbitrary shapes, especially given the confirmation from the box plot of Fig. 4.10 that about five components are sufficient to account for nearly all the variability between feed marks in a given profile. It would appear that the theoretically motivated ideal components discussed in the Theory section are reasonable.

Figure 4.11 shows part of a longer roughness profile. Superimposed are the piecewise feed marks made of idealized components A, B, C, and D. As can be seen, the fit is reasonable. Note, importantly, that often very good finishing does not offer a clear component C (the plastic shelf phenomenon), as the plastic "noise" becomes too great relative to the components. Importantly, modes C and D were found to vary much less from mark to mark on a part than their absolute, constant values (with respect to the ideal scallop) for all the feed
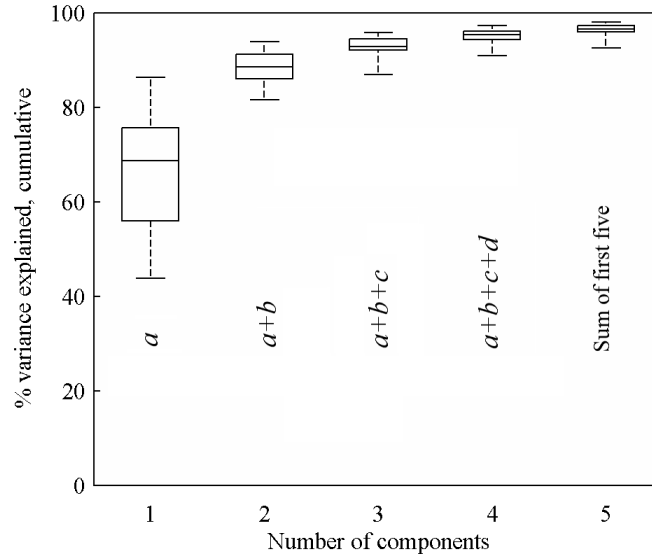
Figure 4.10: Though plain, perhaps the most important result of the paper. The total variance explained by number of principal components included. Shown, up to five of the principal components, the other 595 components accounting for the remaining approximately five percent variance. The box is one quartile in either direction about the mean and the whiskers are the extreme outliers of the data set.

marks of that part.

4.4.4 Quantitative influences of modes of cutting variability on roughness parameters

Perhaps the principle advantage of decomposing feed marks into idealized components that are related to the physical mechanisms involved in cutting is the ability to quantify the influences of these effects. The simplest way to do so is mathematically to remove specific components from the profiles and to evaluate ordinary roughness parameters on those hypothetical profiles. Consider Figures 4.12 and 4.13. As described, the experimental roughness profiles are shown next to their hypothetical equivalents with radial depth component A removed. With the variations in feed mark depth removed, roughness parameter R_v (deepest valley), which is particularly significant to fatigue, is dramatically altered. Removing all four idealized components A, B, C, and D further reduces the apparent values of R_v.
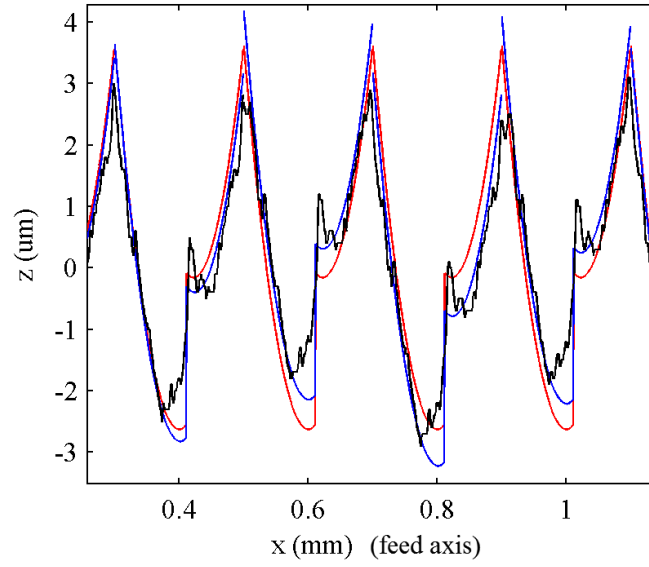
Figure 4.11: A fit of idealized feed mark components to an experimental roughness profile. This is a profile from experiment 6 in Table 4.1. In red (the truly periodic smooth curve), a fit using only idealized components C and D. In blue (the function that hugs the data better), a fit using all four idealized components A, B, C, and D.
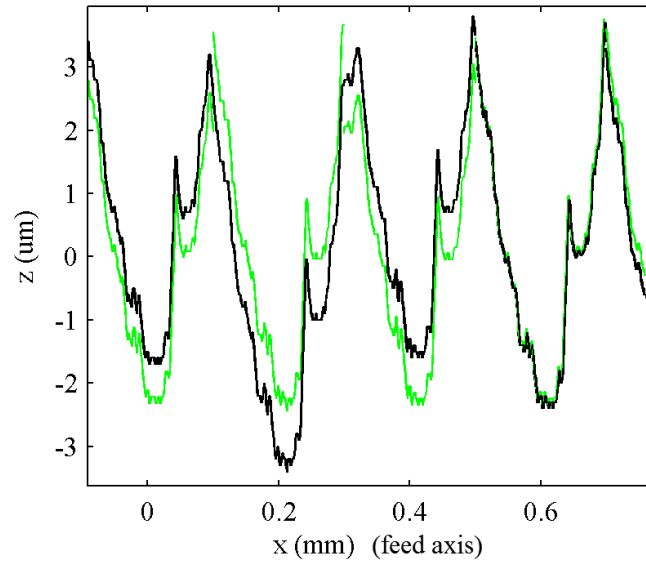
Figure 4.12: An experimental roughness profile (in black). In green, the profile with feed mark depths (component A) subtracted away. Roughness parameter R_v (deepest valley) goes from 3.04 μm to 2.49 μm (18% reduction). Removing all four components A, B, C, and D reduces R_v further to 2.32 μm (24% reduction). This is a profile from experiment 4 in Table 4.1.
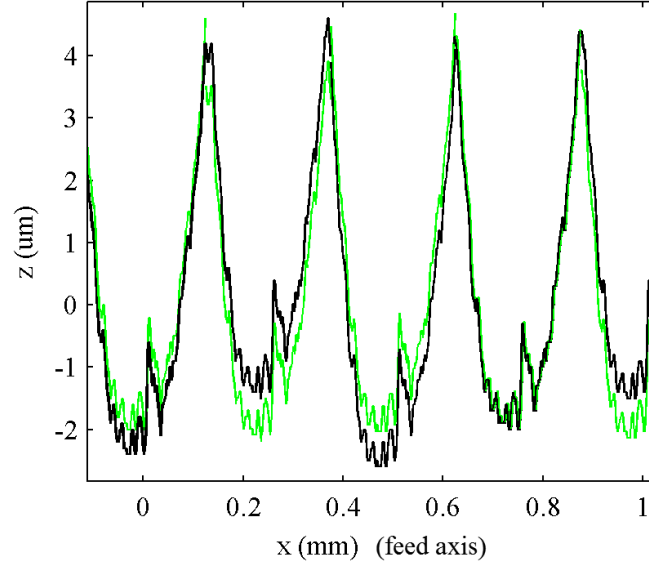
Figure 4.13: Similarly to Fig. 4.12, an experimental roughness profile (in black). In green, the profile with feed mark depths (component A) subtracted away. Roughness parameter R_v (deepest valley) goes from 2.52 μm to 2.15 μm (15% reduction). Removing all four components A, B, C, and D reduces R_v further to 2.05 μm (19% reduction). This is a profile from experiment 10 in Table 4.1.

4.5   Conclusion

Principal component analysis enabled a handful of modes of variability to emerge from the data and account for nearly all the differences between feed marks, and did so in a purely exploratory manner, *i.e.*, without coercing the data by fitting expected forms to the marks by regression. A handful of competing, approximately independent physical mechanisms are therefore sufficient to explain nearly all the variability. Furthermore, the strongest four of the principal components closely resemble theoretically expected feed mark deformations, specifically, radial and lateral displacement of the cutting tool, (local, intra-mark) plough-ing, and side flow. The components were therefore easily idealized to simple mathematical forms. This further enabled quantification of the percent contributions of individual modes of variability to ordinary roughness parameters.

We believe that because measuring linear roughness profiles is quick, convenient, and non-destructive, and utilizes equipment already common in shops, that the automation of mathematical roughness profile decomposition, and subsequent quantification of the percent-age contributions of physical phenomena to roughness parameters already in use by manu-facturers may aid machining specialists with the task of process optimization. Additional, "free" process knowledge can help narrow in on the physical causes of issues faced, requiring

fewer costly trial parts. If that goal can be achieved in practice, manufacturer expenses will be directly impacted.

To the best of our knowledge, the following are novel: idealization of the feed marks in the ways shown above; suggestion of the relationship between the idealized components and the analytically expected plastic roughness effects of side flow and local ploughing, which are characteristic of hard turning; quantification of the percentage contributions of specific physical effects to arbitrary roughness parameters; fully automated analysis from a single roughness profile, with the help of automated feed mark identification.

In our following papers, we intend to offer experimental proof of the physical causes of the idealized components observed.

4.6 Conflict of Interest

The authors declare that they have no competing interests.

4.7 Acknowledgements

CHAPTER 5

ARTICLE 3: FEED MARK DEPTHS IN LINEAR SURFACE ROUGHNESS PROFILES OF FINISH HARD TURNED METAL PARTS COMPARED WITH THE RADIAL COMPONENT OF CUTTING VIBRATIONS

ABSTRACT

In this paper we discuss how one specific physical mechanism active during hard finish turning of metal parts be attributed a percent contribution to arbitrary amplitude-derived surface roughness parameters, in a fully computer-automated way, using only a roughness measuring machine and a personal computer. The ability to do so would benefit manufacturers by narrowing in on the specific causes of unacceptable surface roughness, and may reduce the number of trial parts when optimizing a cut, help maintain stable production, and prevent the scrapping of parts. As part of the development of that ability, this paper investigates whether the variations in cutting tool trace cross-sections (feed marks) in linear roughness profiles can safely be fully attributed to the radial component of cutting tool vibration. This is accomplished by comparing online accelerometer readings with roughness profiles, making use of "correlated domain identification" (CDI) and simple feed mark decomposition.

5.1 Introduction

Suppose we could, in a production environment, acquire a single roughness profile from a turned part, submit the profile to automated analysis software, and obtain estimates of the percent contributions of specific physical phenomena including vibration and ploughing to whichever roughness parameters the designers happen to have specified for the part. This ability would equip a machining specialist with detailed process information directly applicable to manipulation of the many variables of the process (feed, speed, depth of cut, tool

geometry, edge preparation, cutting fluid application, and so on), for the sake of maintaining stable production, preventing the scrapping of parts, and reducing the number of trial parts when optimizing a process (especially when unit cost is high). The development of the above ability is the goal of the current series of papers by P.R. Provencher and M. Balazinski:

- Finding the feed marks: The first paper (Provencher and Balaziski, 2016) in the series introduced automated identification of feed marks in linear roughness profiles, completely independently of feed mark shape, using a technique the authors called "correlated domain identification" (CDI). As shown, knowing the feed mark period (equal to the machining feed length) is insufficient to decompose feed marks according to process signatures; the feed mark phase (see Section 5.2.1) in the roughness profile is also needed, especially in finish hard turning when feed mark shape is dominated by plastic effects and may not resemble the typically drawn ideal "scallops" at all.

- Decomposing the feed marks into phenomenon signatures (manuscript in preparation): The second paper in the series treated the use of idealized principal components of feed marks as signatures of radial and axial vibration, and of plastic effects particularly important in hard turning, that is side flow and local (intra-feed-mark) ploughing. These idealizations were selected according to the dominating principal components and matched literature expectations of feed mark deformations by cutting phenomena. A computer was then able to eliminate any or all signatures to generate hypothetical profiles and estimate most any arbitrary roughness parameters on the hypothetical profiles devoid of those effects, expressing the phenomena by their percent contributions to the roughness parameters. The authors also automated the analysis.

- Substantiating one of the signatures: The current paper demonstrates that the signature associated with radial vibration is indeed accounted for both in spatial frequency and in amplitude by the radial component of the vibrations during turning.

The above series expresses some of the challenges of computer-automating roughness profile analysis to express the quantitative contributions of competing cutting effects on arbitrary roughness parameters. The focus of the current paper is explicitly to investigate the hypothesis that the relative depths of the feed marks in axial roughness profiles of turned parts are fully explained by the radial component of cutting tool vibration. Closely related work has been done, but to the best of our knowledge there is no publication explicitly defending that claim.

In this work, we consider surface roughness of hard finish turned parts. Specifically, we exploit the fact that a single linear roughness profile that crosses the helical tool trace multiple times contains "snapshots" in time of the state of the cut. That statistical sample

can be leveraged to quantify process dynamics. "Dynamics" here is intended in a broad sense, including not only vibration but also plastic side flow, ploughing, and all other mechanisms that exhibit a dynamic stability, rather than static contribution to post-machining part microgeometry.

It is important to note that the topic here is decomposition of feed marks, which should be distinguished from the modeling of machining. Decomposition estimates the influence of machining effects from a roughness profile, whereas modeling of turning, much more common, starts from machining effects to simulate surface generation. Benardos and Vosniakos authored an important review paper on predicting roughness (Benardos and Vosniakos, 2003).

The most closely related work to the current paper, other than the papers described above by our own research group, is that of F. Ancio *et al.*, who have been able to reconstruct part microgeometry from online readings of cutting tool acceleration, beginning with a paper in 2012 (Ancio et al., 2012) and developed further in 2014 (Ancio et al., 2015). In 2013, Ancio *et al.* introduced the use of principal component analysis on roughness profiles of machined parts (Ancio et al., 2013), demonstrating that a superposition of a few patterns suffices to describe most of the roughness of the surfaces studied. In 2016, Ancio *et al.* suggesting a methodology for principal component analysis on turned parts (Ancio et al., 2016). Significantly, they suggested that cutting traces contain information about the physical processes generating machined surfaces, which includes vibrations and material responses.

W. Grzesik has also published on the relationship of cutting effects and intra-feed mark surface roughness morphology. In 2011, W. Grzesik and S. Brol published a simple method for decribing feed marks (Grzesik and Brol, 2011), consisting of fitting parabolas to linear profiles. That method is sometimes justified for round-nosed cutting tools, but is somewhat limited in finish hard turning where plastic effects may dominate even the scallop-shaped ideal tool nose trace. Grzesik and Brol used that method to measure the vertical and lateral displacements of feed marks and feed mark elongations, expressing belief that those deformations relate to plastic side flow, spring-back, cutting edge preparation, cutting edge wear, and other considerations. Importantly, Grzesik and Brol acknowledge that roughness profiles contain information about the surface-generating physical mechanisms. Crucially, Grzesik and Brol also expressed the belief that the relative depths of feed marks are due to material response. While true, the intention of the current paper is to demonstrate that the radial component of tool vibration is a direct, clear, and sufficient explanation for variation in feed mark depth across a roughness profile.

In J.P. Davim's *Metal Cutting: Research Advances*, W. Grzesik and S. Brol published a chapter (Grzesik and Brol, 2010) about generation and modelling of surface roughness. The paper describes surface roughness generation as a dynamic process of material removal and

elastic-plastic deformation, with the analytical nominal shape of feed marks based on tool geometry and minimal undeformed chip thickness. The chapter also discusses plastic flow and numerical treatment of other effects such as cutting edge preparation.

For the current paper, online measurements of cutting tool acceleration were compared with roughness. The surface roughness was decomposed in a fully automated way, utilizing correlated domain identification (CDI) to identify feed mark locations (Provencher and Balaziski, 2016) and feed mark decomposition (as in the above manuscript under preparation). It was shown that the radial component of tool acceleration fully accounts for the variations in feed mark depth, both in terms of spatial frequency and vibrational amplitude.

Specific conclusions include:

- Azimuthal (cutting speed direction) (see Fig. 5.1) roughness profiles of turned parts contain information about vibrational frequencies, but not the depth distribution.

- Axial roughness profiles of turned parts contain vibrational depth distribution information, but not the vibrational frequencies.

- Radial turning vibrations fully account for feed mark depths, in both spatial frequency and depth amplitude.

- The claim is sustained that the depth component of feed mark decomposition is a quantitative indicator of the influence of radial vibration on the surface roughness of turned parts.

- Consequently, it is valid to estimate percent contribution of radial vibration to any amplitude roughness parameter, using only a linear roughness measuring machine and mathematical removal of vibration effects from profiles.

- Turning vibrational frequencies may be estimated using only a linear roughness measuring machine.

- Turning vibrational amplitudes may be estimated using only a linear roughness measuring machine.

5.2 Theory

The principle of the experiment is summarized in Fig. 5.2.

5.2.1 Feed mark identification by correlated domain identification

In finish hard turning, it is often the case that plastic effects dominate roughness profiles, such that it is unclear where the feed marks are located within the roughness profiles. It
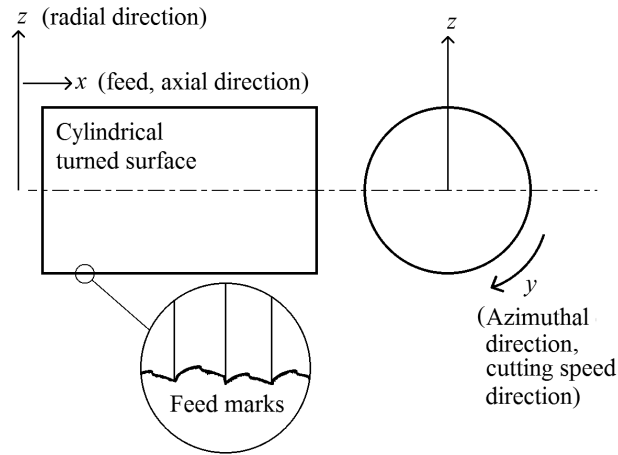
Figure 5.1: The coordinate system used.
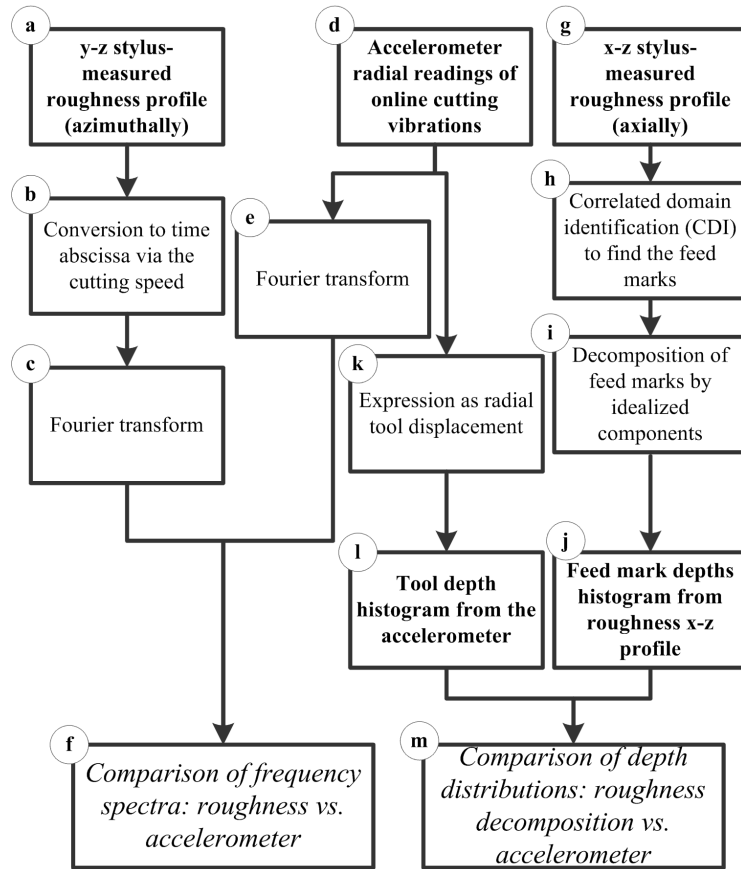
Figure 5.2: The experiment at a glance

is therefore not generally possible to find the feed marks by visual inspection nor by fitting idealized feed mark shapes such as parabolas. For the identification of feed marks within linear roughness profiles to be computer automated, it is therefore preferable to use "correlated domain identification" (CDI) (Provencher and Balaziski, 2016). The method is illustrated in Fig. 5.3. It consists of dividing a roughness profile that contains feed marks into segments of twice the feed, and computing point-by-point correlation of those segments. The resulting correlation map is block-diagonal by virtue of the principle that random variations are correlated with each other within a given feed mark, as that feed mark is the trace of a single passage of the cutting tool; likewise, random variations of a given feed mark are not correlated with random variations of other feed marks within the roughness profile.

The phase (lateral position) of the block-diagonal pattern indicates the end points of the feed marks within the roughness profile. That phase is determined using the "qualifier function", also introduced in the above-cited paper. The qualifier function is essentially the mean correlation of the block-diagonal region, expressed as a function of hypothetical block-diagonal region phase, and represents a technique for identifying where the block-diagonal region is situated within the double-feed correlation map.
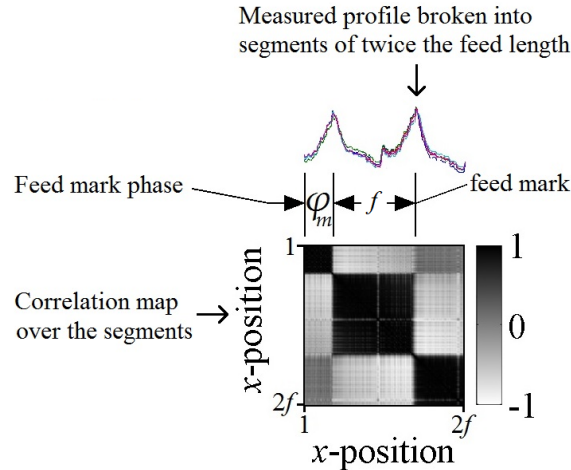
Figure 5.3: Illustration of the CDI method for identifying feed mark phase by exploiting cutting process variabilities and the snapshots in time that feed marks represent. This method has the advantages of requiring no assumptions about nominal feed mark shape, and may reveal the feed mark locations even when the feed marks are not identifiable by visual inspection. Shown here are double-feed segments and how they correspond with the phase of the block-diagonal region of the correlation map. Correlation scales from -1 to 1.

5.2.2 Decomposition of feed marks

At the top of the introduction, we described a manuscript under preparation in which we showed that principal component analysis of feed marks leads to a handful of signatures that account for nearly all the variability between feed marks in any given x-z roughness profile. In that paper, the most important mode of variability was a variation in the depths of feed marks relative to each other, as averaged across the points within each feed mark in an x-z roughness profile.

It is intuitively reasonable that feed mark depths in x-z roughness profiles are caused by the radial component of tool vibration with respect to the workpiece. Can mathematically leveling the feed marks in a roughness profile and re-evaluating a roughness parameter truly quantify the influence of radial vibration? As part of our paper series, it is necessary to verify that claim.

Each feed mark in an x-z roughness profile, as a computer automatically identifies them using the CDI technique described above, may be averaged to obtain an estimate of its depth relative to the other feed marks in the roughness profile. It is that set of depths that was compared with online accelerometer readings, both in terms of y-z spatial frequency and x-z amplitude (coordinate system in Fig. 5.1).

5.3 Experiment

A triaxial accelerometer was mounted on the tool holder for online measurement of tool accelerations. A cylindrical part was turned. After machining, a roughness profile was acquired axially, and another roughness profile was acquired in the azimuthal direction (the cutting speed direction). The coordinate system is shown in the diagram of Fig. 5.1. Each profile was repeated several times to verify the consistency of the results.

The accelerometer was a PCB Piezotronics triaxial accelerometer, model 356A16. The accelerometer's range is 0.5 to 5000 Hz with a sensitivity of 96.3 mV/g i.e. 9.82 mV/(m/s^2). The accelerometer is shown mounted on the tool holder in Fig. 5.4. The accelerometer was attached to the tool holder directly with the accelerometer's mounting screw in a tapped hole in the tool holder.

The lathe used was a Mazak QT-Nexus-200 lathe using a DCLNL-12-4B tool holder from SECO. The specimen was cut using a new edge of a CNMG120408-FF1, grade TP1500 (multilayer Al2O3, Ti(C,N)) cutting insert manufactured by SECO. The specimen was a $\varnothing$2" AISI 4340 bar tempered to 48 HRC. Metalworking fluid was used. The cut was done at 78 m/min and 0.2 mm/rev, to a depth of 0.5 mm.

The roughness measuring machine utilized is a Mitutoyo Formtracer SVC-4000 roughness
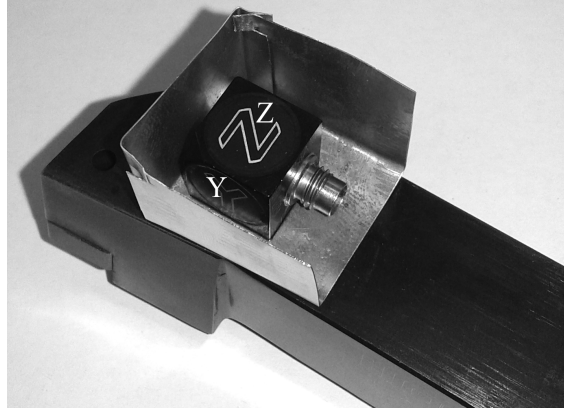
Figure 5.4: The lathe tool holder with the accelerometer attached. The sheet metal is a guard against chips. The axis of the accelerometer labelled "Y" in the photo is the radial direction (z) in the coordinate system of the paper (Fig. 5.1).

measuring machine. The profiles were acquired by the skidless contact stylus method, with a 2 μm radius and 60 μm tip angle.

5.4 Results

5.4.1 Comparison of frequency spectra

A y-z roughness profile is shown in Fig. 5.5, taken along the center of a cutting tool trace, following the curvature of the cylindrical part. That roughness profile is subjected to a discrete fourier transform. Its abscissa is expressed in time units by means of the cutting speed. The result is shown in Fig. 5.7. Fig. 5.6 shows the radial component of the online accelerometer readings as a function of time. That signal's spectrum is also shown in Fig. 5.7.

5.4.2 Comparison of depth distributions

Part (a short excerpt for visual clarity) of an x-z roughness profile is shown in Fig. 5.8. Correlated domain identification was performed on the profile, producing the double-feed correlation map of Fig. 5.9. The phase of the block-diagonal pattern was determined using the qualifier function shown in Fig. 5.10, as in the paper introducing the technique (Provencher and Balaziski, 2016). The result of this fully computer-automated process is shown in Fig. 5.11, where it is shown how the x-z roughness profile is divided into feed marks. The mean values of every feed mark (relative to the roughness profile center line) from the x-z roughness profile so divided is plotted as a histogram in Fig. 5.13.
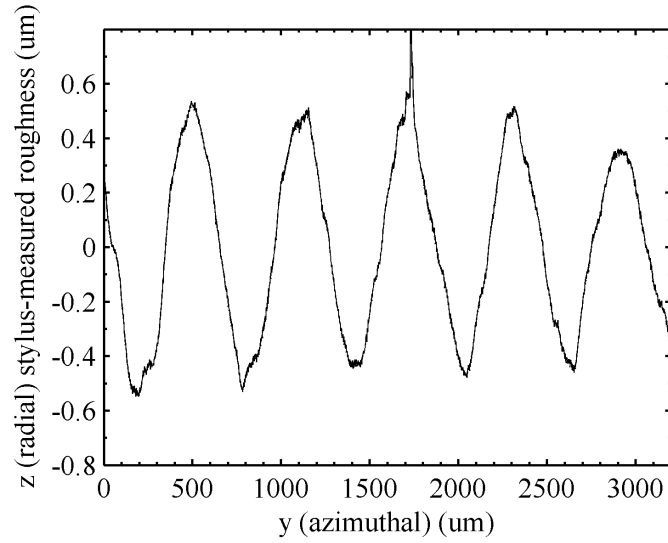
Figure 5.5: A y-z (azimuthal) stylus-measured roughness profile, along the center of a feed mark. The cutting speed direction is along the horizontal axis of the plot. Because the profile of the measured surface is circular, the roughness profile has been additively rectified to eliminate that curvature. Note that the dips and heights are *not feed marks* as they tend to be in axial roughness profiles like the x-z roughness profile in Fig. 5.8. Note also that the trace is quite gentle, despite the accidented appearance brought about by vastly different scales on the plot axes. This is step **a** in Fig. 5.2.
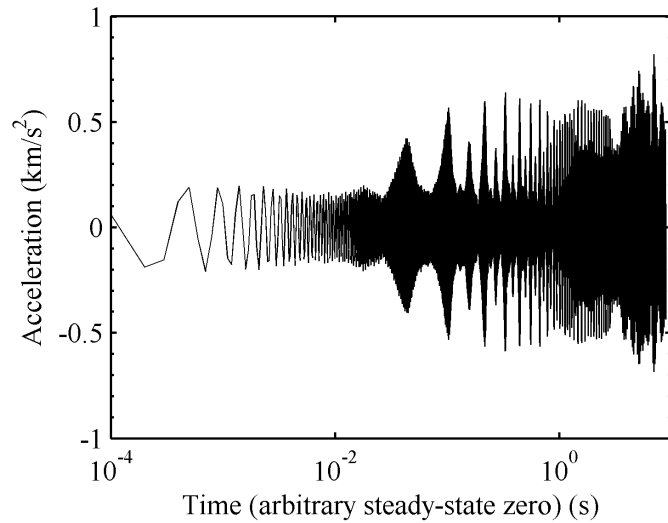
Figure 5.6: The radial component of the accelerometer readings. The time axis is plotted on a log scale to illustrate the signal behavior over both short and long intervals. This is step **d** in Fig. 5.2.
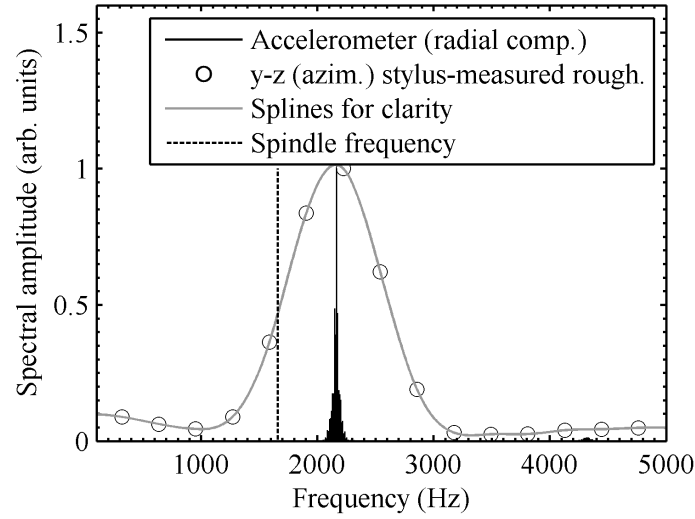
Figure 5.7: A frequency space comparison of the radial accelerometer readings and the y-z (azimuthal) profile of Fig. 5.5. The solid line represents the spectrum of the radial accelerometer signal. The dots represent the spectrum of the y-z profile (subjected to Gaussian windowing to eliminate ringing artifacts), converted to time units via the cutting speed. The splines, added to the plot for clarity, have no physical significance. The lathe spindle rate is also shown. This is step **f** in Fig. 5.2.

In Fig. 5.12, the radial component of the online accelerometer readings is shown after integration to yield radial tool displacement as a function of the progression of the cut. That displacement profile was also used to produce a histogram, one of accelerometer-determined tool depth, shown in Fig. 5.13 alongside the stylus-measured x-z roughness profile feed mark depth distribution.

5.5 Discussion

5.5.1 Discussion of the frequency spectra

Figure 5.7 compares the radial component of the online accelerometer readings with the y-z stylus-measured roughness profile of Fig. 5.5. Immediately apparent in that figure is the sharply limited frequency resolution of the y-z roughness profile spectrum. The frequency resolution limitation is the result of computing a spectrum from a short roughness profile. The source roughness profile is short because the curvature of the part in the y-direction prohibits our roughness measuring machine from acquiring long signals, due to the mechanical range limitations of the device.

A second consequence of performing a Fourier transform on a short signal is the appear-
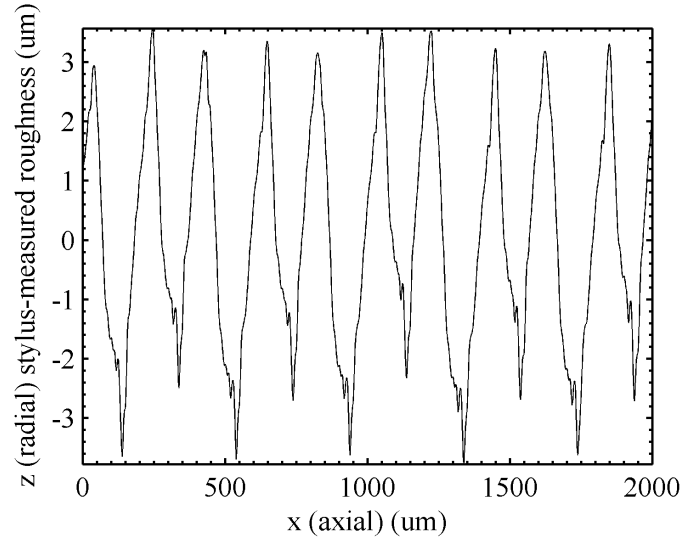
Figure 5.8:   An excerpt of an x-z (axial) stylus-measured roughness profile, showing the feed marks which are the traces of the passage of the cutting tool. The profile is quite gentle despite the accidented appearance suggested by the relative scales of the plot axes. This is step **g** in Fig. 5.2.
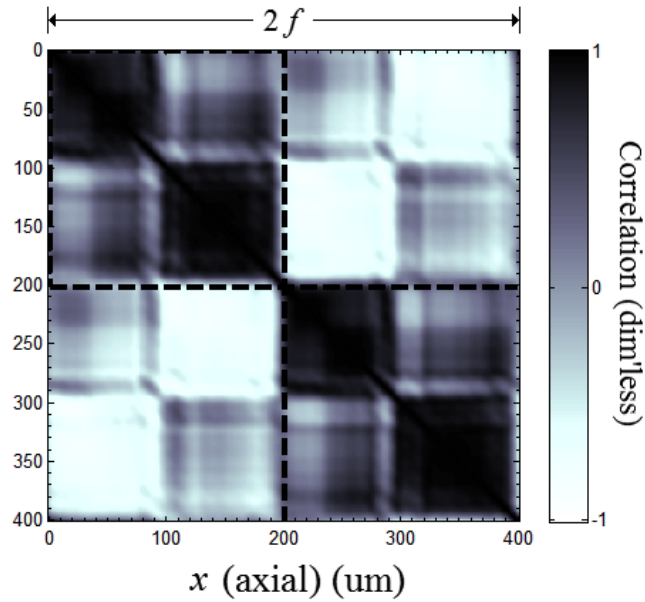
Figure 5.9:   As part of the automated analysis, the correlation map over twice the feed langth in the axial direction, used to determine feed mark position in axial roughness profiles, corresponding to the correlated domain identification (CDI) technique shown in Fig. 5.3. This is the x-z (axial) stylus-measured profile correlated with itself in segments of twice the feed. The dashed lines indicate the edges of the feed marks of the x-z roughness profile of Fig. 5.8. This is step **h** in Fig. 5.2, as are Figs 5.10 and 5.11.
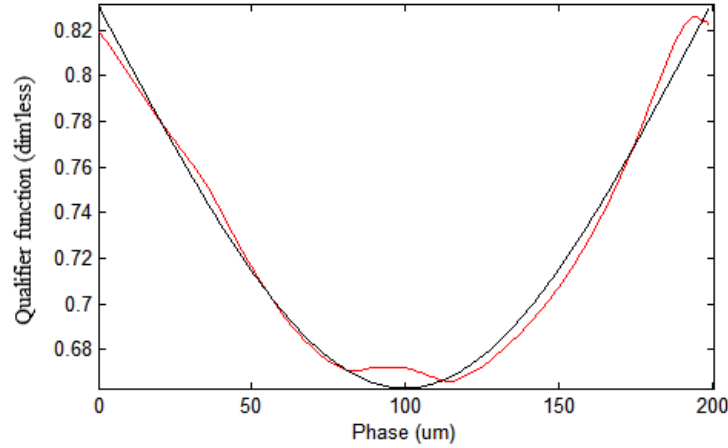
Figure 5.10: As part of the automated analysis, the qualifier function for the correlated domain identification (CDI) technique. The smooth line is the theoretical ideal, and the bumpy red line is from the correlation map of Fig. 5.9. Note that this is completely unrelated to cutting tool shape, and is scallop-shaped by mere coincidence. This is step **h** in Fig. 5.2, as are Figs 5.9 and 5.11.
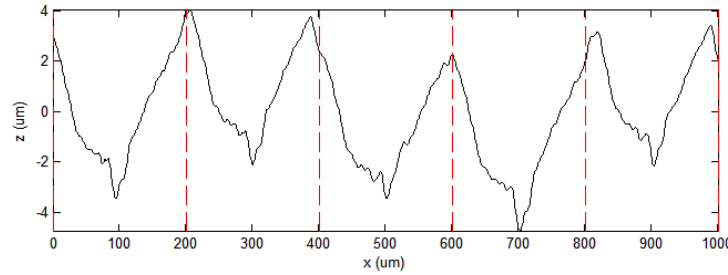
Figure 5.11: An excerpt of the result of the computer-automated feed mark identification. The dashed lines represent the edges of the feed marks as identified using CDI. This is step **h** in Fig. 5.2, as are Figs 5.9 and 5.10.

ance of ringing artifacts, which would appear as additional peaks in the spectrum. That problem was avoided by transforming the y-z profile after applying a Gaussian window (symmetrically, with the edges of the roughness profile at three standard deviations). By comparison, the accelerometer signal was transformed with a simple rectangular window, and a transform artifact is indeed visible around 4300 Hz, be it twice the frequency of the dominant mode. (Alternatively, the double-frequency peak could be a genuinely physical vibrational harmonic, but in any case the second peak is visibly negligible.)

Of course, we expect that longer y-z signals (preferably with the abilities to coordinate the roughness measuring machine axis stepper motors and simultaneously rotate the stylus, as some models may) would greatly improve the frequency resolution from the y-z roughness
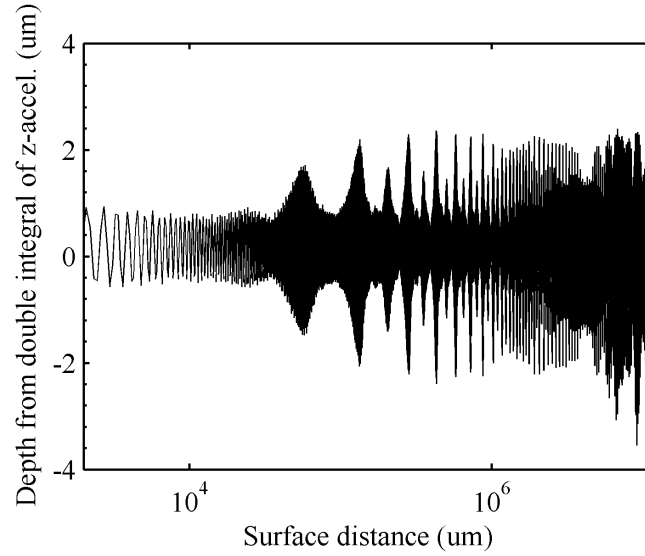
Figure 5.12: The radial displacement of the tool as a function of time, as determined by trapezoidal integration (twice) of the acceleration signal of Fig. 5.6. Again, the time axis (converted to space units via the cutting speed) is logarithmic to illustrate the system's behavior over short and long spans. This is step **k** in Fig. 5.2.
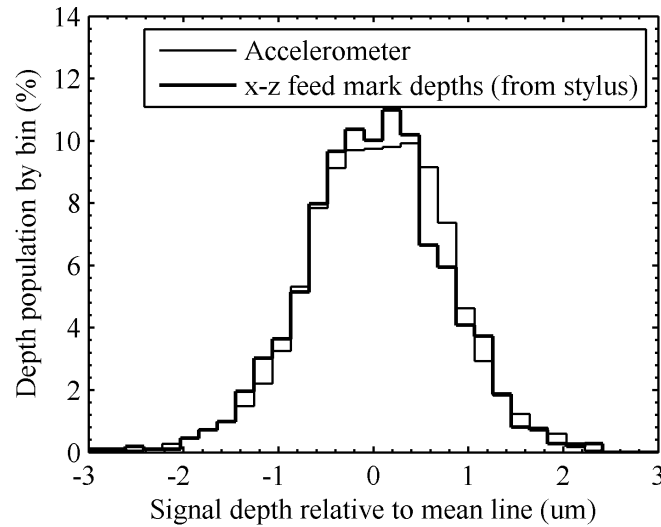
Figure 5.13: A comparison of histograms. The finer line represents the tool depth distribution (relative to the mean) determined from the accelerometer-derived signal of Fig. 5.12. The bold line is the histogram of x-z feed mark depths, from the decomposition of feed marks. This is step **m** in Fig. 5.2.

profile. Indeed, shortening the signal before performing the Fourier transform worsened the frequency resolution and increased transform ringing (not shown).

Despite the technical issues above, it is clear that the dominant frequency of both spectra in Fig. 5.7 coincide. That is a fortunate result as it confirms that feed mark depth is caused *at least in part* by the radial component of cutting vibrations. Confirmation that the feed mark depths are fully caused by those vibrations is in Subsection 5.5.2.

It is natural then to ask whether that dominant frequency is related to the spindle speed. As shown in the same figure, Fig. 5.7, the spindle speed is not responsible. Rather, given the stationarity of the vibrations (in the sense that the cut was relatively stable), it is reasonable to state that dominant vibrational frequency is a mode of the machine tool-tool-workpiece system. Consequently, it is reasonable to conclude (and perhaps, intuitively obvious) that the y-z roughness profile from the part contains an estimate of the dominant vibrational mode of the mechanical system.

A final remark, though the cut was stable, the careful reader will have noticed that the accelerometer signal in Fig. 5.12 contains the expected high-frequency component corresponding with the dominant frequency, but also a lower-frequency envelope resembling beats, suggesting twin low-frequency peaks. Indeed, a log plot of the accelerometer spectrum reveals two minor low-frequency peaks, explaining the beat-envelope.

5.5.2   Discussion of the depth histograms

The correlation map of Fig. 5.9 exhibits the block-diagonal pattern with feed-size blocks that is expected from an x-z roughness profile of a turned part. In addition to that pattern, the map also exhibits a sub-structure, consisting of two smaller blocks of about half the feed length within each feed mark. We have found that particular substructure to be very common in our research on hard turning. Interpreting the correlation map intra-feed-mark substructure blindly, the smaller pattern suggests that a given feed mark contains two regions, each region having internally correlated irregularities, as though different mechanisms had generated the halves of the feed mark. Calling upon process knowledge, indeed, we *do* expect two distinct local mechanisms in feed mark morphology, because part of the feed mark corresponds to local ploughing, in the region where the cutting tool fails to engage the workpiece material, that is, in the region that is locally beneath the minimum chip thickness. However, we do not intend to substantiate that claim in the current paper.

The ensuing qualifier function of Fig. 5.10 indicates that the feed mark phase identified in Fig. 5.9 (shown by the dotted boxes) is very clear, in the manner previously published (Provencher and Balaziski, 2016). That is to say, the qualifier function, representing the

mean correlation value within the block-diagonal region, is maximum at phase zero.[1] The x-z roughness profile of Fig. 5.11, where feed mark phase is shown with dashed lines, indicates that the feed mark edges automatically identified by the computer using the CDI method are intuitively very reasonable by visual inspection of the roughness profile.

The average depths of the feed marks so identified in the x-z profile were collected as a histogram in Fig. 5.13. The same figure superimposes a depth histogram from the accelerometer. This is the most important graph of the current paper. Knowing, from Subsection 5.5.1, above, that roughness profiles correspond in y-z spatial frequency with radial acceleration, the confirmation from Fig. 5.13 that the radial component of tool vibration also fully accounts for feed mark depths in x-z profiles confirms the hypothesis of this paper.

5.6 Conclusion

We were able to show the following:

- Azimuthal (cutting speed direction) roughness profiles of turned parts contain information about vibrational frequencies, but not the depth distribution.

- Axial roughness profiles of turned parts contain vibrational depth distribution information, but not the vibrational frequencies.

- Radial turning vibrations fully account for feed mark depths, in both spatial frequency and depth amplitude.

- The claim is sustained that the depth component of feed mark decomposition is a quantitative indicator of the influence of radial vibration on the surface roughness of turned parts.

- Consequently, it is valid to estimate percent contribution of radial vibration to any amplitude roughness parameter, using only a linear roughness measuring machine and mathematical removal of vibration effects from profiles.

- Turning vibrational frequencies may be estimated using only a linear roughness measuring machine.

- Turning vibrational amplitudes may be estimated using only a linear roughness measuring machine.

Naturally, claiming the above in a general manner for hard turning would require many tests under many conditions.

---

[1]Note that the figures were redrawn after identifying the phase, to generate the figures with the feed mark phase set to zero.

Though the conclusions of the paper are relatively simple, the hypothesis that radial vibration accounts for feed mark depth need no longer be a blind assumption. In particular, experimental verification that feed mark depths in x-z roughness profiles do quantify radial vibration was necessary as a step towards the goal of the series of papers described at the top of this paper: To develop the ability to acquire a single roughness profile from a turned part, submit the profile to automated analysis software, and obtain estimates of the percent contributions of individual distinct physical phenomena to whichever roughness parameters the designers happen to have specified for the part.

5.7   Acknowledgements

CHAPTER 6

GRAPHICAL SOFTWARE IMPLEMENTATION

The work was financed largely by way of a CRIAQ project, sponsored as indicated in the Acknowledgements section. As part of the deliverables of that project, a graphical software implementation of the techniques developed in this thesis was produced, all of it coded from scratch. The implementation includes treatment and filtering of experimental roughness profiles and the ability to estimate the contribution of radial vibration and of total variabilities to surface roughness parameters. It also includes other work, including a tool for estimation of microgeometrical stress concentration by finite elements, and the ability to produce response surfaces from designed experiments.

The codes are also neatly documented and many have command-line versions for future developers.

6.1 Roughness Profile Treatment and Filtering

This part of the software involves the following:

- Interpretation of raw roughness profile files from roughness measuring machines. The profile files may vary in format by manufacturer.

- Inclination correction and frequency filtering.

- Evaluation of some ordinary roughness parameters.

Frequency filtering is done using a Gaussian filter in the manner described by the ISO standard (ISO 11562:1996, 1996), allowing for a frequency band from the signal to be preserved as "roughness" (i.e., eliminating high and low frequencies as desired). Sometimes, a user may wish to filter frequencies manually; when the filter characteristics are modified, the effects on the roughness profile and on the roughness parameters update immediately. The filtering panel is shown in Fig. 6.1.

6.2 Estimation of Cutting Variability Contributions to Roughness

This step is the software implementation of the goal of this thesis, which is the estimation of the percent contributions of specific cutting effects to arbitrary amplitude-based roughness parameters. The steps of this portion of the software are as follows:

- Determination of the effective machining length.

- Determination of the phase of the feed marks in the roughness profile.

- Estimation of the percent contributions of radial vibration and of all variabilities to roughness parameters.

6.2.1 Determination of the effective feed length

The nominal feed length should normally be known; it is the feed per revolution value set on the lathe. However, it is important for this analysis to be somewhat more precise. Even assuming that the roughness measuring machine axes are calibrated perfectly, the feed marks appearing in a roughness profile will normally be slightly shorter than the nominal feed length due to parallax error between the axis of the turned part and the axis of the roughness measurement machine. For this reason, the power spectrum (Fourier transform) of the roughness profile is used to estimate the feed-induced periodicity as it appears in the roughnes profile more precisely than by merely using the nominal feed length.[1] The power spectrum panel in the graphical software is shown in Fig. 6.2.

The software automatically estimates the effective feed based on the spatial frequency of greatest amplitude. Note that because of the discrete nature of the discrete Fourier transform, the true maximum is estimated by interpolation between the highest point and second-highest point, as shown in Fig. 6.2. On the panel, there also appears a graph with two colored rectangles. As the user tweaks the effective feed (if desired), the user should seek to maximise the apparent sharpness of the colored rectangles of that graph. This is in fact the top half of the Correlated Domain Identification (CDI) correlation map introduced in Article One (Chapter 3) and shown below implemented in the software.

6.2.2 Determination of the phase of the feed marks in the roughness profile

After the above steps of roughness profile frequency filtering and determination of the effective feed length, it is necessary to determine the locations of the feed marks in the roughness profile. This is done using the Correlated Domain Identification (CDI) technique developed in Article One (Chapter 3). The implementation is shown in Fig. 6.3. The computer automatically estimates the locations of the feed marks, but the user may inspect the correlation map to identify the feed mark block diagonal pattern manually. The panel also includes the qualifier function to aid in selecting the correct feed mark phase. (As always, the shape of the

---

[1]Using the nominal feed length was a mistake realized after Article One (Chapter 3). This is discussed in the General Discussion.

qualifier function is completely unrelated to feed mark shape, and this technique functions for any feed mark shape.)

6.2.3 Estimation of the percent contributions of cutting effects to roughness parameters

Once the feed mark phase has been identified, the feed marks may be decomposed. Because only the feed mark variability mode that describes relative feed mark depths was experimentally verified as indeed corresponding to the physical mechanism responsible (radial cutting vibration), the graphical implementation only estimates the contribution of that component to roughness parameters, and the contributions of all all variabilities combined. In Fig. 6.4, the contributions are expressed as percentages, indicating what values the roughness parameters might have without radial vibration and without any variability between feed marks. The radio buttons are used to have the program display what the roughness profile might look like without those variabilities.

6.3 Finite element estimation of microgeometrical stress concentration

The graphical software also includes an ability that is not directly related to the goal of this thesis, but that was developed in parallel. It is a tool which takes an experimental roughness profile as input, places it on the top of a virtual block, meshes that system, and estimates microgeometrical stress concetration by finite elements. The purpose was to provide an alternative to the usual means of estimating microgeometrical stress concentration, which is either: to estimate stress concentration by applying a parabola to the roughness profile manually in order to estimate stress concentration as though the local roughness were an elliptical notch (Arola and Williams, 2002) (that technique is prone to a significant operator effect); or, to estimate stress concentration using an expression involving some roughness parameters (Arola and Williams, 2002), typically a parameter of amplitude and one of lateral peak spacing. Finite element estimation of microgeometrical stress concentration is not novel.

The model of the graphical software uses two-dimensional eight-node biquadratic quadrilateral elements, and supposes that stress is applied on the ends of the block (see Fig. 6.5). The model is purely elastic and is meshed to prevent stress singularities (which would cause stress to increase without limit for increasingly fine meshes). The model converges for its parameters (mesh size and block depth, explained below), and approaches analytically expected stresses for reasonably fine meshes. The code was written to be efficient, and was coded from scratch.

The stress singularities were avoided by meshing using elements with parabolic edges.

The parabolic edges were furthermore constrained to meet at a common slope, such that meshed roughness profile, and indeed the displacement field of the entire model, is everywhere spatially once differentiable. The result is a model that converges for element size.

Whereas similar models are often use an elastic-plastic model to avoid stress singularity, those models consequently require material properties as inputs. In keeping with the principle of this thesis, which is to derive quick information about a part in production using only a single roughness profile, the use of an elastic model simplifies the modeling process for the convenience of the operator.

Another issue does not arise from the finite element model but from the measurement resolution of the apparatus used to acquire the experimental roughness profile. Finer roughness measurements will always reveal finer surface details, each potentially raising stress at the surface of the meshed block. This issue is operationally resolved by considering that the assumptions of material homogeneity and of the elastic model cannot be expected to hold at scales approaching the grain size. Therefore, before meshing, the computer digitally resamples the roughness profile at a rate such that the digital roughness profile points are spaced by a distance equal to the characteristic scale of the material. The characteristic scale may simply be chosen to be a representative grain size.

The setup panel for the finite element model is shown in Fig. 6.6. The result of the simulation is shown in Fig. 6.7.

Convergence for mesh size is shown in Fig. 6.8. Convergence for block thickness is shown in Fig. 6.9, in which the "block thickness ratio" is defined in Fig. 6.10. Validation using known stresses is shown in Fig. 6.11 and is accomplished by means of elliptical notches.

6.4   Response Surface Generation

The final feature of the graphical software is the ability to display roughness parameters including estimates of roughness parameter values in the absence of particular components of feed mark variability and including finite element stress concentration. The panel is shown in Fig. 6.12. The response surface panel accepts designed experiments with any number of independent variables and any number of response variables, and plots the 3-dimensional cross-section of the fitted hypersurface. It may also display uncertainty surfaces for any confidence level and the projections of the data points into the 3-dimensional space of the plot.
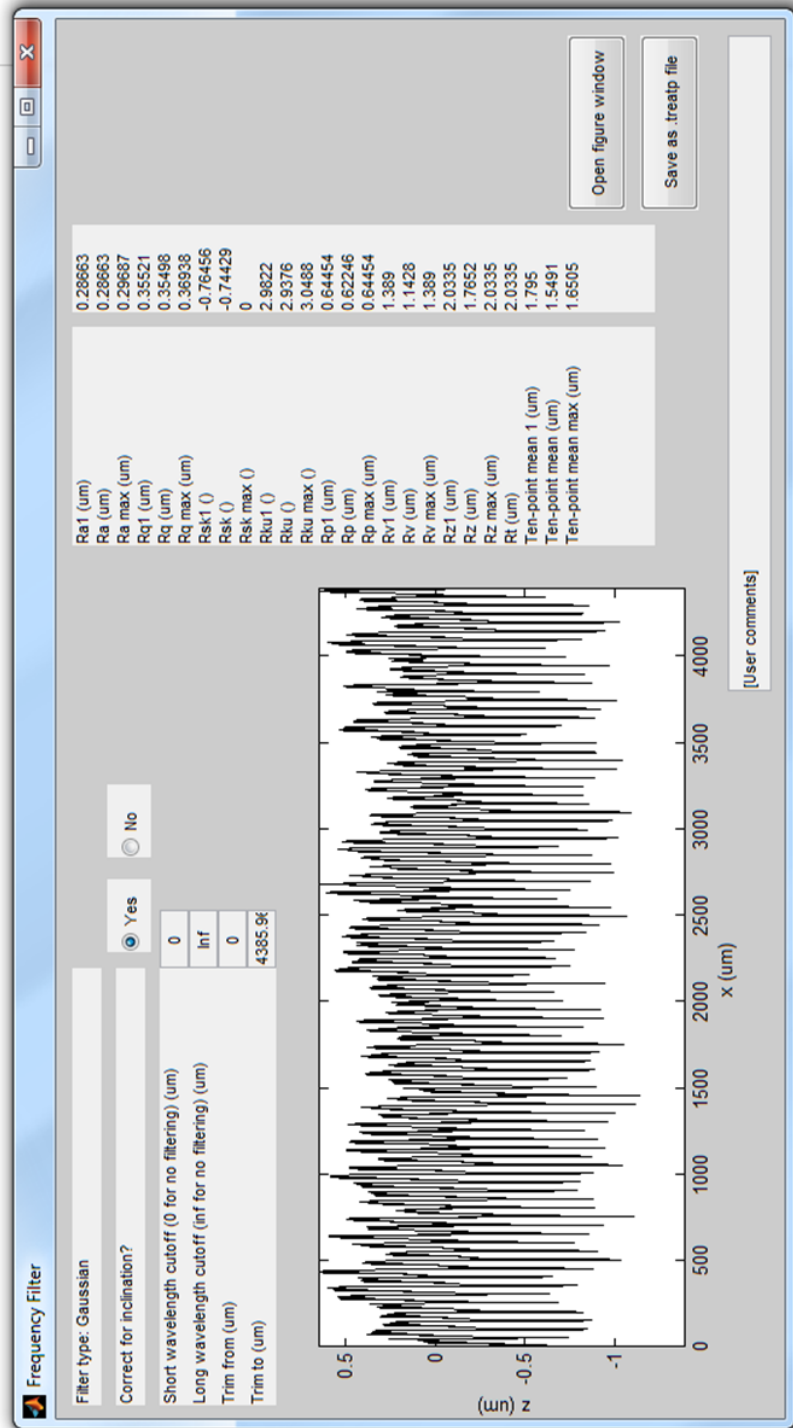
Figure 6.1: The frequency filtering panel of the graphical software implementation
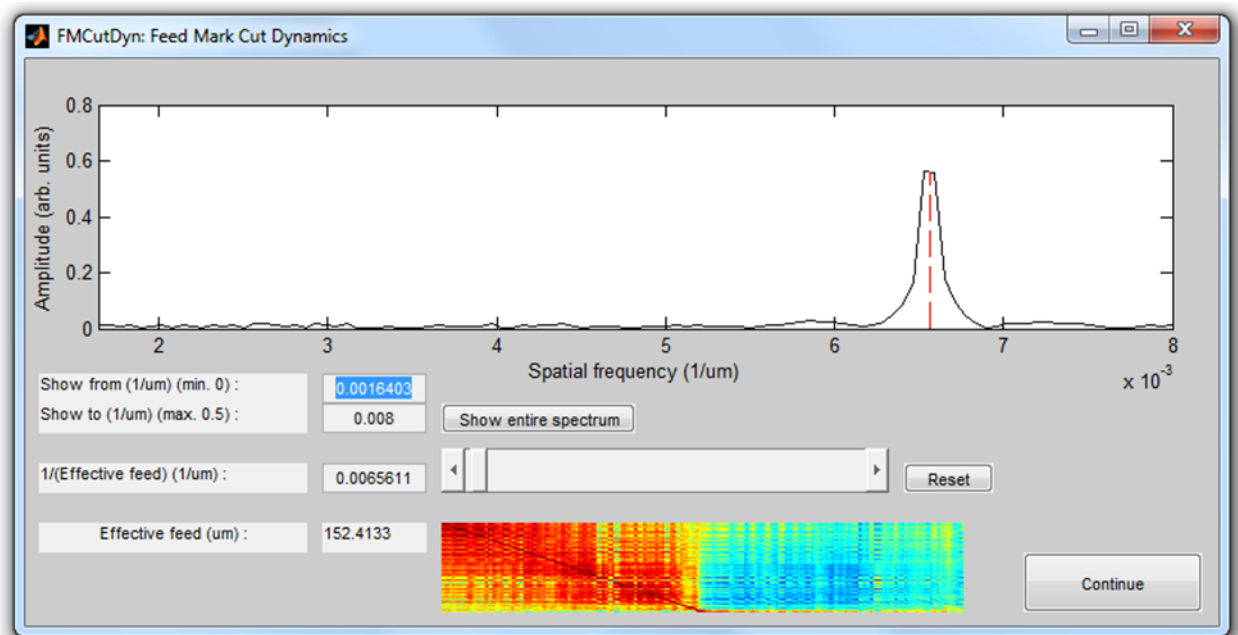
Figure 6.2: The power spectrum panel of the graphical software implementation. The colored rectangles are explained in-text.
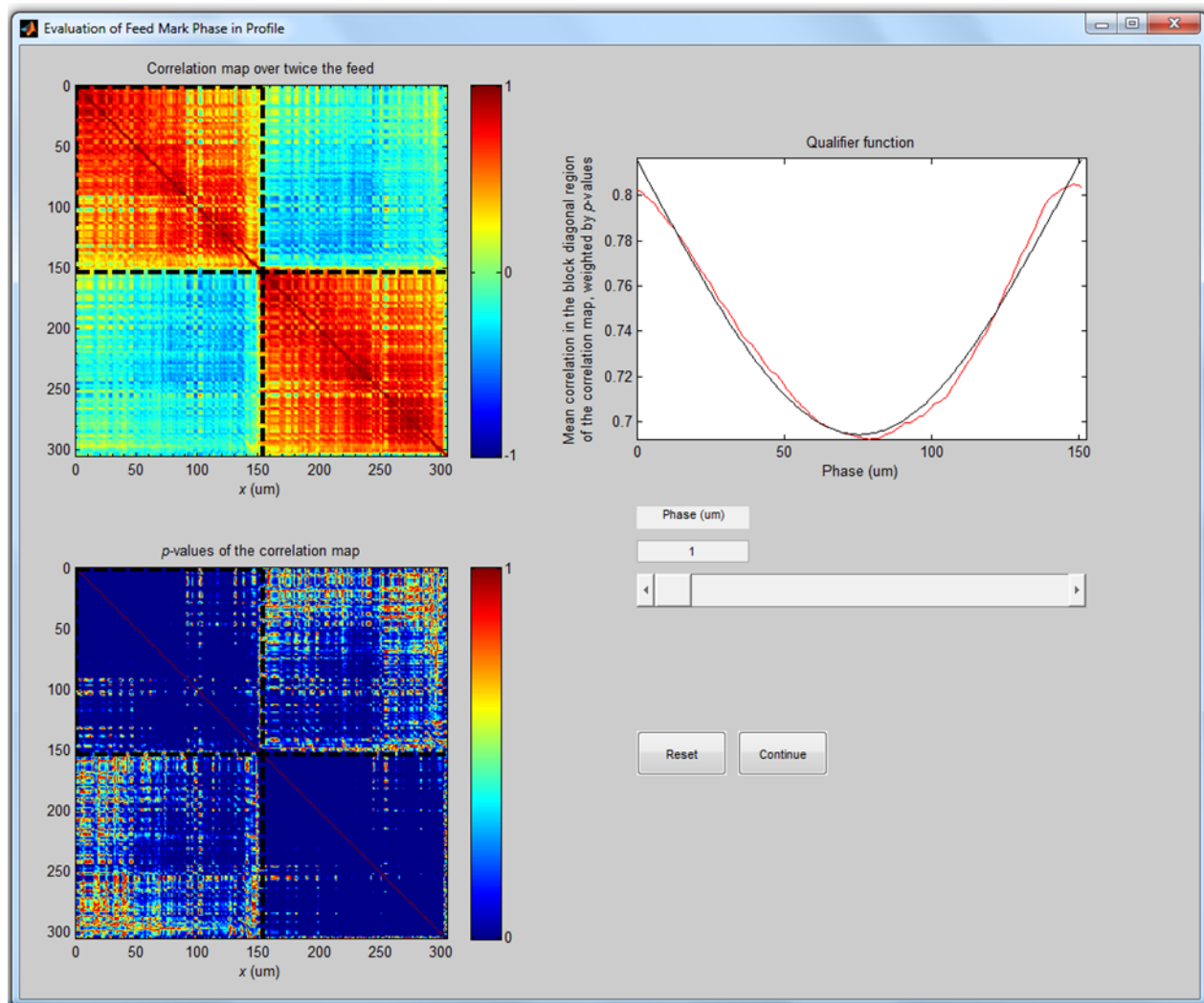
Figure 6.3: The correlation map panel of the graphical software implementation. This is the Correlated Domain Identification (CDI) technique developed in Article One (Chapter 3).
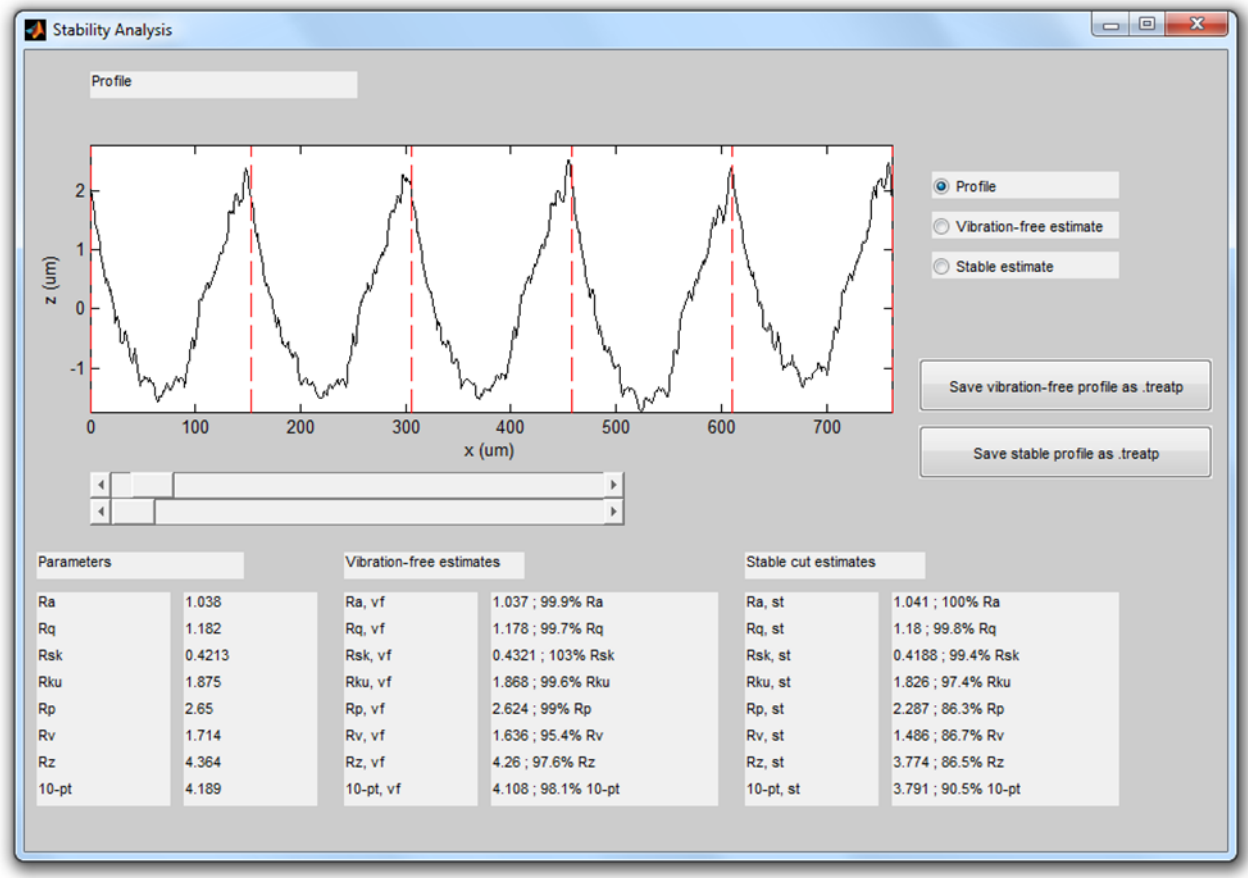
Figure 6.4: The panel of the graphical implementation estimating the contributions of feed mark variabilities
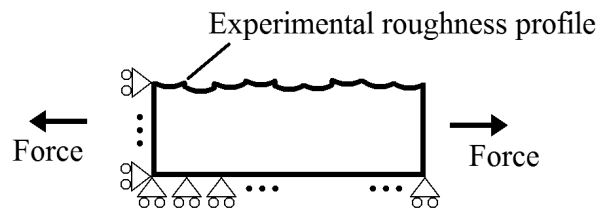
Figure 6.5: Diagram of the finite element model used
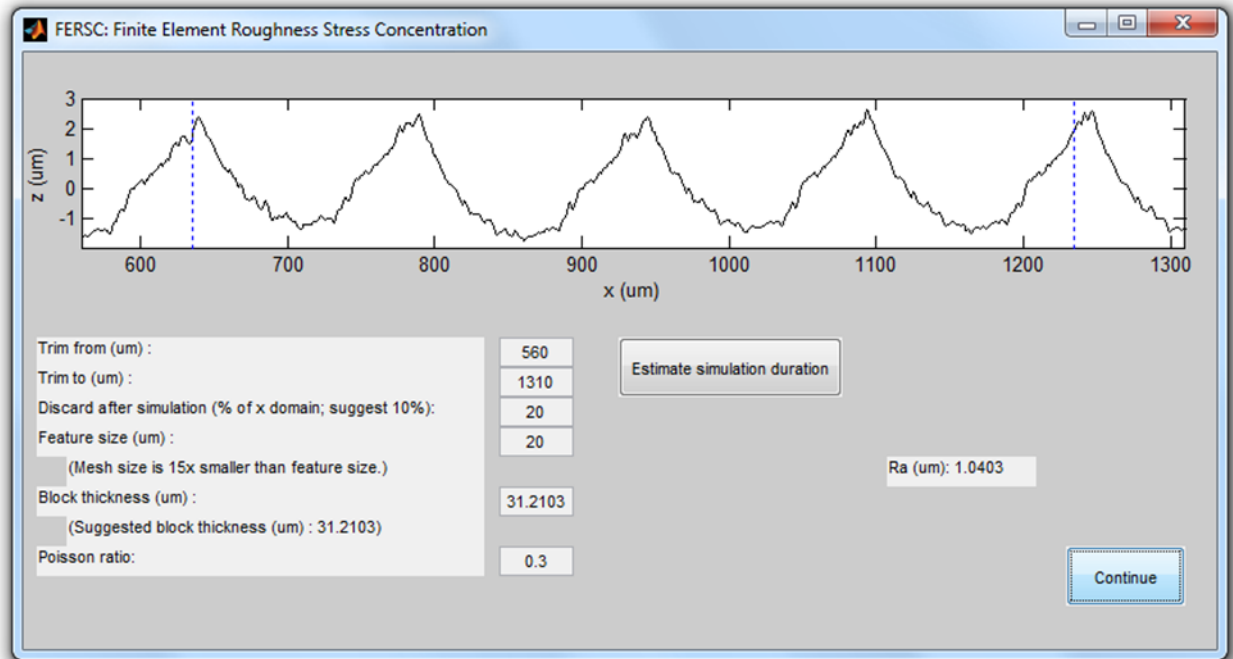
Figure 6.6: The setup panel for the finite element estimation of microgeometrical stress concentration
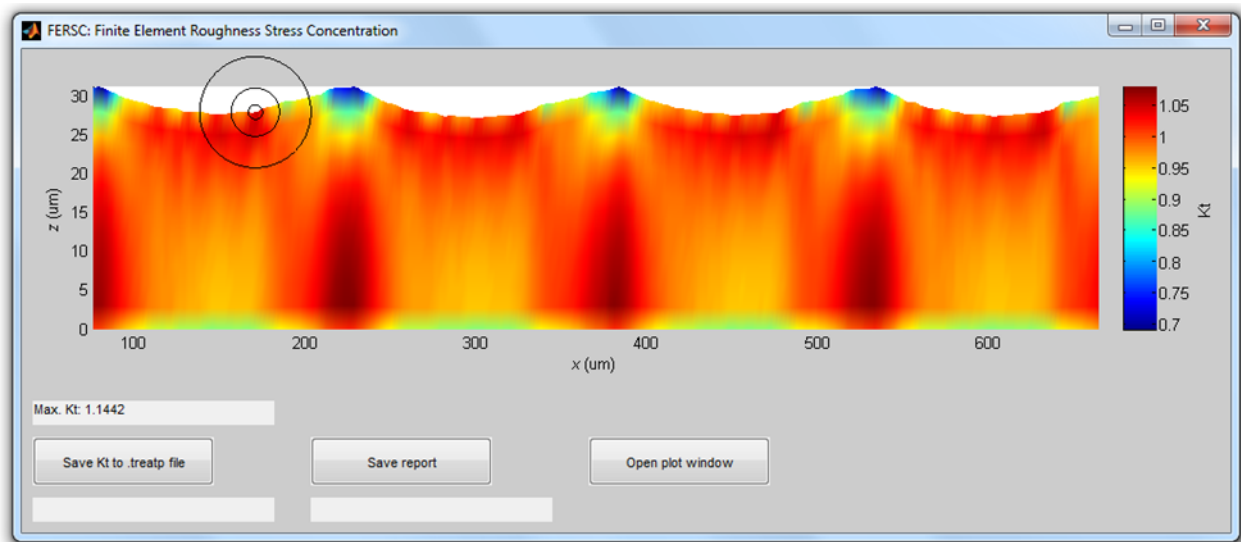
Figure 6.7: The result panel for the finite element estimation of microgeometrical stress concentration, showing the location of maximal stress. Note that although the model is computed to scale, the plot axes are not to scale, giving the appearance of dense vertical stripes.
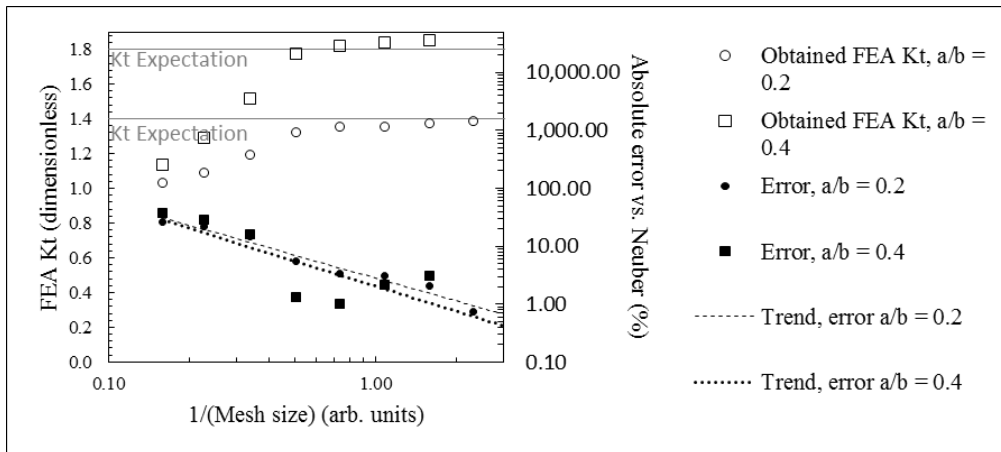
Figure 6.8: Mesh size convergence. a/b represents the proportions of an elliptical notch, for which the analytical maximum stress concentration is known. The graph shows that convergence for mesh size is obtained, and the convergence approaches the analytically expected values.
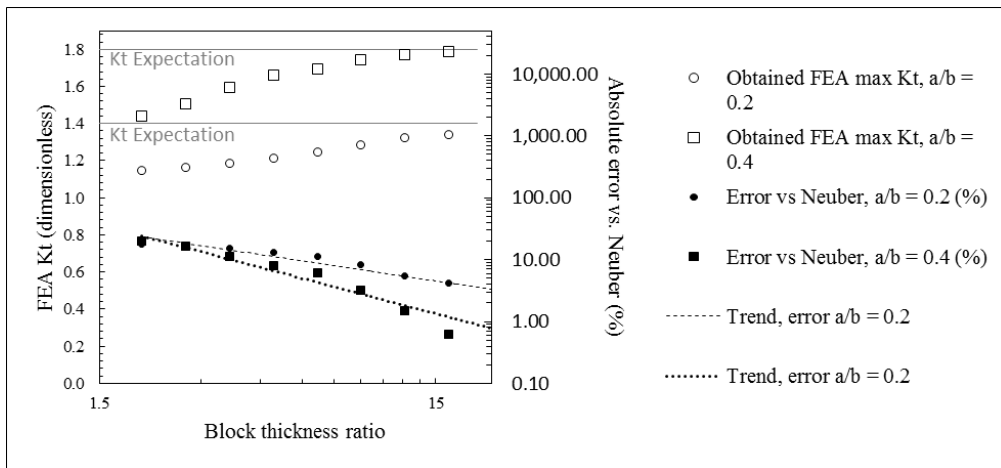
Figure 6.9: Convergence for finite element block thickness
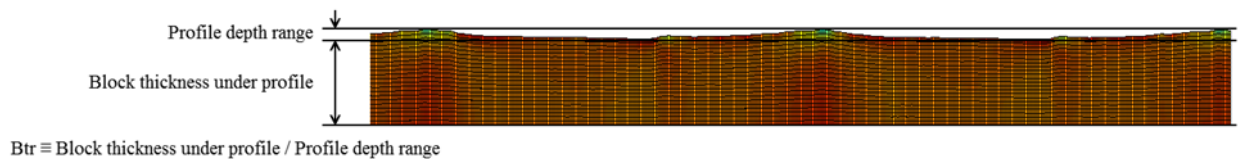
Figure 6.10: Definition of "block thickness ratio" as used in Fig. 6.9
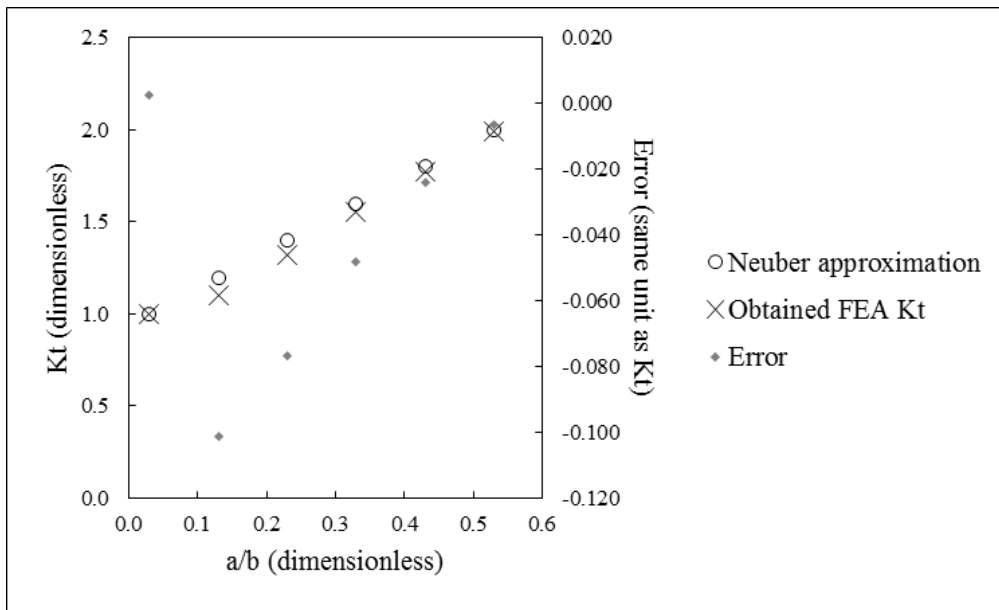
Figure 6.11: Validation of the finite element model using elliptical notches of known maximum stress concentration. Typical settings were used, to represent results using a relatively coarse mesh and computation in under a minute on an ordinary desktop computer (∼3 GHz, single thread processing).
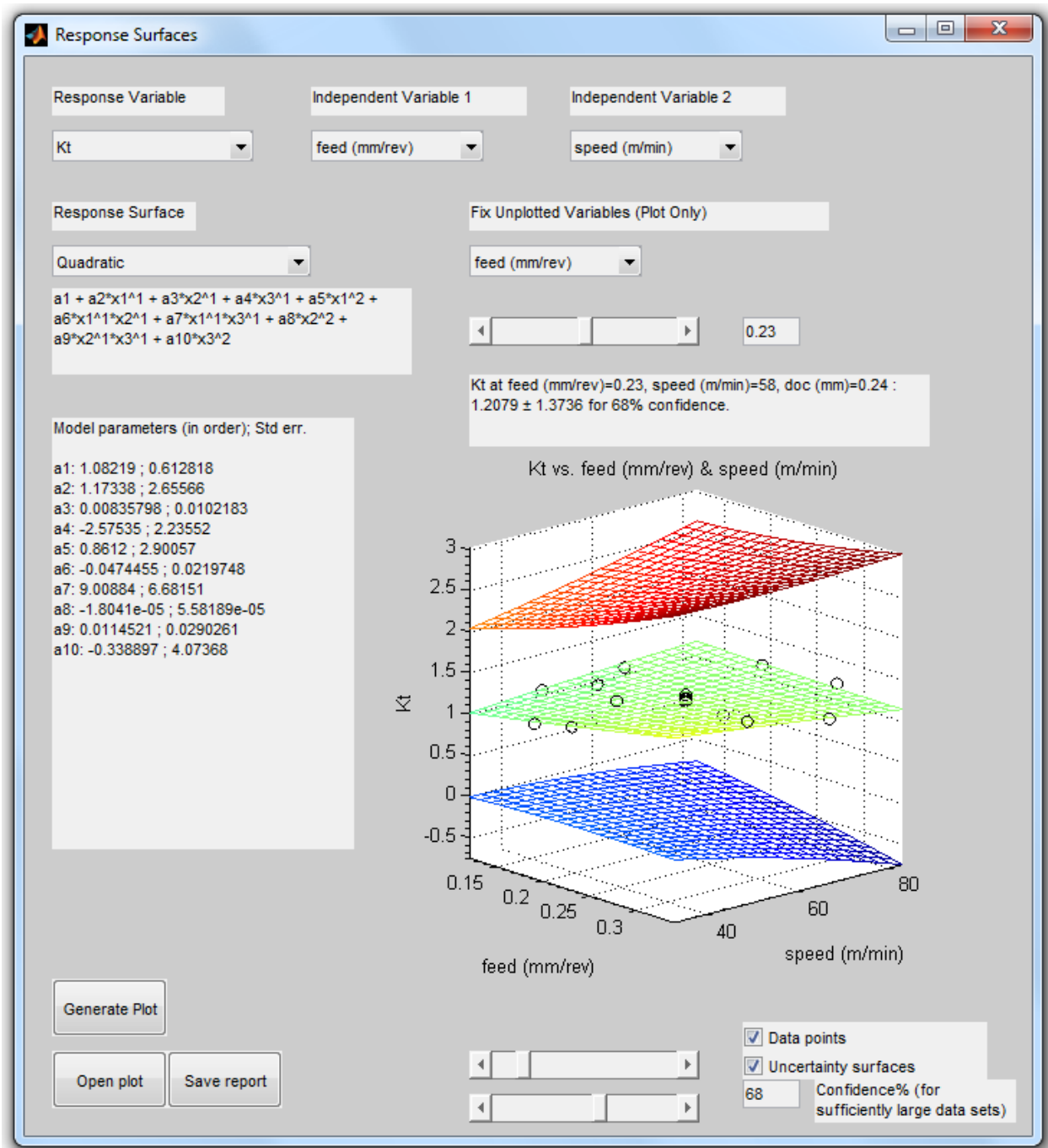
Figure 6.12: The response surface panel of the software developed

CHAPTER 7

GENERAL DISCUSSION

Here, the principal results of the work are discussed in light of what has been learned. This includes a brief description of some unsuccessful approaches that are not involved in the papers included in this thesis. There follows a discussion of the scientific results of the work. In particular, the importance of using precisely determined effective feed mark length when dissecting roughness profiles should be stressed. Indeed, not having used effective feed is a mistake made in Article One. Finally, we discuss in what ways the work of this thesis has contributed to producing a practical support tool for production, and some limitations of the work.

7.1 Unsuccessful Approaches

Throughout the work leading to this thesis, many unsuccessful approaches were attempted. The mention here of some of those attempts should not suggest that those strategies *cannot* work, merely that they didn't work and why they were abandoned.

Early in the research, several months were spent attempting to generate convincing hypothetical predicted roughness profiles at untested machining conditions, based upon roughness profiles from surrounding, tested conditions. This proved frustratingly unreliable, and led to the later strategy of idealized modes of variability. The reason that interpolating profiles themselves is unreliable may be understood in the light that a roughness profile or feed mark encoded as a $z(x_i)$ digital signal of n points behaves as a system with n degrees of freedom, and where the number n depends on the signal length and the sampling rate. Such a description inevitably has either insufficient or superfluous degrees of freedom and none are related to the physics of surface generation nor to the physics of part performance. A hypothetical profile at interpolating machining conditions may provide a reasonable estimated profile some of the time, but never reliably. Indeed, in practice and for good reason, roughness profiles are reduced to one or a handful of scalar roughness parameters, and *those* provide interpolations as response surfaces. These descriptors are significantly more reliable and the response surfaces may usually be validated successfully with validation runs.

Before trying principal components, other parametrizations of roughness profiles were attempted. In particular, time series prediction methods including the use of Lyapunov exponents were tried, but the time series prediction approach did not work at all and was

abandoned after a month. It is possible that it could work.[1]

Could principal components of feed marks be interpolated between machining conditions? A subset of the principal components from a profile could be chosen to describe the feed mark morphology using a reasonable number of degrees of freedom, and those degrees might be reasonably related to the physics of the situation. Two major problems present themselves there. First, the dominant principal components from a roughness profile in an experiment design are difficult to equate in a computer-automated way to the visually different principal components of another roughness profile in the experiment campaign. The principal components are also not always obviously related to physical modes of variability. Second, profiles with different feed lengths make direct comparison impossible, requiring some means of scale transformation. The barrier for that scale comparison is the scale-dependence of intra-mark structure such as the intra-mark location of local ploughing. Much more plausible is the comparison of idealized components as presented in Article Two. Even then, it may be difficult to interpolate between roughness profiles in any manner that is reliable, practical and automatable enough to use in a support tool for production.

Indeed, description of roughness profiles using principal components, rather than idealizations of the components, also works poorly. Again, principal components don't always relate directly to physical modes of feed mark variability. In addition, using the first few principal components only and neglecting the rest produces "hairy" feed mark representations, because the sum of the many unused principal components may indeed have a significant contribution even with a variance sum under 5%.

Independent Component Analysis (ICA) may be more reliable for estimation of the modes of variability. ICA was attempted, but unfortunately was too heavy computationally to be practical, is significantly more complex than principal component analysis, and didn't offer any significant boost to the reliability of the results.

It is worth mentioning also that the techniques developed in this thesis were tried on roughness profiles of turned *composite* parts, and that didn't work at all. The fibrous structure of the composite parts added far too much noise to the signals.

As a final example of an abandoned approach, describing a roughness profile by the statistical spread (e.g. standard deviation) of its principal component scores by feed mark didn't work at all. This is because the statistical distributions of the scores among the feed marks of a profile of the feed mark principal components of that profile are often not even

---

[1]In the author's opinion, the most meaningful and successful time series parameters would be selected not purely mathematically but rather based upon process knowledge. In particular, any chaotic behavior might be best described starting from a physical model of turning as a dynamical system (a system that influences itself recursively).

remotely Gaussian, even involving multiple peaks.[2]

7.2 Scientific Results

Some major points from the papers in this thesis are briefly recapped here.

7.2.1 Feed mark correlation maps

Correlation maps over segments of roughness profiles are a new idea first published in Article One. The correlation maps conveniently illustrate inter-mark and intra-mark structure. In particular, these maps are the basis of the Correlated Domain Identification (CDI) method of Article One for the identification of the phase of the feed marks in roughness profiles, irrespective of feed mark shape, and often even when the feed marks cannot be identified visually.

The identification of the feed marks by correlation map exploits the fact that each feed mark is generated by a distinct physical event, that is, by a separate pass of the cutting tool. As such, the random variabilities in the profile are correlated with one another within feed marks, but not between feed marks. This results in the block diagonal structure that in most cases clearly shows the positions of the feed marks in the roughness profile.

In Article One, it was also shown that random variabilities in feed marks may sometimes be correlated with the variabilities of neighboring feed marks. This may be due to certain effects active during the cut lasting longer than a single revolution of the workpiece on the lathe. Sometimes, there appears to be a negative correlation between adjacent feed marks. This would suggest the presence of a periodic mechanism with a period that is an integer multiple of one revolution.

It is very important when decomposing feed marks to use a precisely evaluated effective feed length, which is usually slightly shorter than the nominal feed mark length. One mistake made in Article One was to use nominal feed length. Doing so results in blurry correlation matrices, and often causes false structure to appear in the correlation matrices due to a systematic overlap of segments, as the segments fall out of phase with the real feed marks along the length of the roughness profile. That type of false structure may, in hindsight, be the cause of the apparent structure in Fig. 3.8, for example.

As shown in Fig. 6.2, one means of determining the effective feed length precisely is to use the power spectrum. Because the power spectrum necessarily has limited frequency resolution, the location of the feed peak may be estimated by interpolation between the

---

[2]In the author's opinion, a realistic roughness profile prediction should nonetheless involve some stochastic component to make each feed mark unique!

greatest near-feed peak and the tallest neighboring point, as also shown in Fig. 6.2.

Sometimes, it may not be convenient or possible to measure very long roughness profiles from a surface. In those cases, it has been found that using the feed marks from multiple independent repeat roughness measurements from a surface is a very decent substitute for a long profile, though that claim is not conclusively shown in this thesis. The validity of co-opting marks from multiple profiles from a single surface is intuitively expected, assuming the process is stationary. In any case, it is always better to use larger feed mark samples than small ones. The sensitivity of the qualifier function to the number of feed marks was shown in Fig. 3.16.

Another point visible everywhere but not explored in this thesis is the *intra*-mark block-diagonal structure. It is particularly evident, for example, in Fig. 5.9. It should be verified experimentally to be sure, but it seems clear that that intra-mark block-diagonal pattern indicates that feed marks are subject to two segregated generation mechanisms (this could be termed "halving", from the appearance of the correlation maps.). Indeed, we expect that to be the case, as that would be the local ploughing effect described in Article Two. That is, part of each feed mark in finish hard turning is cut, and part is "burnished" where the tool edge fails to engage the workpiece material due to insufficient chip thickness. It would be interesting to compare residual stress, microcracking, and microstructure between the cut and "burnished" regions.

7.2.2 Modes of feed mark variability

Feed marks in a given roughness profile from a hard finish turned metallic part vary according to a handful of modes of variability[3], as shown in Fig. 4.10. The greatest mode by far corresponds to the radial component of machining vibration, and the other modes detected appear to correspond to axial vibration, local ploughing, and side flow.

Principal Component Analysis (PCA) reveals those modes without coercing the data by fitting. However, PCA does not distinguish the modes cleanly nor reliably. Independent Component Analysis may divide the modes more reliably, but it is also heavier computationally, and is still fallible. For these reasons, idealized versions of the modes, inspired both from the PCA breakdowns and process knowledge expectations from the literature, are a preferred means of breaking down the feed marks.

Some modes of variability, specifically ploughing and side flow, may be best treated as a static contribution to all the feed marks of a roughness profile. As described in the literature review, some researchers have proposed means of estimating the contribution of material

---

[3]As mentioned before, Ancio *et al.* remarked that a few principal components suffice in their 2016 paper (Ancio et al., 2016).

response as a whole to roughness profiles. It may not in fact be necessary to quantify material response variability; it may suffice to express the dynamic contribution of radial vibration and the static contribution of material response.

Of course, scientifically, it would be most interesting to verify experimentally that the ploughing and side flow modes of variability are indeed fully accounted for by those mechanisms.

7.2.3   The radial vibration variability mode

The radial component of machining vibration fully accounts for the relative depths of feed marks in x-z roughness profiles, both in spatial frequency on the surface and in amplitude. The result that the amplitude of variability in feed mark depth is fully accounted for by the radial component of vibration is shown in Fig. 5.13. Verifying that was a necessary step towards creating the support tool for production. It sustains the claim that the depth mode when decomposing feed marks is a quantitative indicator of the influence of radial vibration on the surface roughness of hard turned parts.

A secondary result of Article Three is that azimuthal (cutting speed direction) roughness profiles of turned parts contain information about vibrational frequencies and that axial roughness profiles of turned parts contain vibrational depth distribution information. This result is borderline intuitively obvious but it is good to see that claim demonstrated experimentally. A roughness measuring machine may therefore be enough to estimate the dominant machining vibrational frequencies, and perhaps more importantly, quantify the influence of the vibration on arbitrary roughness amplitude parameters.

Indeed, as Article Three concludes, it is therefore valid to subtract away this radial vibration variability mode digitally from an experimental roughness profile in order to estimate the percent contribution of radial vibration to any amplitude roughness parameter, using only a linear roughness measuring machine. While studying roughness profiles, it was found often that the variation in feed mark depth contributed much more or sometimes much less than visual appraisal seemed to indicate. Quantitative expression of the contribution of vibration to a roughness parameter would seem to be much more accurate than eyeballing.

Naturally, digitally modified experimental roughness profiles do not express reality. This is true as soon as a roughness profile undergoes any transformation, including frequency filtering. The estimation of variability mode contributions is at best an indicator and is never a substitute for critical thinking on the part of a machining specialist.

7.3 Development as a Support Tool for Production

This thesis involves practical contributions in addition to scientific contributions. As shown, a documented graphical software tool was developed and delivered to the industrial partners listed in the Acknowledgements section, which are Pratt & Whitney Canada and Héroux-Devtek. The software automates as much of the analysis as possible, and requires only a roughness measuring machine to use.

In sum, the software created gives the ability to collect a single linear roughness profile from a hard finish turned part for the following to be estimated: the percent contribution of radial cutting vibration to various roughness parameters, microgeometrical stress concentration, and in the case of a designed experiment, empirical predictions of the above using response surfaces.

Importantly, the support tool was made with all the principles outlines in Section 1.3 in mind. It requires no special equipment, provides practical results (the contributions to arbitrary roughness parameters rather than to esoteric parameters unused by industry), and is simple to employ.

Indeed, analysis is as automated as possible in the software for the convenience of the operator:

- The software automatically suggests a filtering cutoff.

- It automatically appraises the roughness profile to suggest a precise estimate of the effective feed length.

- The software automatically identifies the phase of the feed marks.

- The software also saves all the roughness parameters to file, including the vibration-free estimate versions, and can load them up all at once when generating the designed experiment files used with the response surface capability.

- The response surface portion automatically generates the prediction model for any number of predictor variables and any number of response variables, and can display uncertainty surfaces.

- All the results the software provides are saved as human-readable text files or as graphs.

Additionally, the finite elements portion of the software is a purely geometrical analysis. It requires only a roughness profile and a characteristic grain size. It does not require any other knowledge of the material.

A note on algorithm efficiency. Considerable effort was put into making all the codes quick to use on an ordinary desktop computer ($\sim$3 GHz, single-thread). In particular, the

CDI method was written so that upon computation of the qualifier function, for each value of phase, the mean correlation of the block-diagonal region at that phase recycles the calculation for the previous phase value. The software as a whole could also likely be made even more efficient by rewriting key parts in the C programming language rather than Matlab, but is already sufficiently fast for the author's taste. Analysis is done in seconds (normally fewer than five, a considerable improvement over the minutes it took earlier in the study). The finite elements portion takes the most time and may take seconds to hours depending on length of the roughness profile and the relative size of the crystal grains.

7.4 Limitations of the Study

This thesis is subject to several limitations. In scope, it is limited to hard finish turning of cylindrical metal parts. The experiments described in the papers also make use of a limited selection of workpiece materials. Furthermore, only one of the the modes of feed mark variability (albeit, the most influential one by far) was verified experimentally to be caused by its suspected mechanism.

The support tool is of good quality and the codes are documented for reuse by any future developers. As described above, the methods are mostly automated for the convenience of the operator (Section 7.3). It must be stressed however that the software created is not of commercial quality. And, though the burden on the operator was reduced as much as possible, the analysis still requires some critical thinking. Indeed, if the double-feed correlation map of a roughness profile does not exhibit a block-diagonal structure, then the feed marks do not vary detectably in depth (though that, and other pitfalls, are noted in the software manual, not included in this thesis).

As well, it is important to remark again that this thesis focuses on modes of feed mark variability, not upon static contributions to all feed marks. Static contributions are touched upon in Article Three, and have been discussed by other authors in the literature, and the focus of the current study remains variabilities. Indeed, in practice, for finely finished critical surfaces, process stability, part reliability, and reproducibility of the surface integrity may often be more important than maximizing surface quality. In production, when roughness requirements are met, improving the roughness further may not be economical; however, maintaining a reliable output should be! That is the reasoning behind the focus on variability.

CHAPTER 8

CONCLUSIONS AND RECOMMENDATIONS

The work described in this thesis falls into two major categories: scientific results and development of a practical graphical software implementation suitable for use as a support tool for production. The results are summarized in more detail in Sections 7.2 and 7.3. Some limitations of the work are also explained in Chapter 7.

Operationally put, this describes a new method by which a computer may automatically locate the feed marks in linear roughness profiles by exploiting random variabilities of the cutting process. Modes of cutting variability were identified and idealized, such that a computer may automatically decompose a roughness profile into the contributions of specific mechanisms to the roughness of a given part. The mechanisms identified are the radial and axial components of machining vibration, local intra-mark ploughing, and side flow. The signature of radial vibration was verified experimentally, confirming that radial vibration fully accounts for variation in feed mark depth, not only in terms of spatial frequency on the part surface, but also in amplitude.

Those results were exploited to create a practical software tool. The tool enables an operator to submit a single linear roughness profile from a hard finish turned metallic part and obtain estimates of the percent contributions of radial vibration and of all modes combined to the values of arbitrary roughness parameters of profile amplitude. The software developed includes other features including finite element estimation of microgeometrical stress concentration and response surface generation. The software tool is designed to be quick and easy to use, requiring no special expertise and no special equipment, and to yield practical results such as radial vibration increasing R_a or some other parameter by some $x\%$.

The work is limited by the narrow selection of workpiece materials and cutting tools used and directly concerns only cylindrical hard finish turned metallic parts.

Future work was taken into consideration. The codes developed were documented and the code was segregated into clean individual program functions, such that future work need not recreate thoroughly evolved code.

The author suggests that future researchers consider verifying that ploughing and side flow indeed fully account for the feed mark decomposition signatures described in the work. Perhaps this could be accomplished by controlling workpiece hardness and examining very local, directional deformation of microstructure. Closely related to that, for fatigue applications, it may be very valuable to develop understanding of the local, intra-mark ploughing

effect as it relates to microstructure, residual stress, and microcracking. It is well-known that that intra-mark "burnishing" effect may have a positive effect on fatigue life, but because hardness and residual stress tests are rarely performed on an intra-mark scale, there may be much to learn there. As explained in Section 7.2, a surface can be quite different locally in one half of a feed mark versus the other half.

CHAPTER 9

ORIGINAL CONTRIBUTIONS

The author of this thesis personally committed virtually all the work described himself. The choice of research path, hypotheses, choice of methods, experiment design, data acquisition setup and coding, measurements, application of and development of mathemetical methods, analysis, analysis scripting, programming, illustrations, and paper and thesis writing were all done in their entirety by the author. Exceptions are grant applications, machining, and the mechanical mounting of the accelerometer. In addition, several persons have lent advice throughout the work. They are formally recognized in the main Acknowledgements section.

The following are the larger original contributions of this thesis:

- Use of correlation maps of roughness profiles, and specifically the use of correlation maps over segments of twice the feed length.

- Identification of feed marks in linear roughness profiles regardless of feed mark shape, even when marks are indistinguishable by eye.

- Identification of feed mark modes of variability corresponding to local ploughing and side flow, and idealization of those modes.

- Validation that the feed mark variability mode corresponding to the radial component of cutting vibration is indeed fully accounted for by that mechanism.

- Estimation of the percent contributions of specific mechanisms (radial vibration, axial vibration, ploughing, and side flow) to arbitrary amplitude-based roughness parameters.

- Creation of an almost entirely automated graphical software implementation suitable for use in production.

As stated before, expression as a contribution to any parameter facilitates applicability in manufacturing, in which production is usually concerned with meeting specific scalar surface roughness requirements such as average roughness R_a rather than exotic roughness parameters. Automation of the analysis is important in order to avoid requiring special expertise in the techniques developed for manufacturer implementation. Linear roughness profiles are attractive for the quick, inexpensive, and non-destructive nature of their acquisition, and for the widespread availability of linear roughness measuring machines in machine shops. The final software tool was a deliverable to the partner companies who contributed financially to this Ph.D., which are Héroux-Devtek and Pratt & Whitney Canada.

REFERENCES

Albrecht, P. (1960). New developments in the theory of the metal-cutting process: part I. the ploughing process in metal cutting. *Journal of Engineering for Industry*, 82(4):348–357.

Allen, R. and Mills, D. (2004). *Signal Analysis: Time, Frequency, Scale, and Structure*. Wiley.

Ancio, F., Gámez, A., and Marcos, M. (2015). Factors influencing the generation of a machined surface. application to turned pieces. *Journal of Materials Processing Technology*, 215:50 – 61.

Ancio, F., Gámez, A., and Marcos, M. (2016). Study of turned surfaces by principal component analysis. *Precision Engineering*, 43:418–428.

Ancio, F., Gámez, A., Salguero, J., Batista, M., and Marcos, M. (2013). Principal components based analysis of surface quality of horizontal turned samples. *Advanced Science Letters*, 19(2).

Ancio, F., Gámez, A., Salguero, J., and Marcos, M. (2012). Test methodology to relate machined surface roughness and acceleration. *Advanced Materials Research*, 498:249–254.

Arola, D. and Williams, C. (2002). Estimating the fatigue stress concentration factor of machined surfaces. *International Journal of Fatigue*, 24(9):923–930.

ASME B46.1 - 2009 (2009). Surface texture (surface roughness, waviness, and lay). Standard, American Society of Mechanical Engineers, New York, USA.

Astakhov, P. V. (2010). *Surface Integrity in Machining*, chapter Surface Integrity – Definition and Importance in Functional Performance, pages 1–35. Springer London, London. `http://dx.doi.org/10.1007/978-1-84882-874-2_1`.

Benardos, P. and Vosniakos, G.-C. (2003). Predicting surface roughness in machining: A review. *International journal of machine tools and manufacture*, 43(8):833–844.

Boscaino, G., Praticò, F., and Vaiana, R. (2003). Spectral texture indicators significance in relation to flexible pavements surface performance. *Proceeding of XXII World Road Congress*, pages 19–25.

Brown, C. A. (2012). Roughness. In Bruce, R. W., editor, *Handbook of Lubrication and Tribology, Volume II*. CRC Press. `10.1201/b12265-5`.

Carroll, C. W., Sufi, N. W., and Chang, R. C. (1989). Suppression of tool marks to enhance detection of surface defects. volume 1164, pages 212–221. `10.1117/12.962825`.

Chen, Q., Yang, S., and Li, Z. (1999). Surface roughness evaluation by using wavelets analysis. *Precision Engineering*, 23(3):209 – 212. `http://dx.doi.org/10.1016/S0141-6359(99)00013-6`.

Cheng, K. (2008). *Machining Dynamics: Fundamentals, Applications and Practices*. Springer Series in Advanced Manufacturing. Springer London.

Dietzsch, M., Papenfuß, K., and Hartmann, T. (1998). The MOTIF-method (ISO 12085) - a suitable description for functional, manufactural and metrological requirements. *International Journal of Machine Tools and Manufacture*, 38(5):625 – 632. `http://dx.doi.org/10.1016/S0890-6955(97)00110-7`.

DIN 4760 (1982). Form deviations; concepts; classification system. Standard, Deutches Institut Fuer Normung, Berlin, Germany.

Ehmann, K. and Hong, M. (1994). A generalized model of the surface generation process in metal cutting. *CIRP Annals - Manufacturing Technology*, 43(1):483 – 486.

Field, M. and Kahles, J. (1964). The surface integrity of machined & ground high strength steels. Technical Report DMIC Report 210, Delaware Industries Manufacturnig Corporation.

Field, M., Kahles, J., and Cammett, J. (1972). A review of measuring methods for surface integrity. *Annals of the CIRP*, 21/2:219 – 239.

Fujii, N. and Shirai, T. (2000). Surface property measuring device. US Patent 6,164,124.

Gegg, B., Suh, C., and Luo, A. (2011). *Machine Tool Vibrations and Cutting Dynamics*. SpringerLink: Bücher. Springer New York.

Greenwood, J. and Wu, J. (2001). Surface roughness and contact: An apology. *Meccanica*, 36(6):617–630. `http://dx.doi.org/10.1023/A:1016340601964`.

Griffiths, B. (2001). 1 - setting the scene. In Griffiths, B., editor, *Manufacturing Surface Technology*, pages 1 – 29. Kogan Page Science, Oxford. `https://doi.org/10.1016/B978-185718029-9/50002-0`.

Grzesik, W. (2011). *Mechanics of Cutting and Chip Formation*, pages 87–114. Springer London, London. `http://dx.doi.org/10.1007/978-1-84996-450-0_3`.

Grzesik, W. and Brol, S. (2009). Wavelet and fractal approach to surface roughness characterization after finish turning of different workpiece materials. *Journal of Materials Processing Technology*, 209(5):2522 – 2531. `http://dx.doi.org/10.1016/j.jmatprotec.2008.06.009`.

Grzesik, W. and Brol, S. (2010). *Metal Cutting: Research Advances*, chapter Generation and Modelling of the Surface Roughness in Machining Using Geometrically Defined Cutting Tools, pages 163 – 185. Nova Science Publishers, New York, USA.

Grzesik, W. and Brol, S. (2011). Identification of surface generation mechanisms based on process feed-back and decomposition of feed marks. *Advanced Materials Research*, 223:505 – 513. `10.4028/www.scientific.net/AMR.223.505`.

He, C., Zong, W., and Sun, T. (2016). Origins for the size effect of surface roughness in diamond turning. *International Journal of Machine Tools and Manufacture*, 106:22 – 42.

ISO 11562:1996 (1996). Spécification géométrique des produits (GPS) – état de surface: Méthode du profil – caractéristiques métrologiques des filtres à phase correcte. Standard, International Organization for Standardization, Geneva, CH.

ISO 12085:1996 (1996). Geometrical product specifications (GPS) – surface texture: Profile method – motif parameters. Standard, International Organization for Standardization, Geneva, CH.

ISO 25178-2:2012 (2012). Geometrical product specifications (GPS) – surface texture: Areal – part 2: Terms, definitions and surface texture parameters. Standard, International Organization for Standardization, Geneva, CH.

ISO 4287:1997 (1997). Geometrical product specifications (GPS) – surface texture: Profile method – terms, definitions, and surface texture parameters. Standard, International Organization for Standardization, Geneva, CH.

ISO/TS 16610-29:2006 (2006). Geometrical product specifications (GPS) – filtration – part 29: Linear profile filters: Spline wavelets. Standard, International Organization for Standardization, Geneva, CH.

Jawahir, I., Brinksmeier, E., M'Saoubi, R., Aspinwall, D., Outeiro, J., Meyer, D., Umbrello, D., and Jayal, A. (2011). Surface integrity in material removal processes: Recent advances. *CIRP Annals - Manufacturing Technology*, 60(2):603 – 626. `http://dx.doi.org/10.1016/j.cirp.2011.05.002`.

JIS B 0601-2001 (2001). Geometrical product specification (GPS) - surface texture: Profile method - terms, definitions and surface texture parameters. Standard, Japanese Industrial Standards Committee.

Kim, B. and Chu, C. (1999). Texture prediction of milled surfaces using texture superposition method. *Computer-Aided Design*, 31(8):485 – 494.

Kishawy, H. and Elbestawi, M. (1999). Effects of process parameters on material side flow during hard turning. *International Journal of Machine Tools and Manufacture*, 39(7):1017 – 1030.

Klocke, F. and Kuchle, A. (2011). *Manufacturing Processes 1: Cutting*. RWTH edition. Springer Berlin Heidelberg.

Kong, M., Lee, W., Cheung, C., and To, S. (2006). A study of materials swelling and recovery in single-point diamond turning of ductile materials. *Journal of Materials Processing Technology*, 180(1-3):210 – 215.

Lin, S. and Chang, M. (1998). A study on the effects of vibrations on the surface finish using a surface topography simulation model for turning. *International Journal of Machine Tools and Manufacture*, 38(7):763 – 782. `http://dx.doi.org/10.1016/S0890-6955(97)00073-4`.

Petropoulos, P. G., Pandazaras, N. C., and Davim, P. J. (2010). *Surface Integrity in Machining*, chapter Surface Texture Characterization and Evaluation Related to Machining, pages 37–66. Springer London, London. `http://dx.doi.org/10.1007/978-1-84882-874-2_2`.

Provencher, P. R. and Balaziski, M. (2016). Automatic identification of feed marks in machined surface roughness profiles by correlating random variations. *The International Journal of Advanced Manufacturing Technology*, 82(5):1305–1315. `http://dx.doi.org/10.1007/s00170-015-7461-z`.

Quintana, G., Ciurana, J., and Campa, F. (2009). *Machine Tools for High Performance Machining*, chapter Machine Tool Spindles. Springer-Verlag London, London.

Rimpault, X., Chatelain, J.-F., Klemberg-Sapieha, J.-E., and Balazinski, M. (Accepted May 2016). Surface profile texture characterization of trimmed laminated composite in the stacking sequence direction. *Measurement*.

Sahoo, P., Barman, T., and Davim, J. (2011). *Fractal Analysis in Machining*. Springer Briefs in Applied Sciences and Technology. Springer Berlin Heidelberg.

Schulze, V., Schaal, N., Kuster, F., and Wegener, K. (2015). 15th CIRP conference on modelling of machining operations (15th cmmo) springback in metal cutting with high cutting speeds. *Procedia CIRP*, 31:24 – 28.

SHERPA/ROMEO (2017). Publisher copyright policies & self-archiving, international journal of advanced manufacturing technology. [Online.] `http://www.sherpa.ac.uk/romeo/search.php?issn=0268-3768` [Accessed 17 May 2017.].

Tabenkin, A. (2001). To each his own parameter. *Quality Digest*.

USPTO (2017). Terms of use for USPTO websites. [Online.] `https://www.uspto.gov/terms-use-uspto-websites` [Accessed 17 May 2017.].

Vorburger, T. and Raja, J. (1990). Surface finish metrology tutorial. Technical report, National Institute of Standards and Technology, Maryland, USA.

Wang, S. J., To, S., and Cheung, C. F. (2013). An investigation into material-induced surface roughness in ultra-precision milling. *The International Journal of Advanced Manufacturing Technology*, 68(1):607–616. `http://dx.doi.org/10.1007/s00170-013-4781-8`.

Whitehouse, D. J. . (2011). *Handbook of Surface and Nanometrology, Second Edition*. CRC Press, Florida, USA.

Zahavi, E., Torbilo, V., and Press, S. (1996). *Fatigue Design: Life Expectancy of Machine Parts*. A Solomon press book. Taylor & Francis.

Zecchino, M. (2003). Why average roughness it not enough. *Advanced Materials and Processes*, 161(3):25–28.

Zhang, J. and Liang, S. (2005). Surface roughness in finish turning of hardened steels. *Transactions of the North American Manufacturing Research Institute of SME*, 34:515–522.

Zhanqiang, L., Zhenyu, S., and Yi, W. (2013). Definition and determination of the minimum uncut chip thickness of microcutting. *The International Journal of Advanced Manufacturing Technology*, 69(5):1219–1232.

Zong, W., Huang, Y., Zhang, Y., and Sun, T. (2014). Conservation law of surface roughness in single point diamond turning. *International Journal of Machine Tools and Manufacture*, 84:58 – 63.

APPENDIX A

LIST OF PUBLICATIONS

(Conference talk) Provencher, P.R. & Balazinski, M. (2015) Automated identification of machining feed marks in surface roughness profiles by correlating deviations. *4th International Conference on Virtual Machining Process Technology* (VMPT 2015), in Vancouver, Canada. Proceedings unpublished.

(Journal paper) Provencher, P.R. & Balazinski, M. (2016) Automatic identification of feed marks in machined surface roughness profiles by correlating random variations. *Int J Adv Manuf Technol* 82: 1305. Online version published in 2015 (same journal). `http://dx.doi.org/10.1007/s00170-015-7461-z`

(Submitted to journal) Provencher, P.R. & Balazinski, M. (2017) Principal component idealizations of the dominant modes of variability in the mechanics of the cutting process in metal turning. Submitted to the *Int J Adv Manuf Technol*.

(Submitted to journal) Provencher, P.R. & Balazinski, M. (2017) Feed mark depths in linear surface roughness profiles of finish hard turned metal parts compared with the radial component of cutting vibrations. Submitted to the *Int J Adv Manuf Technol*.

(Unrelated solid-state physics paper, co-author) A.A. Aczel, H.A. Dabkowska, P.R. Provencher, G.M. Luke. (2008) Crystal growth and characterization of the new spin dimer system $Ba_3Cr_2O_8$. *Journal of Crystal Growth* 310:4, pp 870-873.